2015

Utilizing Hydrology and Geomorphology Relationships to Estimate Streamflow Conditions on Maui and O'Ahu, Hawai'I

Brytne Okuhata
Scripps College

Utilizing hydrology and geomorphology relationships to estimate streamflow conditions on Maui and Oʻahu, Hawaiʻi

A Thesis Presented

by

Brytne Okuhata

To the Pomona College Geology Department

In partial fulfillment of

the degree of Bachelor of Arts

Senior Thesis in Geology

April 23, 2015

Advised by:

_____

Dr. Linda Reinen

Primary Research Advisor

_____

Dr. Karl Lang

Reader

Utilizing hydrology and geomorphology relationships to estimate streamflow conditions on Maui and O‘ahu, Hawai‘i

ABSTRACT: As the population on the island of Maui drastically increases, water resource demands continue to rise. In order to match water demands and to manage water resources, it is important to understand streamflow and drainage basin interactions. If relationships between a drainage basin’s hydrologic and geomorphologic characteristics can be quantified, then streamflow conditions of ungaged streams can potentially be estimated. The baseflow recession constant is an important variable to analyze for water management, yet until this study, recession constants were not calculated for the island of Maui, or Hawai‘i as a whole. Recession constants of currently gaged streams on Maui correlated to the permeability and flow conditions of the watersheds. Streams with recession constants >0.95 were generally placed in areas of the island with dike-impounded groundwater and streams with recession constants <0.95 were generally placed in areas with dike-free groundwater. Recession constants <0.90 also indicated near perennial and/or intermittent streams. Hydrologic variables such as baseflow recession constants, low-flow values, and change in storage values are generally correlated to a watershed’s geomorphologic variables such as drainage density, hypsometric integral and concavity index. Based on equations produced from the relationships between a watershed’s hydrology and geomorphology, drainage density and hypsometric integrals are potential indicators of hydrologic variables and streamflow conditions. The same analysis can be done on other islands in Hawai‘i, but the specific relationships between hydrology and geomorphology must be determined for each island. The understanding of baseflow recession constants and relationships between a watershed’s hydrology and geomorphology can contribute to water resource management. Having the potential to predict flow conditions of ungaged streams provides a tool to identify which streams are most ideal as a freshwater source without expending extra resources to unproductively gage streams and drill for water.

Table of Contents

Tables:

1. Introduction

Despite efforts to conserve water in Hawai‘i, demands are increasing as the population of the islands continue to grow. With a population of 1.36 million people, Hawai‘i withdrew 671 million gallons of freshwater per day in 2010 (Maupin et al., 2014). Specifically, Maui's population increased 43.7% within the last 20 years (U.S. Census Bureau, 2010 Census) and the County of Maui Department of Water Supply (MDWS) produced an average of 37.5 million gallons per day (Johnson et al., 2014). That average value of produced water is expected to increase 12 to 57 percent by 2030 (Johnson et al., 2014). In order to meet these increasing demands, fresh groundwater systems need to be studied to determine the availability of the resources (Johnson et al., 2014). Flow conditions provide insight into the type of stream and relative amount of water within each drainage basin. Relationships between hydrologic and geomorphologic parameters of drainage basins have the potential to predict a stream's flow condition, informing us of which streams are the most useful to supply the community with freshwater resources.

The Hawaiian Islands are a group of shield volcanoes produced by multiple lava flows. The interior lava flows are mainly basalt, but then grade out to younger andesite flows, therefore making the interior of the flows more porous and permeable than the exterior of the flows (Cox, 1954). Throughout the islands are fissures in rift zones, which were filled with lava to form dikes (Cox, 1954). The islands' lava flows have a high average permeability, resulting in a high infiltration to rainfall ratio (Cox, 1954). The precipitation works its way down and accumulates as three main groundwater reservoirs: perched groundwater, dike-impounded groundwater, and groundwater floating on salt water (Cox, 1954). The first two reservoirs are the main sources of water supply.

Maui was selected as a case study and O‘ahu was selected as the test case for this thesis because of their growing demand for water. O‘ahu is heavily populated and Maui's population is greatly increasing, therefore making the two islands important locations to study water resources. Since Maui and O‘ahu have similar shield-forming stages, but differ in age and erodability, the two islands can be compared to determine how geomorphologic factors affect the hydrology of the islands.

1.1 Maui's Hydrogeology

Maui is the second largest island in the Hawaiian island chain, with an area of 728 square miles (Stearns and Macdonald, 1942). Maui is formed from two shield volcanoes, Mauna Kahalawai to the west and Haleakalā to the east, which are connected by an isthmus forming a valley in the middle (Figure 1a) - hence the island's nickname: "The Valley Isle" (Stearns and Macdonald, 1942). With its diverse environments and ecosystems, Maui is unique to the Hawaiian island chain. The island experiences different micro-climates between districts, with the city of Hana on the east side of the island being wet and warm, the city of Lahaina on the west side hot and dry, and the summit of Haleakalā cold and semi-arid. Maui's volcanic layers are intruded by dikes (Figure 1b), which were created as magma rose through narrow, vertical cracks within the volcanoes and solidified (Stearns and Macdonald, 1942). The dikes' lower permeability, relative to the lava flows, impedes groundwater flow, causing groundwater to flow parallel to the dike's orientation (El-Kadi and Moncur, 2006). Closer to the dike-free coasts of the island are lens-shaped water bodies, known as freshwater-lens groundwater systems (Figure 1b), which are perched within volcanic basalt that is of higher-permeability than the dikes themselves (Johnson et al., 2014). Since freshwater is less dense than saline groundwater, the freshwater sits atop the saltwater and lower-permeability geologic layers, and typically flows toward the ocean (Johnson et al., 2014).

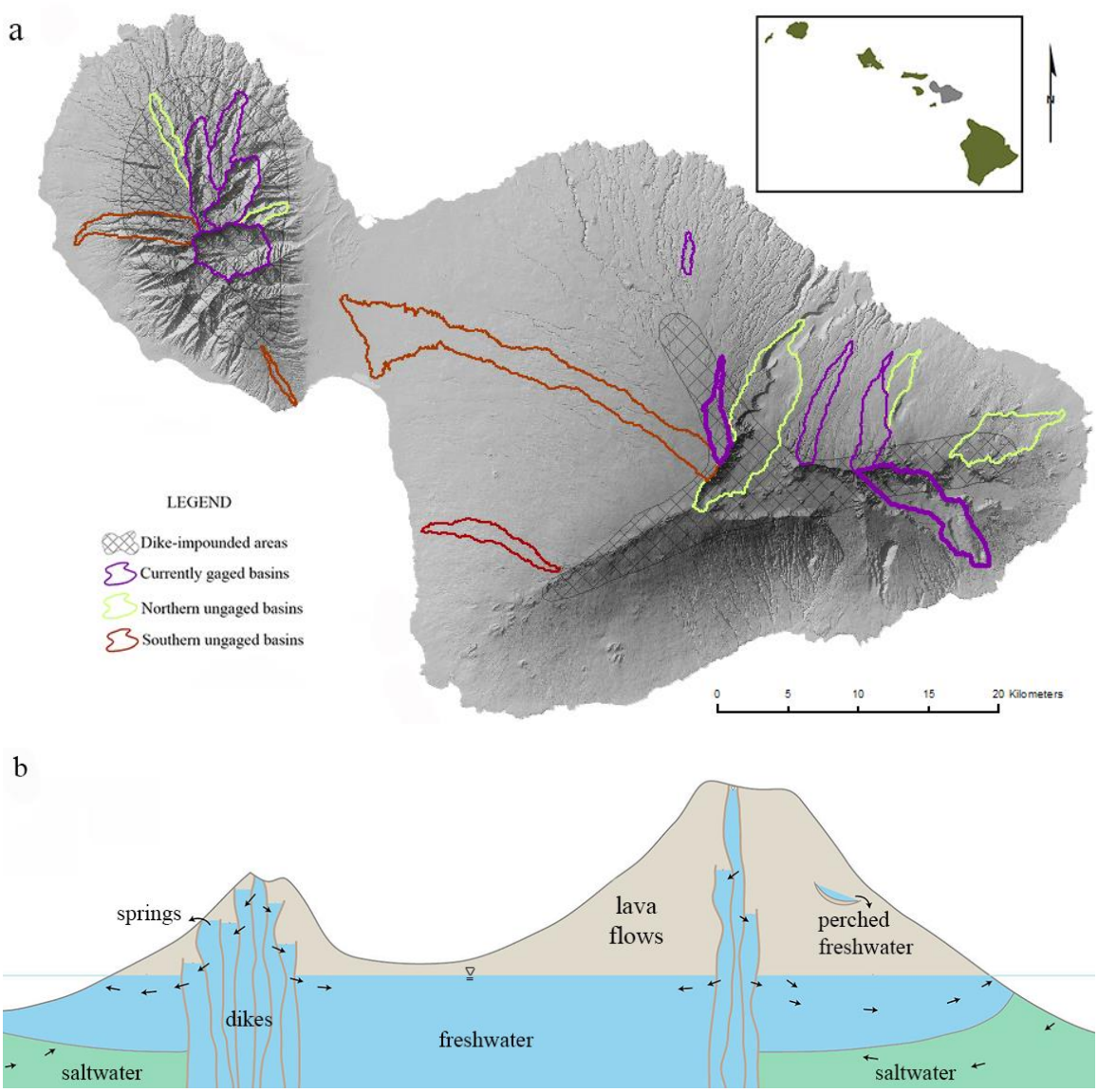

Figure 1. Case study location and hydrogeology schematic. (a) Map of Maui displayed with drainage basins used in this thesis and dike-impounded areas. Dike outlines provided by Maoya Bassiouni, USGS, pers.comm. July 2014. Inset map displays State of Hawai‘i with Maui shaded in grey. (b) Illustration of dike intrusions causing compartmentalization of groundwater. Illustration was recreated for Maui based on figure from Gingerich and Oki, 2000. Illustration not drawn to scale.

Haleakalā’s summit, Pu‘u ‘Ula‘ula, stands at 10,023 feet above sea level, exhibiting a classic shield shape with broad slopes (Johnson et al., 2014). The western slopes of Haleakalā are drier and broader compared to the wetter eastern slopes. Mauna Kahalawai, also known as the West Maui Mountains, contains deeply carved valleys due to erosion. Its summit, Pu‘u Kukui, stands at 5,788 feet above sea level (Johnson et al., 2014). The most rainfall occurs on the slopes of the

island at 2,000 to 6,000 feet above sea level, but can vary from island to island depending on the location and topography (Oki, 2004). Because of the relatively steep topography of the Hawaiian Islands, the northeastern sides of the islands receive more rainfall (Figure 2) due to the tradewinds from the north Pacific anticyclone (Johnson et al., 2014; Oki et al., 2010). The islands experience a wet season from October to April, where tradewinds blow 50-80 percent of the time, and a dry season from May to September, where tradewinds blow 80-95 percent of the time (Gingerich, 2008; Oki et al., 2010). The island of Maui receives an average rainfall of 81 inches per year; Puʻu Kukui in particular receives an average rainfall of 360 inches per year, and the northeastern mid-slopes of Haleakalā receive an average rainfall of 200 inches per year (Johnson et al., 2014). In comparison, the southwestern slopes of Haleakalā receive 25 inches of rain per year, as this area falls within the rain shadow (Johnson et al., 2014).

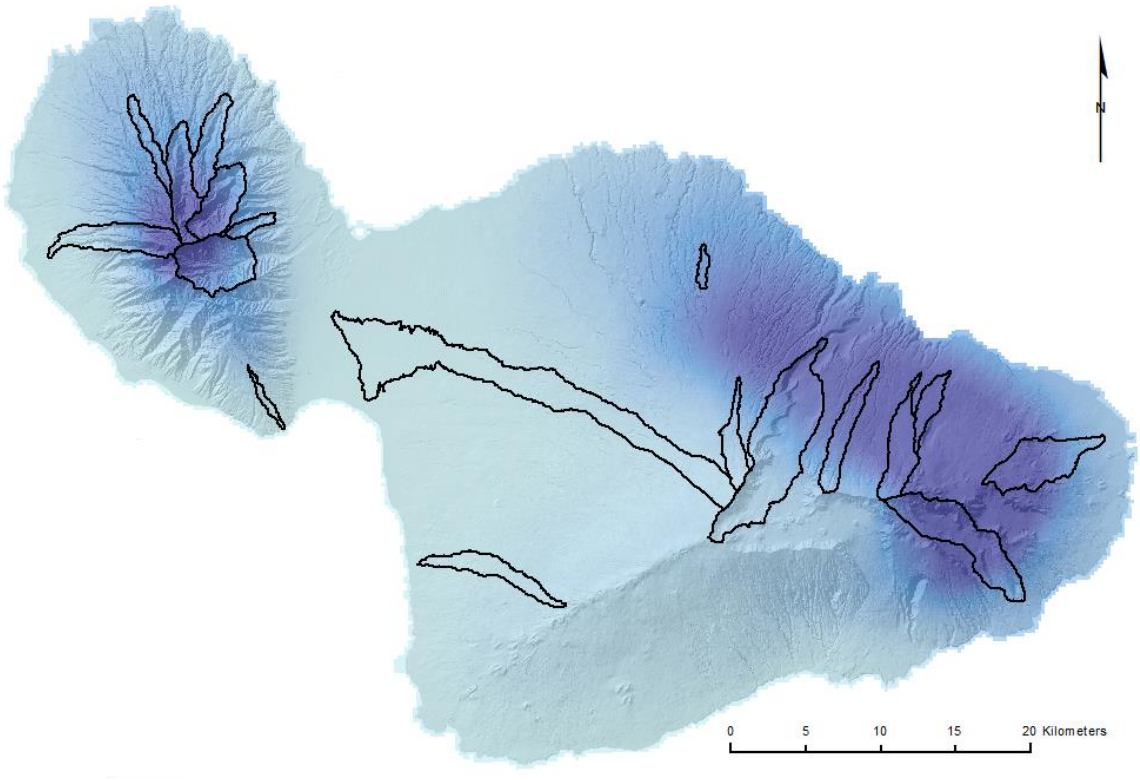

Figure 2. Map of Maui displaying average annual rainfall in inches (Giambelluca et al., 2013). All of the drainage basins used in this study are outlined in black.

Maui's location, topography, and climate system affect the island's complex hydrogeologic system. It has been found that one of Maui's streams, Waiheʻe, has a baseflow greater than its recharge (Johnson et al., 2014). This result provides evidence for groundwater sharing between watersheds, which was previously seen on Oʻahu in the 1940s, when the Haiku tunnel was created (Hirashima, 1963). This tunnel went through four dikes and consequently drained water at a rate of 11 million gallons per day for several months throughout the construction process (Hirashima, 1963). Continuous withdrawal caused water that typically drained into Kahaluʻu Stream to feed into Haiku Valley (Hirashima, 1963). This relationship is evidenced by a decrease in discharge from Kahaluʻu Stream by 26% (Hirashima, 1963). Despite the fact that the groundwater sharing on Oʻahu was caused by anthropogenic affects, it is believed that groundwater sharing is naturally occurring at Waiheʻe Stream on Maui (Delwyn Oki, USGS, pers. Comm. July 2014).

1.2 Oʻahu's Setting and Hydrogeology

Oʻahu, with an area of 596 square miles, is the third largest island in the Hawaiian island chain (Engott et al., 2015). Oʻahu was formed by two shield volcanoes which have eroded away to form steep mountains with deeply cut valleys (Engott et al., 2015). The older western side of the island is made of lava from Waiʻanae Volcano and the younger eastern side of the island is made of lava from Koʻolau Volcano (Figure 3). Oʻahu is made of two shield-stage lava flows which are intruded by dikes that are less-permeable than the basaltic lava flows. There are specifically at least 1,000 dikes per mile within the central area of the two rift zones that cut through the elongated volcanoes (Figure 3) (Engott et al., 2015). Similarly to Maui, Oʻahu also has areas of freshwater lens-shaped bodies, which are surrounded by lava flows of greater permeability. As in the case of Haleakalā, the eastern Koʻolau mountains receive more precipitation than the Waiʻanae mountains, which fall into the rain shadow (Figure 4) (Engott et al., 2015).

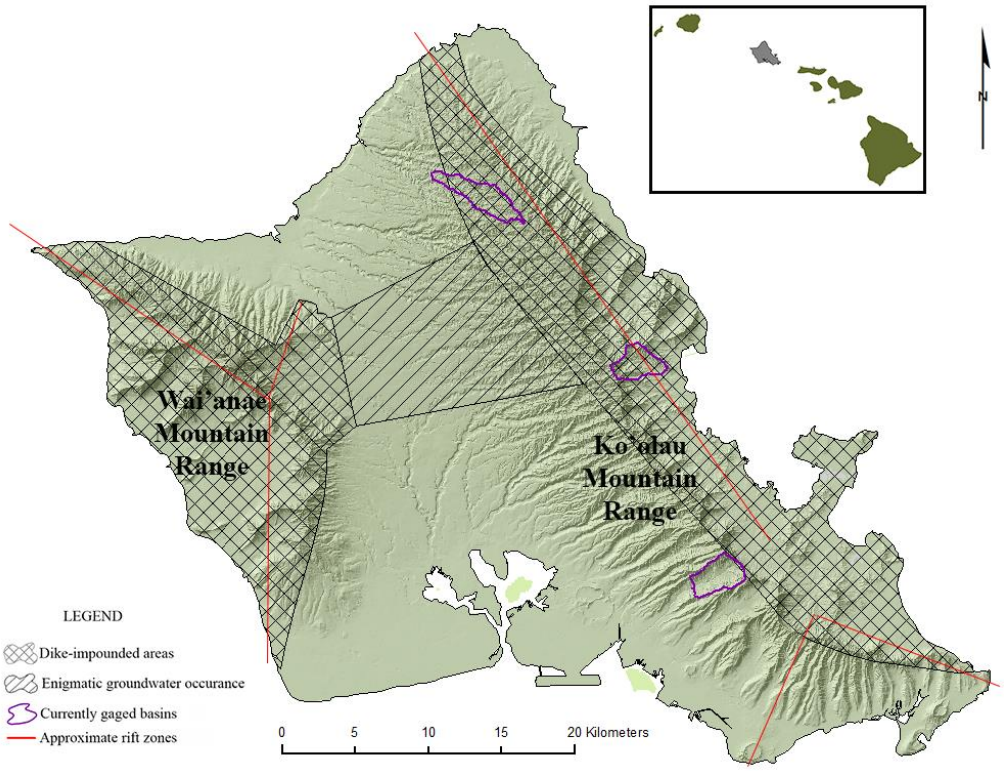

Figure 3. Map of Oʻahu displaying drainage basins and dike-impounded areas. Dike outlines provided by Maoya Bassiouni, USGS, pers.comm. July 2014. Inset map displays State of Hawaiʻi with Oʻahu shaded in grey.

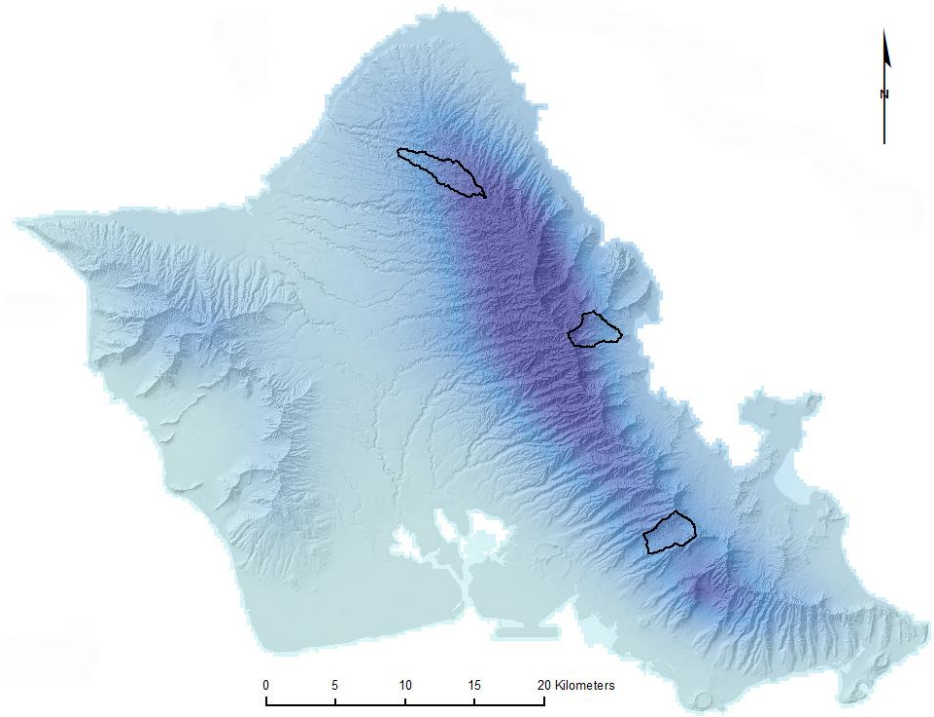

Figure 4. Map of Oʻahu displaying average annual rainfall (inches) with isohyets (Giambelluca et al., 2013). Three of the currently gaged drainage basins are outlined with black.

1.3 Recession Constants, k

Low-flow recession constants inform us of the natural storages that capture and feed groundwater into streams, which reveal the hydrogeologic settings of the area (Tallaksen, 1995). Groundwater discharge analysis compares drainage basin characteristics with the geology of the area (Knisel, 1963). Recession constants are dimensionless values that delineate the rate at which a stream's flow decreases as the stream is being recharged with groundwater (Vogel and Kroll, 1996). Recession constants are calculated based on exponential functions between time and stream discharge (Figure 5).

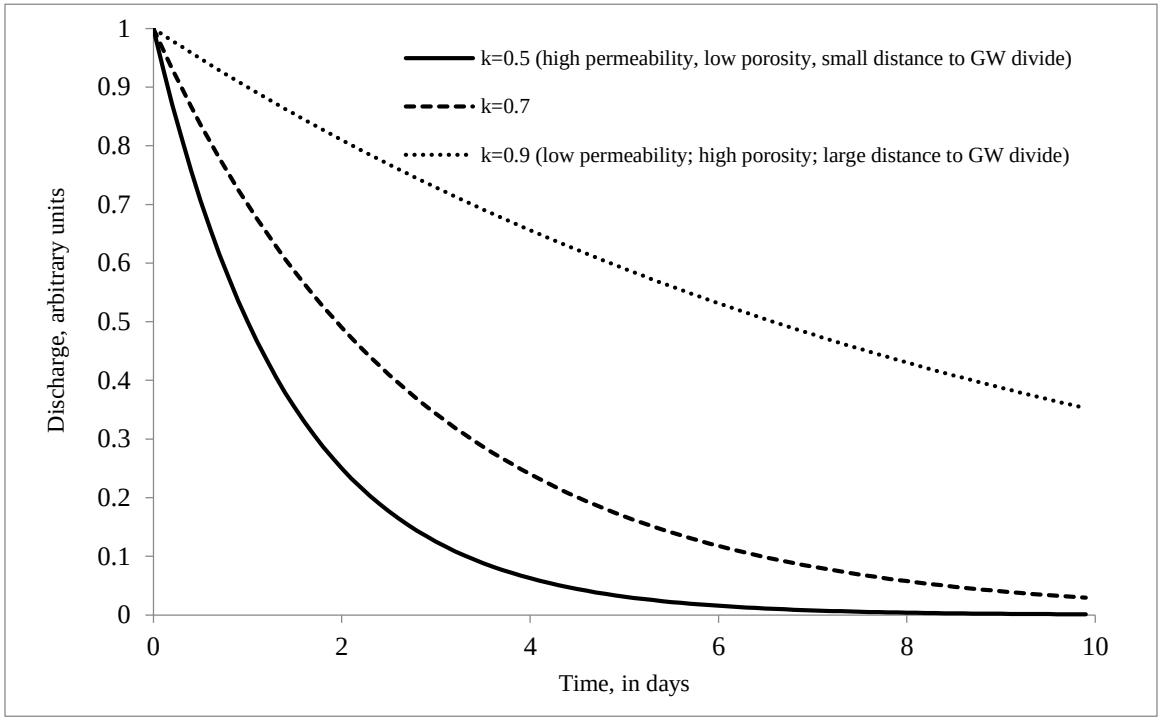

Figure 5. Graph displaying how the steepness of a hydrograph's falling limb correlates to the relative recession constant value. Lower recession constants correlate to steeper falling limbs. Hydrographs with steeper falling limbs are typically set in areas of higher permeability, lower porosity, and small distances to the groundwater divide. Higher recession constants correlate to flatter falling limbs. Hydrographs with flatter falling limbs are typically set in areas of lower permeability (i.e. dike-impounded areas), higher porosity, and larger distances to the groundwater divide. Graph created by D.S. Oki.

The recession constant, *k*, is derived from the discharge equation

$$Q = Q_o e^{-\alpha t} \quad (1)$$

where the recession the recession constant, *k*, is determined by the equation

$$k = e^{-\alpha} \quad (2)$$

as noted in Thomas et al. (2013). An exponential function quantifies the relationship where the dependent variable proportionally changes the same change as the independent variable. Recession constants are calculated from the baseflow recession curve, which indicates when the streamflow is returning to flow derived from groundwater (Fetter, 2001). This can help determine the hydrogeologic settings of the streams and indicate the stream's low-flow discharge variability, which can be used for various purposes such as irrigation, water supply, and quantity estimates (Tallaksen, 1995). High recession constants indicate steadier hydrographs with flat falling limbs, suggesting a slower depletion of base runoff (Carlston, 1963). Lower recession constants indicate flashier hydrographs with steeper falling limbs, suggesting a more rapid depletion of base runoff (Carlston, 1963). Recession constants are useful in estimating aquifer properties and potential recharge. The baseflow recession curve follows the rising limb of the hydrograph, which is an increase in discharge, usually caused by rainfall, and the falling limb, which indicates that the discharge and stream level are decreasing (Figure 6) (Fetter, 2001). Recession constants could potentially identify perennial and intermittent streams, which would indicate the usefulness of a stream for water resources. Despite the importance of these low-flow recession constants, there are currently no published recession constants for streams in Hawai‘i.

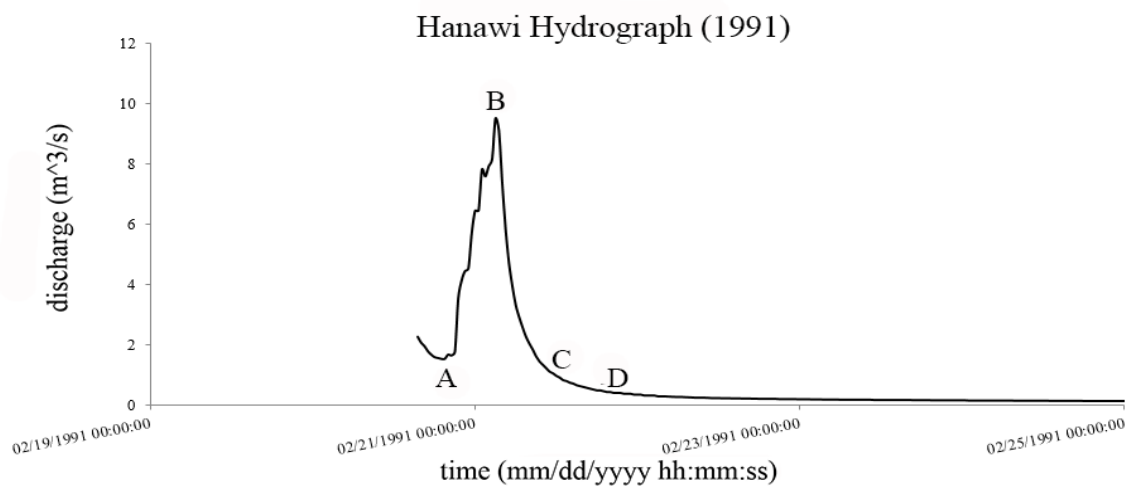

Figure 6. Example of a desired "clean" hydrograph following a storm event with little to no peaks interrupting the recession. AB is the rising limb, BC is the falling limb, CD is the base flow recession. Points C and D are visually determined while picking out the recession curve.

1.4 Geomorphology

The shape and form of a watershed is closely linked to its hydrologic response (Rodriguez-Iturbe and Valdes, 1979). The movement of groundwater and surface water helps to shape a watershed, which can control how the water moves. The geomorphology of a watershed impacts the rate of discharge from a drainage basin (Langbein et al., 1947), therefore influencing the baseflow recession constants of that basin. Geomorphologic parameters, such as drainage density, hypsometric integral, and concavity index are critical features that influence a watershed's stream discharge. Drainage density is the total length of the streams within a drainage basin divided by the area of that basin (Bierman and Montgomery, 2014). The drainage density value indicates how well a watershed drains. Higher drainage densities indicate that a basin drains quickly because there are more conduits/streams draining water within a unit area, by decreasing the lag time to peak discharge (Harlin, 1984). The higher drainage density is reflected by pronounced discharge peaks and steeper falling limbs. According to the National Institute of Hydrology (http://www.nih.ernet.in/learning_hyd.html), lower drainage densities indicate that a basin is not well drained, therefore reflected by hydrographs with shallow rising and falling limbs.

Hypsometric integral values reflect the erosional maturity of the drainage basin (Sarp et al., 2011) as well as how prone the basin is to more erosion (Singh, 2008). The hypsometric integrals indicate the relative basin relief and amount of land mass found at different elevations of the watershed. Higher hypsometric integrals indicate relative higher relief and lower hypsometric integrals indicate relative lower relief (Bierman and Montgomery, 2014). Therefore, higher hypsometric integrals correlate with less-eroded basins and lower hypsometric integrals with lower relief correlate with heavily eroded basins.

Concavity indices reflect the surface processes believed to have formed the watershed and its stream (Bierman and Montgomery, 2014). Concavity indices <0.3 reflect streams with steeper headwaters, concavity indices between 0.3-0.7 reflect fluvial incision, and concavity indices >0.7 reflect alluvial rivers (Bierman and Montgomery, 2014). Most streams have a negative concavity index, reflecting a concave stream profile, while a positive concavity index reflects a convex stream profile. These three geomorphologic variables are linked to the hydrology of a watershed and can shed light on streamflow conditions.

1.5 Previous Works

By analyzing the relationship between geomorphologic parameters and baseflow recession constants, previous studies have aimed to predict low-flow estimates of streams in the northeast United States. These studies found that groundwater flow is controlled by the physical properties within a drainage basin and resultantly can be seen in the basin's geomorphic qualities. The study sites – the Allegheny Mountains, Massachusetts, and New Jersey – are located in areas that generally experience humid continental conditions with warm (temperatures above 50°F) humid summers and very cold winters (average 26.6°F during coldest month). The summer conditions of these places are somewhat comparable to Hawai'i, but Hawai'i experiences warmer conditions on a more regular basis throughout the year. According to the National Oceanic and Atmospheric Administration (http://www.weather.gov/climate/index.php?wfo=hnl), Hawai'i has an average temperature range of 80-90°F and experiences an average annual humidity of 70% at sea level. The different conditions that Hawai'i experiences could impact the relationships between recession constants and geomorphologic parameters of watersheds.

Zecharias and Brutsaert (1988) examined the relationship between baseflow recession constants and the geomorphic and soil characteristics of watersheds from the Allegheny Mountain section of the Appalachian Plateau. In this study, they determined that the reaction factor, a baseflow recession time scale, is correlated to the land slope, drainage density, hydraulic conductivity, and rock porosity of the watershed. Drainage systems in this area are not strongly impacted by structural controls and slopes demonstrate V-shaped valleys. The climate is humid continental and 75% of the area is covered with forests. Zecharias and Brusaert found that generally, the steamflow of humid forested areas, are comprised of baseflow. This emphasizes the importance of understanding the relationship between the rate at which groundwater flows within a drainage basin and the geomorphic parameters that control that flow, since the discharge of groundwater is dependent on the basin's lithology, which can also be reflected as the basin's morphology.

Vogel and Kroll (1992, 1996) calculated regional regression models from 23 sites in Massachusetts, where it typically experiences humid continental conditions. They found the importance of understanding low-flow statistics in order to manage water quality and water supply. They determined a relationship between low-flow statistics and three different variables – drainage area, basin slope, and baseflow recession constant. They found that baseflow recession constants, drainage area, and basin slope explain over 90% of the low-flow discharge

statistic variability. Therefore, the recession constants could act as indicators of basin hydraulic conductivity and soil porosity, as well as a relationship between low-flow statistics and variables.

Thomas et al. (2013) created regression models to analyze how anthropogenic water withdrawals in New Jersey (which has a high density population) affect the baseflow recession constants. They found that the baseflow recession constants are useful in analyzing rainfall-runoff models, separating baseflow, and estimating low-flow statistics of ungaged streams. Results suggested that geologic characteristics such as drainage density and basin slope are important factors in determining recession constants and that groundwater withdrawal increased recession constant estimates. They found that the geomorphology most impacted the recession constant, suggesting that drainage density was the main cause of variability amongst recession constants.

These studies were all conducted in areas with similar climate conditions in the northeast and mid-Atlantic United States and found relationships between stream discharge, baseflow, low-flow statistics and geomorphological parameters of the drainage basins. They found the importance of analyzing recession constants and geomorphology to determine low-flow statistics for potential water supply. Knisel (1963) noted that hydrologists recognize that geology plays an important role in water yield, so it is not sufficient to only analyze the discharge data, but to also analyze its relationship with geologic and geomorphologic data. Despite the importance of this relationship, nobody has analyzed these hydrologic and geologic relationships in Hawai‘i. A recent report by the USGS Pacific Islands Water Science Center (Johnson et al., 2014) analyzes Hawai‘i’s annual recharge of streams under various climate conditions and the physical conditions that could affect the recharge. By considering multiple variables for the entire island of Maui such as, rainfall, fog interception, direct runoff, irrigation, septic-system leachate, excess water, and moisture storage, this report is currently the most robust stream analysis. However, it does not include recession constants or whole-basin geomorphologic parameters such as drainage density, hypsometry, and concavity, which have proven to be important in the other studies.

1.6 Current Work

The objective of this thesis is to apply this previous research to the unique conditions of Hawai‘i while also introducing low-flow recession constants and whole-scale basin parameters. The findings from this thesis are used to provide insight into how hydrologic and geomorphologic variables relate to each other within a watershed, and specifically how baseflow recession constants can be crucial indicators of a stream and drainage basin’s hydrology. I understand that

the recession constant is a complex parameter that is affected by various factors such as, time, precipitation, peak discharge, lithology, and geomorphology. However, for this study, I chose to primarily focus on how the geomorphology of a watershed relates to the recession constant.

I aim to address the overarching question of whether it is possible to predict streamflow conditions based on hydrologic and geomorphologic variables. The goal is to determine if we can predict the flow conditions of an ungaged stream based on the watershed location and geomorphology. Deriving from the main question, this thesis also aims to determine whether geomorphologic variables can recognize groundwater sharing between Waiheʻe and ʻĪao streams on Maui, and if so, which variables best accomplish this.

2. Methods

In order to identify relationships between geomorphology and hydrology, I used two basic types of data, hydrologic data and geomorphologic data, and compared the two data features to each other.

2.1 Hydrologic Parameters

The hydrologic data collected for this thesis included baseflow recession constants, low-flow values, recharge, baseflow, and change in storage values (Table 1).

2.1.a Baseflow Recession Constant, k

During an internship at the USGS Pacific Islands Water Science Center in the summer of 2014, I calculated baseflow recession constants for the nine currently gaged streams on Maui. Baseflow recession constants (*k*) can inform us what physical factors, such as dikes, influence the way groundwater reacts to recharge. I retrieved all of the available discharge data of the nine current continuously-gaged streams of Maui – Honokōhau, Kahakuloa, Waiheʻe, ʻĪao, Honopou, Waikamoi, West Wailuaiki, Hanawi, and ʻOheʻo – from the USGS Pacific Islands Water Science Center (http://maps.waterdata.usgs.gov/mapper/index.html). The discharge values for each stream were plotted as a hydrograph against time (Figure 7).

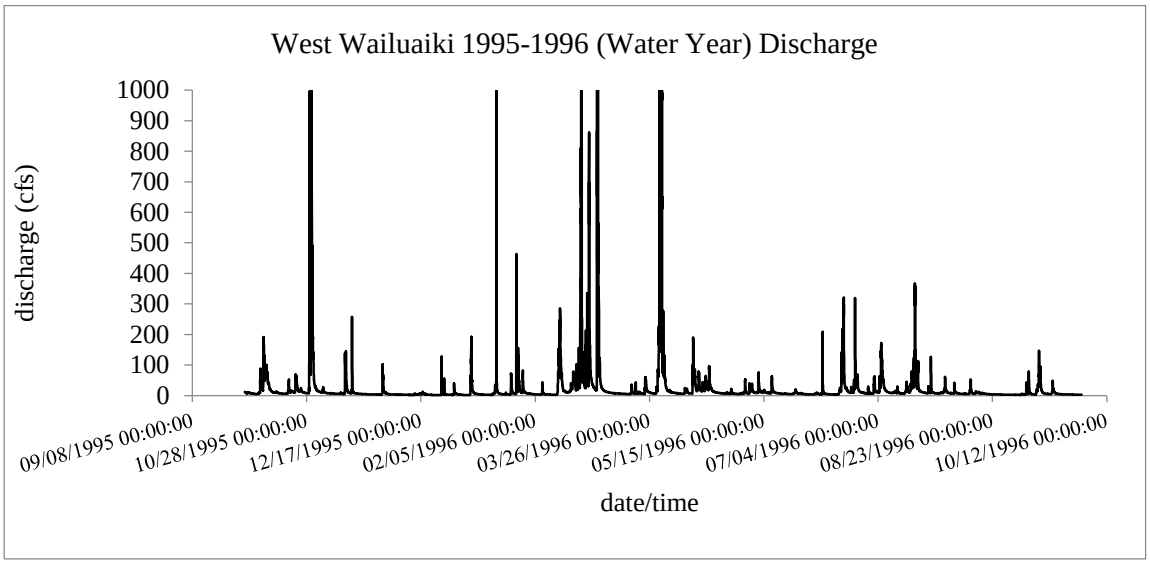

Figure 7. Example of a hydrograph over one water year (October 1 – September 30). Each peak indicates the stream's water discharge after a storm or rain event. Individual peaks and falling limbs were picked out from hydrographs in order to calculate the baseflow recession constants for each stream.

I selected recession curves that are relatively clean (i.e. are not interrupted by large peaks) and follow a discharge peak that is at least five times the median discharge (Appendix A) of the stream. I then visually determined when the recession curve ends by establishing when the curve flattened out, typically when the discharge values stopped receding before a new discharge peak occurred. The recession constant, *k*, was quantified using a best-fit exponential curve equation (Figure 8) (Thomas et al., 2013)

$$Q = Q_o e^{-\alpha t} \quad (1)$$

where the recession constant, *k*, is determined by the equation

$$k = e^{-\alpha} \quad (2)$$

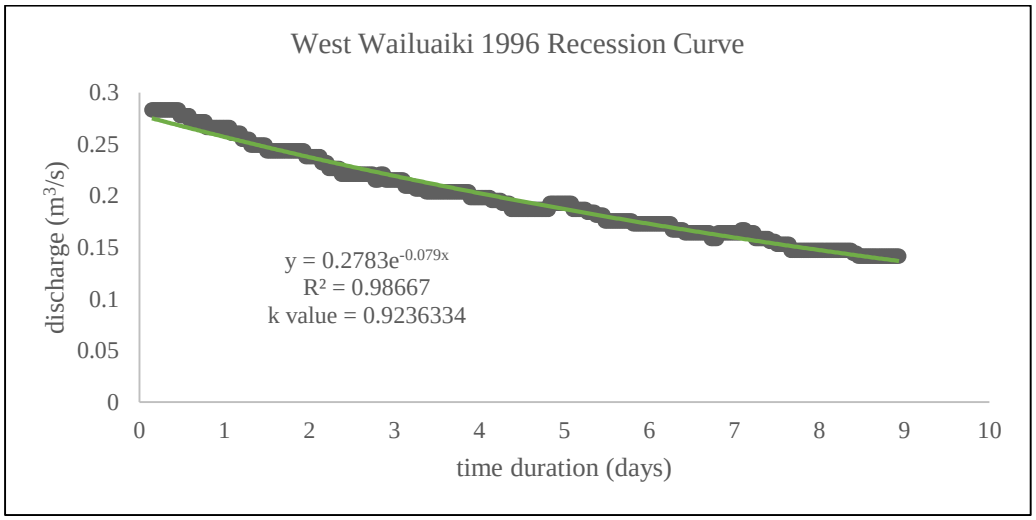

Figure 8. Example of a recession curve with best-fit exponential line (green). Recession constant (*k*) is equal to $e^{-\alpha}$.

It is important to point out that other studies define their recession constant differently and that difference affects the way the data should be analyzed against other geomorphologic variables. Authors such as Brandes et al. (2005) define their recession constant as just α (not –α) from Equation 1. This difference in definition means that *k* and α are inversely related to each other, as according to Equation 2.

An objective automated method to determine the end of the recession period was tested, but this method produced inconsistent results. With this method, I calculated when 90% of the discharge values are the same within a 24-hour period, therefore indicating that the recession is stable and complete. With this method, the COUNTIF function in Excel was used to count the number of flow values within a 24-hour period (12 hours prior to and 12 hours after) that matched the flow value of the current time. Since the discharge values were collected in

intervals of 30 minutes, there are a total of 49 flow values within the 24-hour period (24 values during the 12 hours prior, 24 values during the 12 hours after, and 1 value for the current time). Therefore, if we want 90% of the flow values to match the current flow value, 45 of the 49 flow values need to be matched (Figure 9). However, it was noticed that the recession continued past the estimated end of the recession, so the recession curve was oftentimes cut short, which affects the time duration and recession constants.

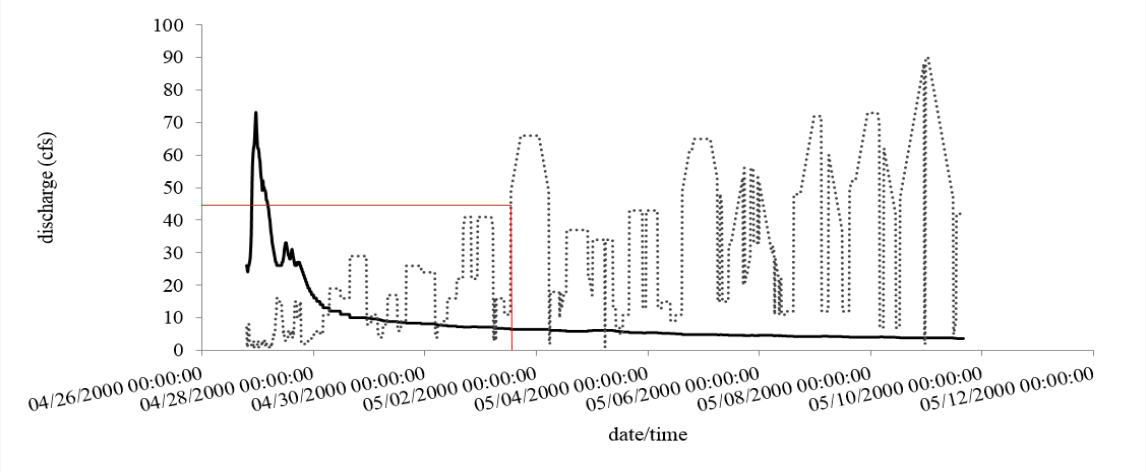

Figure 9. Example hydrograph with objective automated method to determine the end of a recession period. The solid line is the flow and the dotted line corresponds to the number of values that are the same as the flow value indicated at that time. The red lines indicate where the 90% criterion was met. When the dotted line reaches a value of 45, 90% of the flow values within a 24-hour period matches the current flow value, therefore indicating the end of the recession period.

I found that the recession constants correlated to the general lithology of the island, where higher recession constants were calculated from perennial streams in areas in which groundwater is dike-impounded and lower recession constants were calculated from streams in areas with dike-free groundwater or intermittent streams. After noticing the correlation between general lithology and recession constants, I was motivated to analyze whether a stream's flow condition could be predicted from various watershed parameters.

2.1.b Low-flow Values, Q_{95}

The Q_{95} exceedance percentile tells us that a stream's discharge value is expected to exceed the Q_{95} discharge value 95% of the time (Pyrce, 2004). Q_{95} values (along with Q_{90} values) are widely considered as low flow indices (Pyrce, 2004). Low-flow values were computed by creating flow-duration curves for each stream (Figure 10 and Appendix A).

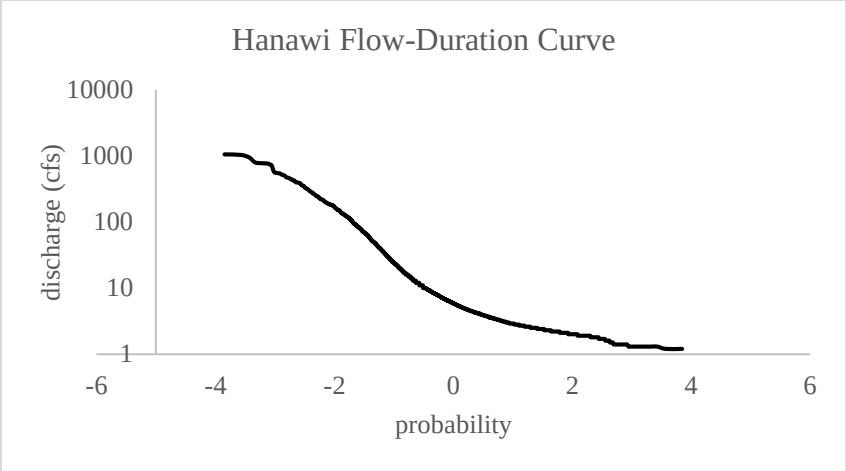

Figure 10. Example flow-duration curve. All flow-duration curves for currently gaged streams on Maui can be found in Appendix A.

2.1.c Recharge

Recharge values were calculated with a GIS data set provided by the USGS Pacific Islands Water Science Center (http://water.usgs.gov/GIS/metadata/usgswrd/XML/sir2014-5168_Maui_water-budget_components.xml) which was used in the Johnson et al. (2014) study (Figure 11). The data set contains a file that divides Maui according to the type of landcover and calculates various hydrologic variables for each landcover polygon. Hydrologic variables include rainfall, runoff, total evapotranspiration, fog, and recharge (all of which are measured in inches per year). Recharge values were clipped for each watershed analyzed in this thesis and converted to units of cubic feet per second (Appendix B). The same process was done for the island of O‘ahu with a data set used in the Engott et al. (2015) study (Figure 12).

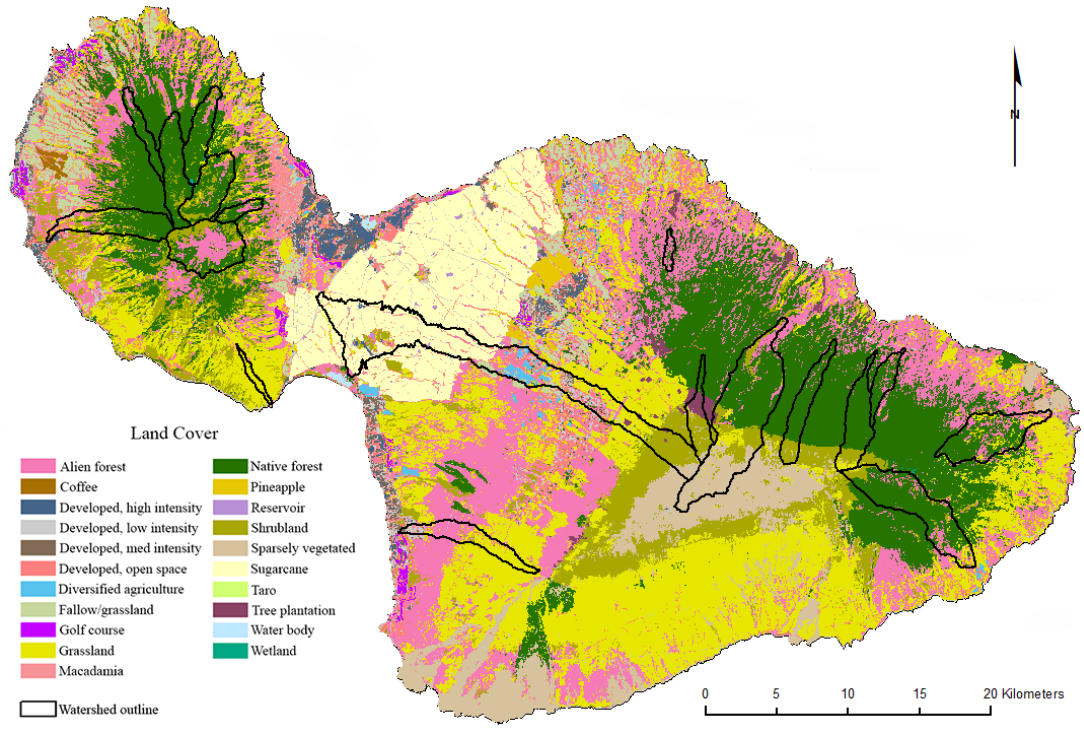

Figure 11. Mean annual water-budget components used to calculate recharge for Maui. The island is divided according to land cover, from which each watershed was clipped out for this thesis. GIS dataset created by A.G. Johnson (2014) from the USGS Pacific Islands Water Science Center.

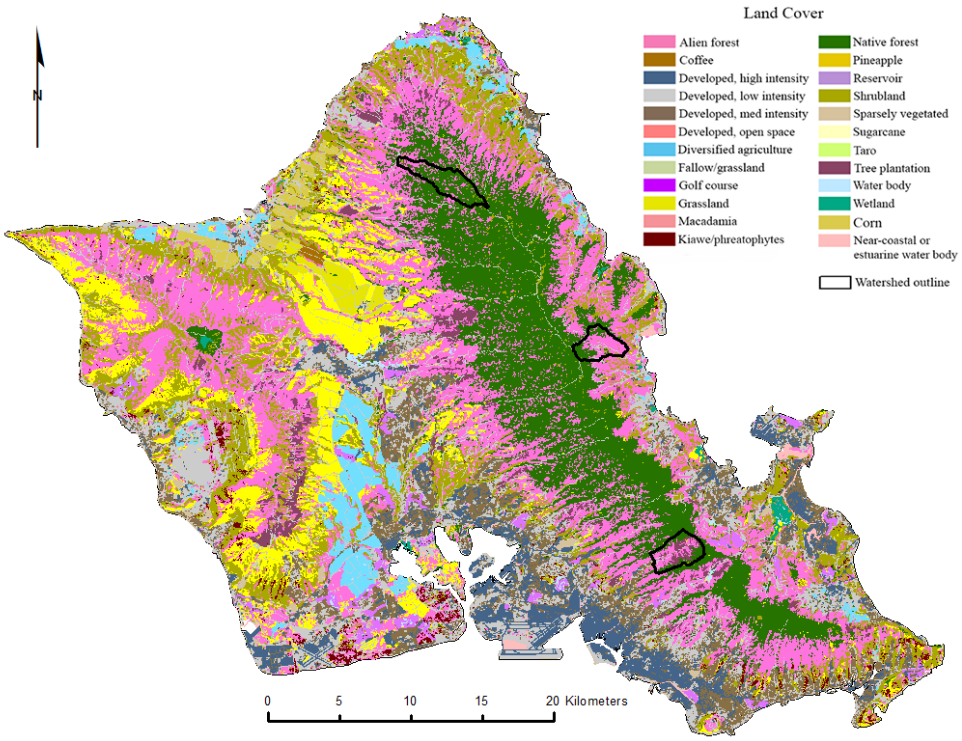

Figure 12. Mean annual water-budget components used to calculate recharge for O‘ahu. The island is divided according to land cover, from which each watershed was clipped out for this thesis. GIS dataset created by J.A. Engott (2015) from the USGS Pacific Islands Water Science Center.

2.1.d Baseflow

Baseflow values were computed using program files provided by the USGS Pacific Islands Water Science Center which were developed by Wahl and Wahl (1995), and streamflow input files from NWIS and USGS (Appendix C).

2.1.e Change in Storage, ΔS

A basic water-budget equation of

$$P = Q + ET + \Delta S \quad (3)$$

where P is precipitation, Q is runoff, ET is evapotranspiration, ΔS is change in storage (Fetter, 2001) was used to calculate the change in storage of each watershed. By reorganizing Equation 3 in terms of ΔS, ΔS can be calculated by

$$\Delta S = P - Q - ET \quad (4)$$

Average annual precipitation and evapotranspiration values were computed from the mean annual water-budget components file from the Johnson et al. (2014) report provided by the USGS Pacific Islands Water Science Center (http://water.usgs.gov/GIS/metadata/usgswrd/XML/sir2014-5168_Maui_water-budget_components.xml). In this file, precipitation values were labeled as 'Rainfall,' evapotranspiration values were labeled as 'Total ET,' and the values are reported in inches per year. The average precipitation and evapotranspiration values were multiplied by the area of the watershed (in square inches) to calculate a volume of precipitation and evapotranspiration in cubic inches per year. Average annual discharge values were retrieved from the USGS Pacific Islands Water Science Center site (under Annual Statistics) for each stream. These values are reported in cubic feet per second, so were therefore converted to cubic inches per year to match the precipitation and evapotranspiration units. Equation 4 was used to compute the change in storage based on the precipitation, evapotranspiration and discharge values for each stream.

2.2 Geomorphology Data

All of the geomorphologic variables were computed using ArcMap reference frame and DEM of Hawai'i. The DEM (Digital Elevation Model) were obtained in October 2014 as NED 1/3 (~10 meter) dataset. DEM were projected in ArcGIS under WGS (World Geodetic System) 1884 UTM (Universal Transverse Mercator) Zone 4N. The DEM for the entire state were downloaded as 14 separate files, which had to be stitched together with the Mosaic tool in ArcMap (Appendix D). From the stitched DEM, geomorphologic variables were computed for the nine currently gaged streams on Maui, as well as nine ungaged streams on Maui, which will be used to predict the hydrological values of those streams.

2.2.a Stream Network

Before computing geomorphologic variables, I had to create a stream network for Maui, and therefore had to determine the cell accumulation threshold. I determined the cell accumulation threshold and stream network using two different methods – a general island method and a watershed-specific method. Rea and Skinner (2012) used two different cell accumulation thresholds, which has been used by other papers. Rea and Skinner created a dense stream network with a 900-cell threshold (x = 2.954) to display delineation and a sparse stream network with a 20,000-cell threshold (x = 4.3) to define catchments. In order to determine a general stream network for the entire island of Maui (Appendix E), I compared the stream network produced to a satellite-image basemap in ArcMap. (Basemaps used in this thesis were created using ArcGIS® software by Esri. ArcGIS® and ArcMap™ are the intellectual property of Esri and are used herein under license. Copyright © Esri. All rights reserved. For more information about Esri® software, please visit www.esri.com.) Stream networks were validated by comparison with satellite images where I was able to see lines of flowing water (Figure 13). I therefore made a stream network to outline the currently flowing streams, and found that a 3,162-cell threshold (x = 3.5) created an average stream network for the entire island.

Figure 13. Evidence of currently flowing streams while determining Method 1 stream network cell-threshold. Streams on satellite basemap are interpreted as the faint white lines that flow through stream channels, which are then traced with blue lines to clearly visualize. Black lines are the stream network created with a 3162 cell-threshold (x=3.5).

In order to determine a watershed-specific stream network, cell accumulation thresholds were determined for each individual stream analyzed on the island of Maui. The stream networks were created using the same methodology as explained in Appendix E, but I determined the specific cell accumulation threshold for each stream by comparing my stream to a stream network map created by the USGS based on a 10-meter DEM (http://streamstatsags.cr.usgs.gov/hi_ss/default.aspx?stabbr=hi&dt=1428991619089). The stream densities I created were matched as closely as possible to the respective stream found on the USGS map. With this method, cell accumulation thresholds ranged from 3,162 (x=3.5) to 31,623 (x=4.5).

2.2.b Drainage Density

Drainage densities were computed by dividing the total stream length by the area of the drainage basin (Appendix F).

2.2.c Hypsometric Integrals and Curves

Hypsometric integrals were computed with the equation

$$HI = \frac{mean\ elevation - minimum\ elevation}{maximum\ elevation - minimum\ elevation} \quad (5)$$

where the elevations were determined as explained in Appendix G.

2.2.d Concavity Index, θ

Concavity indices were determined by plotting the watershed drainage area, A, against the channel slope percent rise to compute a power trendline equation

$$S = k_s A^{-\theta} \quad (6)$$

where S is the channel slope, k_s is the profile steepness, and θ is the concavity index (Zaprowski et al., 2005). Methods to compute the slope and flow for the concavity index are explained in greater detail in Appendix H.

2.3 Analysis

2.3.a Predicting relative amounts of discharge

The hydrologic and geomorphologic variables were calculated for the nine currently gaged streams on Maui. It is not as easy to calculate the hydrologic variables for ungaged streams on the island because gaging stations are needed to collect streamflow statistics. However, it is still possible to compute the geomorphologic variables of ungaged streams using the DEM

and ArcMap reference frame, which does not depend on the availability of stream gaging stations.

In order to determine if a stream's relative discharge can be predicted based on quantifiable hydrologic and geomorphologic variables, the calculated variables of the currently gaged streams were plotted against each other to determine the relationship between the hydrologic and geomorphologic features. Recession constants, low-flow values, and change in storage values were plotted against drainage densities, hypsometric integrals, and concavity indices (where the geomorphologic variables were plotted on the x-axis and the hydrologic variables were plotted on the y-axis). Each plot was fitted with a best-fit line and 95% confidence intervals (Appendix I and J). The geomorphologic values computed from the currently gaged streams were plugged into the appropriate equations to determine the precision of the best-fit equation and to anticipate which relationships should provide the most accurate predictions. The geomorphologic values from the nine ungaged streams were then plugged into the appropriate best-fit equation to determine what recession constant, low-flow value, and change in storage value each geomorphologic variable would predict. The predictions of each hydrologic variable were compared to each other to discover which geomorphologic variable(s) could be used to determine the most accurate hydrologic values.

2.3.b Comparing Maui to Oʻahu

The same analysis was carried out with streams on the island of Oʻahu to determine if the islands share similar relationships or if there is variability between each island within the state. The same hydrologic and geomorphologic variables were calculated from stream discharge data for three currently gaged streams on Oʻahu. Since Oʻahu has the same general lithology and climate system as Maui, the geomorphologic data were input into the same best-fit equations used for Maui's predictions. Those hydrological predictions were compared to the actual hydrological values to determine the accuracy of the predictions.

2.3.c Evaluating groundwater sharing between watersheds

To evaluate whether there is groundwater sharing between watersheds, the recharge values computed (Appendix B) were compared to the baseflow values computed (Appendix C).

3. Results

The overarching question of this thesis is whether streamflow conditions can be predicted based on relationships found between hydrologic and geomorphologic variables, and if these predictions can aid in determining which streams would be most ideal to gage in the future in order to receive the most water possible from groundwater resources. To answer these questions, hydrologic and geomorphologic data was calculated for the nine currently gaged streams, five ungaged northern streams, and four ungaged southern streams on Maui (Figure 14 and 15). I tested this method with three of the currently gaged streams on Oʻahu to determine if the method was applicable to different islands (Figure 16). This study focused on three hydrologic variables and three geomorphologic variables in order to resolve if this method of streamflow condition management is possible.

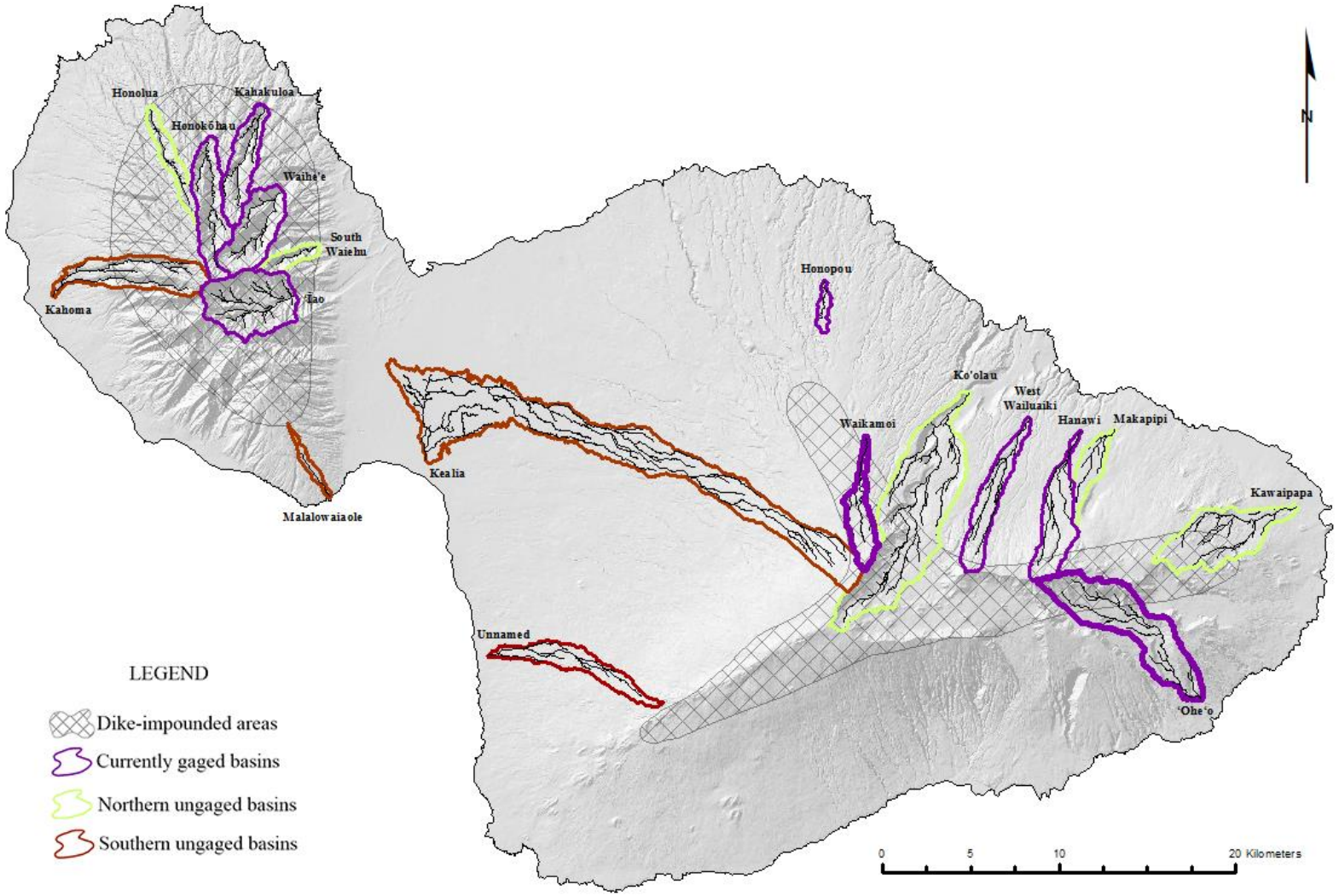

Figure 14. Map of Maui displaying all of the drainage basins created with Method 1 stream networks. Known intermittent stream outlines are bolded. Areas of the island impounded by dikes are displayed with criss-crossed areas (dike outlines provided by M. Bassiouni, USGS, pers. comm. July 2014).

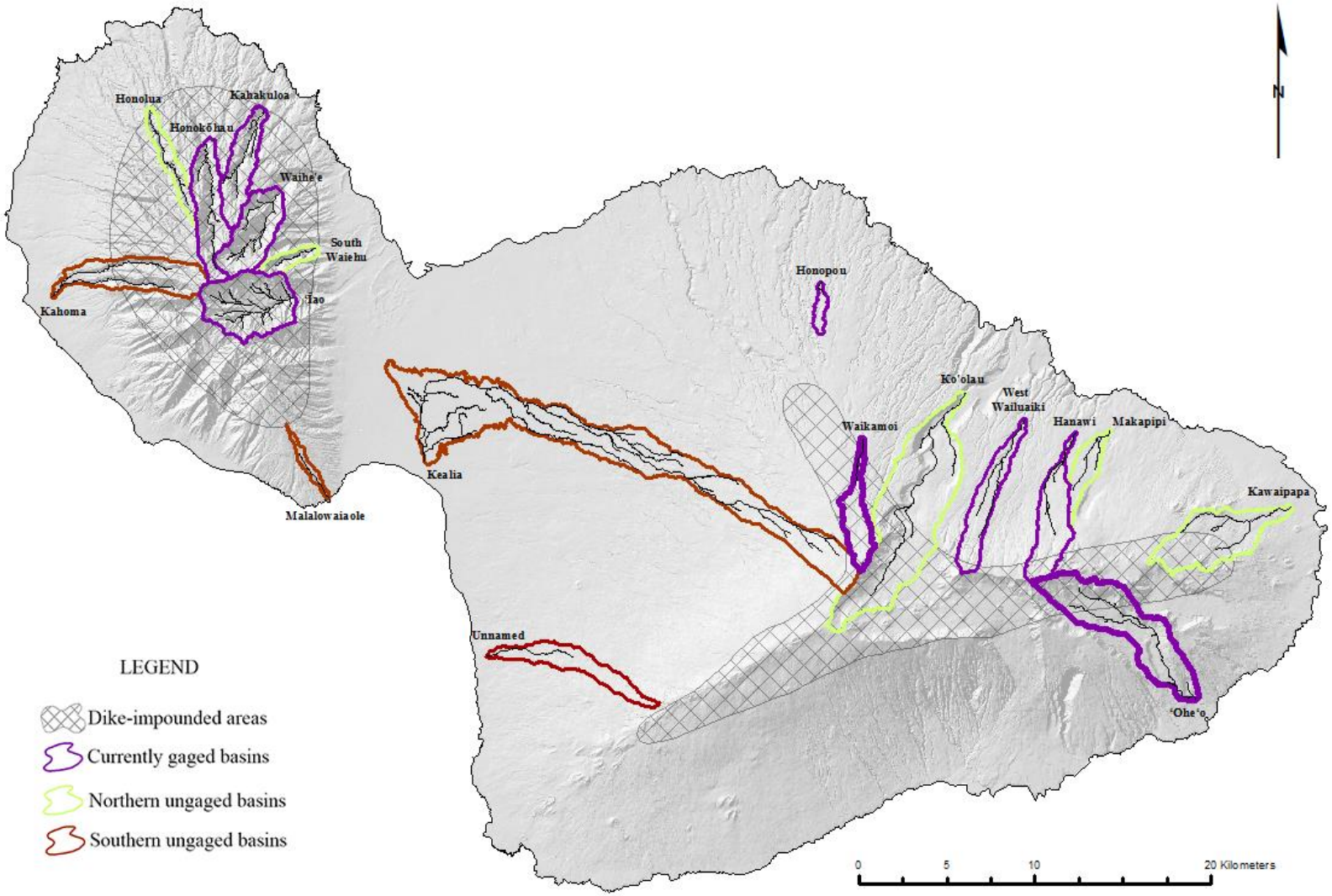

Figure 15. Map of Maui displaying all of the drainage basins created with Method 2 stream networks. Known intermittent stream outlines are bolded. Areas of the island impounded by dikes are displayed with criss-crossed areas (dike outlines provided by M. Bassiouni, USGS, pers. comm. July 2014).

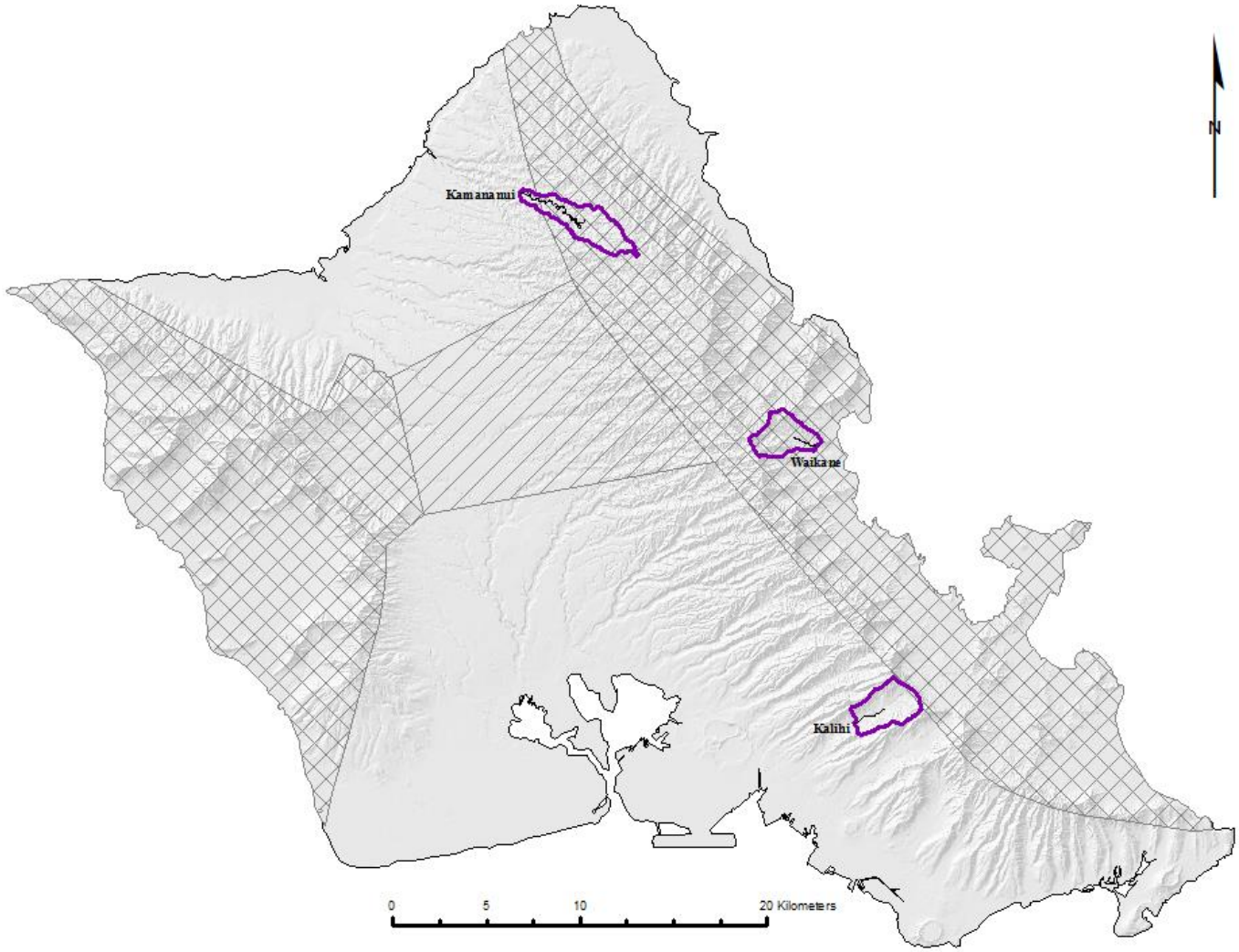

Figure 16. Map of O‘ahu displaying all of the drainage basins analyzed in this thesis. The three currently gaged basins used in this study are outlined with purple. Areas of the island impounded by dikes are displayed with criss-crossed areas and areas with enigmatic groundwater occurrence are displayed with striped areas (dike outlines provided by M. Bassiouni, USGS, pers. comm. July 2014).

3.1 Hydrologic variables

The hydrologic variables used in this thesis are recession constants, low-flow values, and change in storage values.

3.1.a Recession Constants, k

The recession constant is the rate at which stream flow decreases as the stream is being recharged (Vogel and Kroll, 1996). The lithology and aquifer properties of the drainage basins, therefore, influence the recession constants. The recession constant, *k*, is derived from the discharge equation $Q = Q_o e^{-\alpha t}$ (Equation 1), where $k = e^{-\alpha}$ (Equation 2) (Thomas et al., 2013). High recession constants typically correspond to settings of lower permeability, by causing the groundwater to discharge steadily into the stream network (Delwyn Oki, USGS, pers.comm. March 2015). In this study, streams with recession constants greater than 0.95 were typically set in watersheds with at least 50% of its area impounded by less-permeable dikes (Table 1). Low recession constants typically correspond to settings of higher permeability, causing the groundwater to discharge rapidly into the stream network and sometimes reducing the flow to zero. In this study, streams with recession constants less than 0.95 were typically set in watersheds with less than 50% of its area impounded by less-permeable dikes (Table 1). Related to that assessment, very low recession constants that are less than 0.90 correlated with intermittent streams (Table 1). Since intermittent streams are seasonal and therefore only flow during certain times of the year (Bierman and Montgomery, 2014), the groundwater quickly discharges from the stream and drops to zero. This is most likely caused by a change in hydraulic conductivity and a difference in the ability of the aquifer's subsurface to transmit water (Bierman and Montgomery, 2014), resulting in a very low recession constant. The recession constants alone are useful for water resource management because they can differentiate between perennial and intermittent streams. In the case of potential water resources, intermittent streams are much less desirable due to the low discharge and baseflow expected from the stream.

Table 1. Calculated hydrologic variables for gaged and ungaged streams on Maui and Oʻahu. Hydrologic variables include recession constant (k), alpha value (α), low-flow value (Q_{95}), the percent of time water flows in a stream, average annual precipitation (P), average annual discharge (Q), average annual evapotranspiration (ET), and change in storage (ΔS). Dike-impoundment indicates what percent of the drainage basin is impounded by dikes and years used indicates the years used to calculate P, Q, ET, and ΔS.

	Stream	USGS ID	Dike-impoundment (%)	k	α	Q_{95} (cfs)	P (in^3/yr)	Q (in^3/yr)	ET (in^3/yr)	ΔS (in^3/yr)	Years used for P, Q, ET, ΔS
Currently gaged Maui streams	Honokōhau	16620000	100	0.962	0.039	11	4.82E+15	2.08E+12	7.16E+14	4.10E+15	‘78-‘07
	Kahakuloa	16618000	100	0.957	0.044	4	1.72E+15	9.50E+11	4.66E+14	1.25E+15	‘78-‘07
	Waiheʻe	16614000	100	0.982	0.018	33	5.37E+15	3.84E+12	9.28E+14	4.44E+15	‘78-‘07
	ʻĪao	16604500	100	0.956	0.045	16	9.33E+15	3.34E+12	1.82E+15	7.51E+15	‘78-‘07
	Honopou	16587000	0	0.943	0.059	0.47	6.22E+13	2.54E+11	1.93E+13	4.27E+13	‘78-‘07
	Waikamoi	16552800	96.87	0.855	0.157	1.65	6.38E+14	1.00E+11	2.61E+14	3.77E+14	‘78-‘07
	West Wailuaiki	16518000	5.55	0.930	0.073	2.2	2.42E+15	1.81E+12	4.28E+14	1.99E+15	‘78-‘07
	Hanawi	16508000	18.05	0.956	0.045	2.2	3.58E+15	1.26E+12	4.99E+14	3.08E+15	‘78-‘07
	ʻOheʻo	16501200	36.01	0.845	0.167	0.44	2.14E+16	2.74E+12	2.98E+15	1.84E+16	‘78-‘07
Ungaged southern Maui streams	Kahoma	16638500	69.45	-	-	-	-	-	-	-	-
	Malalowaiaole	16647500	0	-	-	-	-	-	-	-	-
	Kealia	-	2.436	-	-	-	-	-	-	-	-
	Unnamed	16664200	0	-	-	-	-	-	-	-	-
Ungaged northern Maui streams	South Waiehu	205426156313601	100	-	-	-	-	-	-	-	-
	Honolua	16623000	100	-	-	-	-	-	-	-	-
	Makapipi	16507000	0	-	-	-	-	-	-	-	-
	Kawaipapa	16502900	44.66	-	-	-	-	-	-	-	-
	Koʻolau	16523000	48.17	-	-	-	-	-	-	-	-
Currently gaged Oahu streams	Kalihi	16229000	3.626	0.938	0.064	0.68	1.42E+15	3.41E+11	6.31E+14	7.90E+14	‘78-‘07
	Kamananui	16325000	91.17	0.830	0.187	0.01	1.65E+15	5.36E+11	5.28E+14	1.12E+15	‘78-‘07
	Waikāne	16294900	100	0.979	0.021	3.8	1.11E+15	5.88E+11	3.80E+14	7.28E+14	‘78-‘07

3.1.b Low-flow Values, Q_{95}

Low-flow values are defined as Q_{95} values, the discharge at which the stream flow is expected to exceed 95% of the time. In the case of water resources, higher Q_{95} values would be most desirable because they indicate that the stream has an overall larger discharge. I found that the drainage basins that are completely impounded by dikes had the highest Q_{95} values compared to the drainage basins that were only partially impounded by dikes (Table 1 and Figure 17). The Q_{95} values were generally positively correlated to the recession constants (Figure 18), which will be further addressed in the discussion.

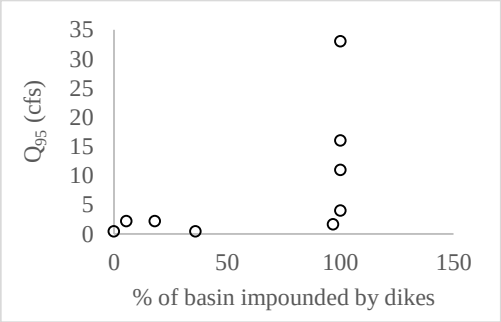

Figure 17. Plot comparing percent of basin impounded by dikes to low-flow value, Q_{95}.

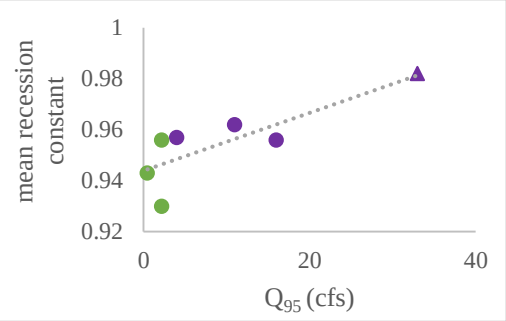

Figure 18. Plot comparing low-flow value, Q_{95}, to mean recession constant. Note the general positive trend. Purple markers indicate streams where k>0.95. Green markers indicate streams where k<0.95. Triangle marker is Waiheʻe stream.

3.1.c Change in Storage, ΔS

The change in storage of a drainage basin is the difference of the watershed's precipitation, discharge, and evapotranspiration (Equation 4). This value indicates how much water is lost to factors other than discharge and evapotranspiration, such as reservoirs, soil, lakes, etc. (Fetter, 2000). A larger change in storage value would not be ideal for water resource purposes because that indicates a lot of water is lost before it is able to drain to gage sites. ΔS values for Maui streams were generally positively correlated to both the recession constant and Q_{95} values (Table 1). The ΔS values, however, did not have strong correlations to the percent of the basin that is impounded by dikes (Figure 19). The ΔS values were generally positively correlated to the recession constants (Figure 20), which will be further addressed in the discussion.

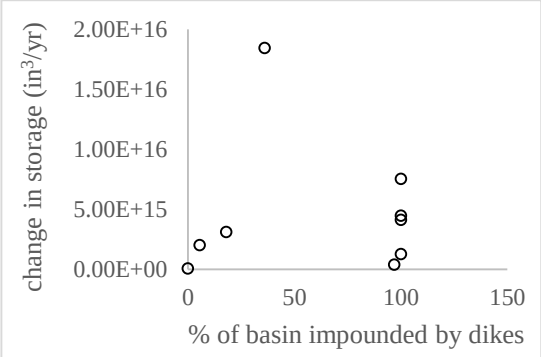

Figure 19. Plot comparing percent of basin impounded by dikes to change in storage, ΔS.

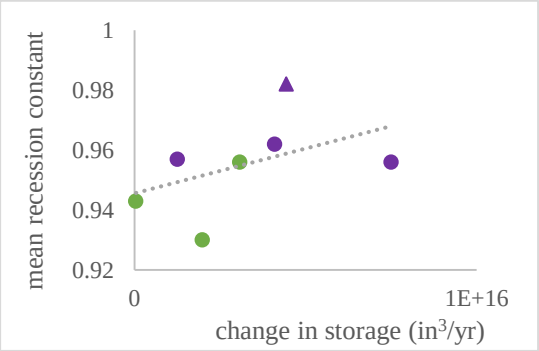

Figure 20. Plot comparing change in storage value, ΔS, to mean recession constant. Note the general positive trend.

3.2 Geomorphic Variables

Drainage density, hypsometric integral, and concavity index were the geomorphologic variables used in this thesis. Unlike the hydrologic variables, streamflow gaging stations are not needed to calculate geomorphic characteristics. The geomorphologic variables can instead be calculated with the DEM in ArcMap. Therefore, the three geomorphologic variables were calculated for both the gaged and ungaged watersheds on the island of Maui (Table 2).

3.2.a Drainage Density

The drainage density informs us of how much a watershed is cut by stream channels and how well the watershed is drained by the stream network (Bierman and Montgomery, 2014). Drainage densities are calculated by dividing the total channel length by the total drainage area; high drainage densities indicate relatively evolved basins that are cut by numerous streams which drain the basin well, while low drainage densities indicate relatively young basins that do not contain many stream channels (Bierman and Montgomery, 2014). Note that drainage densities do not correlate with the percent of the drainage basin that is impounded by dikes (Figure 21).

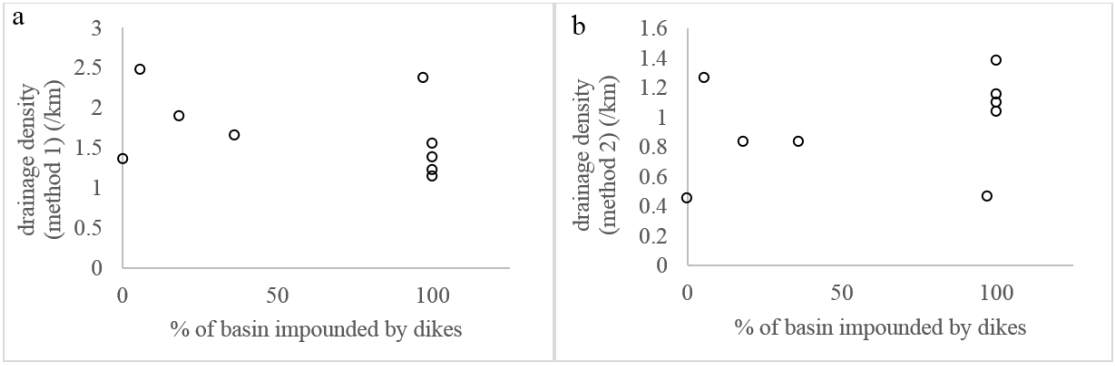

Figure 21. Plots comparing percent of drainage basin impounded by dikes and drainage density. (a) Drainage densities calculated with Method 1. (b) Drainage densities calculated with Method 2.

Table 2. Calculated geomorphologic variables for gaged and ungaged streams on Maui and O‘ahu. Geomorphological variables include drainage basin area (km^2), stream length (km), stream order (Strahler method), drainage density (dd), hypsometric integral (Hyps.Int.), and concavity index (θ). Dike-impoundment indicates what percent of the drainage basin is impounded by dikes. Stream length and drainage density are reported twice, based on the method used to determine cell accumulation threshold.

	Stream	USGS ID	Dike-imp (%)	Basin area (km^2)	Stream length Method 1 (km)	Stream length Method 2 (km)	Stream order	dd Method 1 (/km)	dd Method 2 (/km)	Hyps.Int. (dimension-less)	-θ
Currently gaged Maui streams	Honokōhau	16620000	100	11.07	13.49	11.46	2	1.23	1.04	0.448	-0.532
	Kahakuloa	16618000	100	8.92	14.09	9.95	2	1.57	1.11	0.461	-0.425
	Waihe‘e	16614000	100	11.09	12.80	12.8	3	1.16	1.16	0.402	-0.485
	‘Īao	16604500	100	15.84	22.2	22.2	3	1.39	1.39	0.354	-0.442
	Honopou	16587000	0	1.53	2.71	0.91	1	1.36	0.45	0.545	0.448
	Waikamoi	16552800	96.87	6.43	14.35	2.83	3	2.39	0.47	0.545	-0.208
	West Wailuaiki	16518000	5.55	9.21	22.36	11.48	3	2.48	1.28	0.420	-0.397
	Hanawi	16508000	18.05	10.92	20.90	9.26	3	1.90	0.84	0.495	-0.41
	‘Ohe‘o	16501200	36.01	22.32	36.46	18.53	3	1.66	0.84	0.440	-0.29
Ungaged southern Maui streams	Kahoma	16638500	69.45	13.16	23.15	15.75	2	1.76	1.18	0.454	-0.601
	Malalowaiaole	16647500	0	1.66	3.13	3.13	1	1.89	1.89	0.467	-0.273
	Kealia	-	2.436	58.5	134.76	99.46	3	2.30	1.7	0.215	-1.048
	Unnamed	16664200	0	9.31	21.68	5.62	3	2.33	0.60	0.350	-0.379
Ungaged northern Maui streams	South Waiehu	205426156313601	100	2.63	3.11	3.11	1	1.18	1.18	0.376	-0.784
	Honolua	16623000	100	4.85	7.61	7.61	2	1.57	1.57	0.432	-0.167
	Makapipi	16507000	0	4.82	9.84	6.70	2	2.04	1.39	0.380	-0.546
	Kawaipapa	16502900	44.66	16.18	28.92	12.82	3	1.79	0.79	0.484	-0.262
	Ko‘olau	16523000	48.17	38.74	62.53	22.85	4	1.61	0.59	0.492	-0.206
Currently gaged Oahu streams	Kalihi	16229000	3.626	6.64	1.98	1.98	1	0.298	0.298	0.328	-1.465
	Kamananui	16325000	91.17	8.12	7.51	7.51	1	0.924	0.924	0.440	-0.309
	Waikāne	16294900	100	5.79	1.56	1.56	1	0.270	0.270	0.298	-2.097

3.2.b Hypsometric Integral

The hypsometric integral indicates the degree of erosion of a drainage basin as well as the processes and factors controlling the formation of the basin (Sarp et al., 2011), while also describing the development stages of the watershed and its proneness to erosion processes (Singh, 2008). It indicates the amount of land mass found at different elevations; high hypsometric integrals are typical of younger basins, and low hypsometric integrals are typical of older basins (Bierman and Montgomery, 2014). When drainage densities and hypsometric integrals were plotted against each other (Figure 22), the relationships between the two variables differed depending on the method used to determine the stream network of the watersheds. When drainage densities were calculated with Method 1 (whole-island stream network), they were positively correlated with the hypsometric integrals (Figure 22a). When drainage densities were calculated with Method 2 (watershed-specific stream networks), they were inversely correlated (Figure 22b), just as was found by Bloomfield et al. (2011). This relationship is as expected, due to the nature of hypsometric integrals explained earlier.

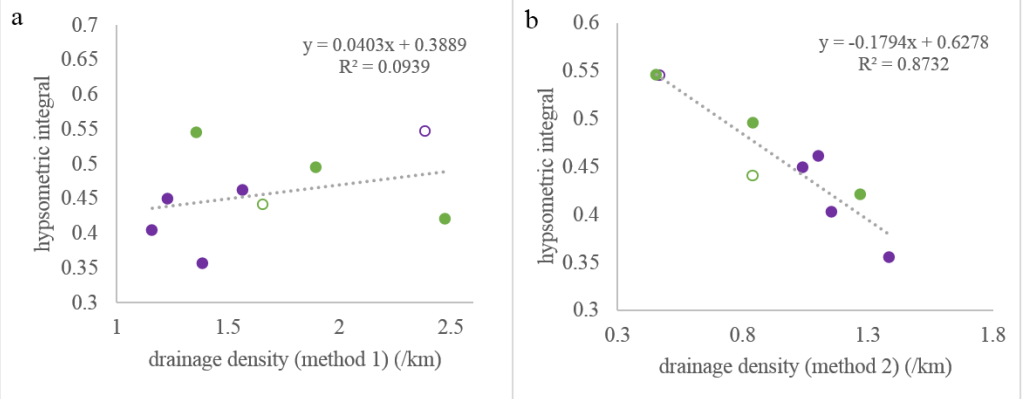

Figure 22. Plots comparing drainage density against hypsometric integral. (a) Drainage densities calculated with Method 1 stream networks. (b) Drainage densities calculated with Method 2 stream networks. Purple markers are streams with at least 50% of its watershed impounded by dikes. Green markers are streams with less than 50% of its watershed impounded by dikes. Open markers (both purple and green) are intermittent streams.

3.2.c Concavity Index

Concavity index values reflect the surface processes that are believed to have formed the stream and/or watershed (Bierman and Montgomery, 2014). Lower concavity indices (<0.3) reflect steeper headwaters and debris flows; medium concavity indices (0.3 – 0.7) reflect streams that are typically dominated by fluvial incision; high concavity indices (>0.7) typically reflect alluvial rivers (Bierman and Montgomery, 2014). When concavity indices were plotted against Method 2

drainage densities and hypsometric integrals (Figure 23), the concavity indices were generally inversely correlated to drainage densities and positively correlated to hypsometric integrals. The different correlations are as expected based on the inverse relationship found between drainage density and hypsometric integrals (Figure 22b). My data displays negative concavity index values because my stream profiles are all concave rather than convex (except for the anomaly, Honopou, which has been omitted from the graphs). The more negative the concavity values are, the more concave the stream profiles are. If streams are more concave, the drainage basins are potentially more eroded than convex streams, which I propose result in higher drainage densities, explaining the inverse relationship between negative concavity indices and drainage densities as seen in Figure 23a.

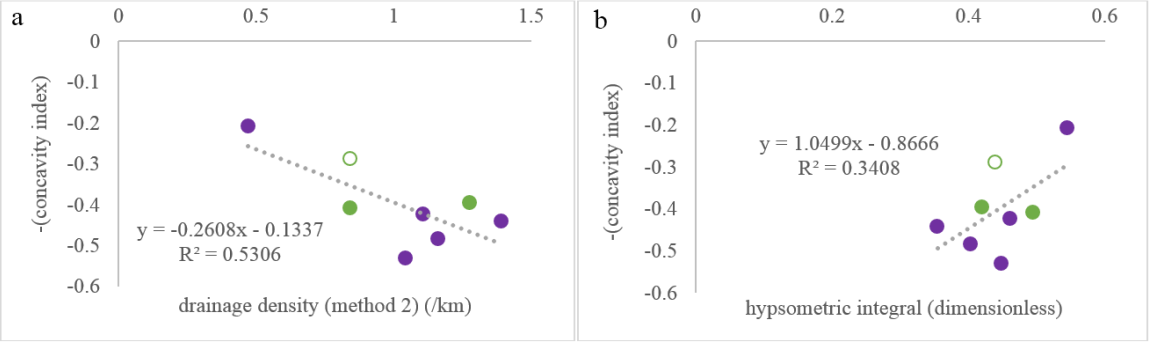

Figure 23. Plots comparing concavity indices against drainage density and hypsometric integral. (a) Concavity indices plotted against Method 2 drainage densities. (b) Concavity indices plotted against hypsometric integrals. In both graphs, Honopou stream has been omitted because it is the only convex stream with a positive concavity index value.

3.3 Comparisons between hydrologic and geomorphologic variables

The hydrologic and geomorphologic variables calculated from Table 1 and 2 were compared to determine if they share relationships that could potentially predict streamflow conditions.

The relationship between drainage densities and mean recession constants of the nine currently gaged streams on Maui differed depending on the method used to determine the stream network and drainage density. When a general stream network was created for the entire island, drainage densities had an inverse relationship with recession constants (Figure 24a, 24b). When stream networks were created for each watershed, drainage densities had a positive relationship with recession constants (Figure 24c, 24d). These relationships will be analyzed further in the discussion section.

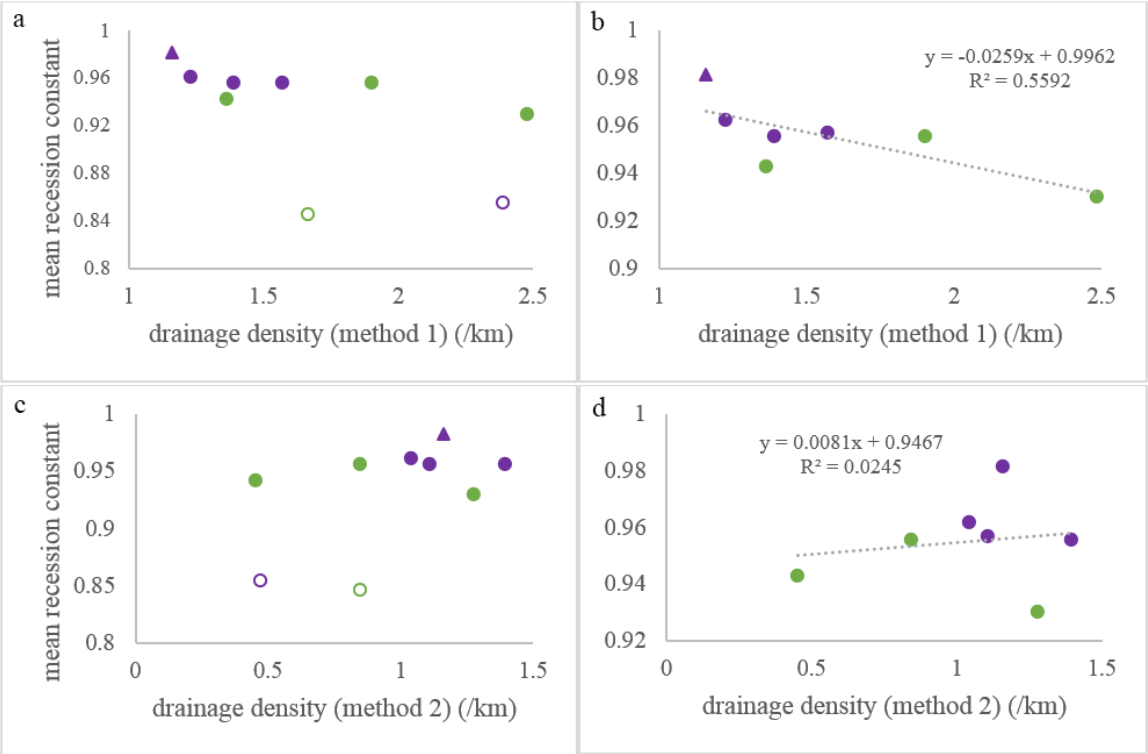

Figure 24. Plots comparing drainage density to mean recession constants. (a) Plot comparing drainage densities calculated with Method 1 stream networks to mean recession constants of nine currently gaged streams on Maui. Note that the drainage density is generally inversely correlated to the recession constant, with Waikamoi Stream (open purple circle) and ʻOheʻo Gulch (open green circle) as the anomalies. (b) Plot comparing Method 1 drainage densities to mean recession constants of perennial streams with best-fit line. (c) Plot comparing Method 2 drainage densities to mean recession constants of nine currently gaged streams on Maui. (d) Plot comparing Method 2 drainage densities to mean recession constants of perennial streams with best-fit line.

The recession constants were also compared to the concavity indices and hypsometric integrals to determine the relationships between the variables. Recession constants and concavity indices were found to have an inverse relationship and were generally divided by how much of the basin is impounded by dikes (Figure 25). Basins with at least 50% of its area impounded by dikes had lower concavity indices and basins with less than 50% of its area impounded by dikes had higher concavity indices. The main outlier is Honopou because it was the only stream with a positive concavity index, reflecting the convex shape of the stream profile. An inverse correlation was also found between the recession constants and hypsometric integrals (Figure 26). When the low-flow values were plotted against the hypsometric integrals, an inverse correlation was also found (Figure 27).

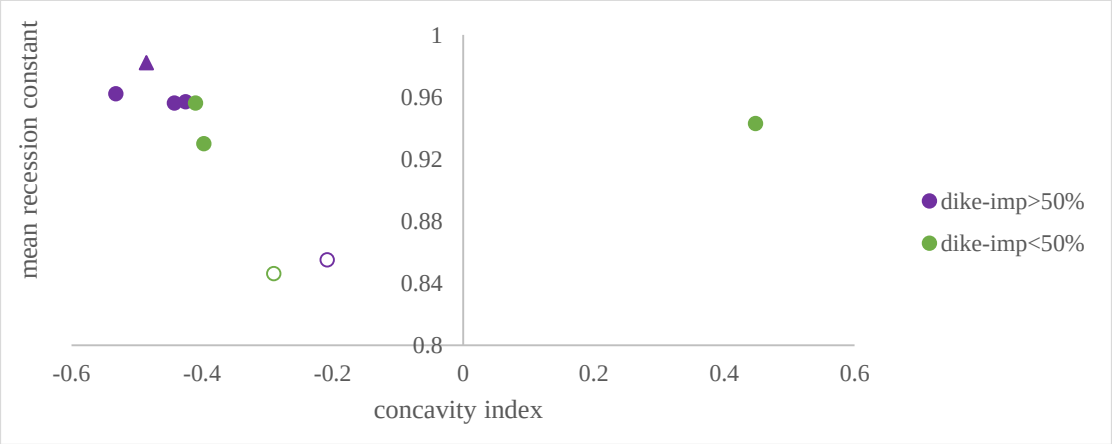

Figure 25. Plot comparing concavity indices to mean recession constants. Note that the concavity indices are inversely proportional to the recession constants, except for Honopou, which has a positive concavity index because the stream's profile is convex. Open markers (both purple and green) are intermittent streams.

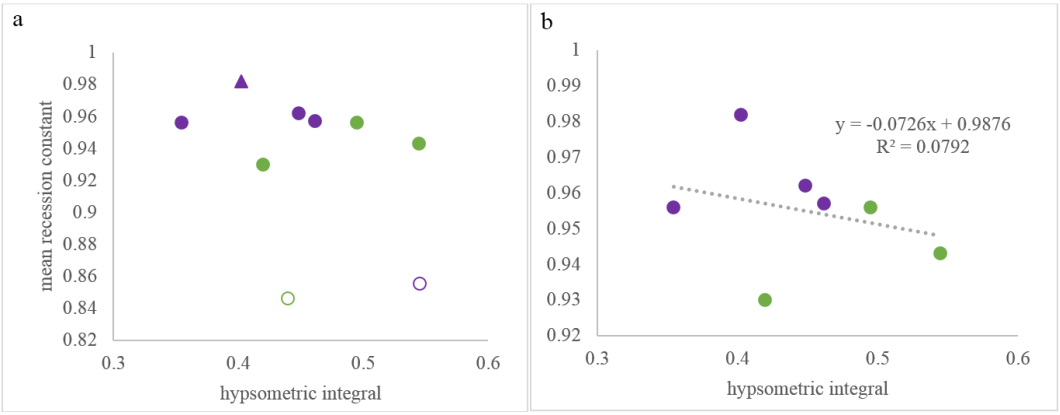

Figure 26. Plots comparing hypsometric integrals to mean recession constants. (a) Plot including the two intermittent streams. Note that the hypsometric integrals are slight inversely proportional to the recession constant, with Waikamoi Stream (open purple circle) and ʻOheʻo Gulch (open green circle) as the anomalies. Purple markers are streams with at least 50% of its watershed impounded by dikes. Green markers are streams with less than 50% of its watershed impounded by dikes. Open markers (both purple and green) are intermittent streams. (b) Plot comparing hypsometric integrals to mean recession constants of perennial streams with best-fit line.

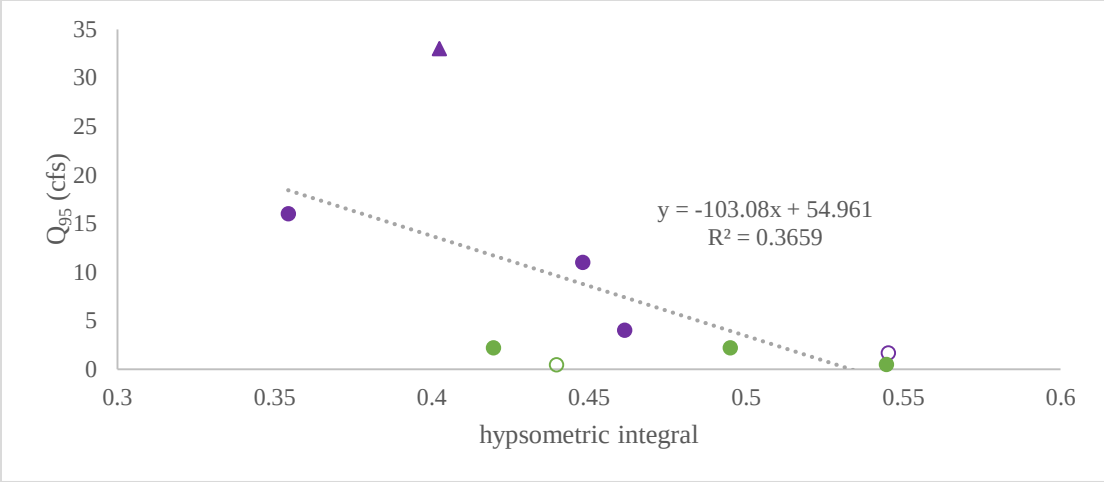

Figure 27. Plot comparing hypsometric integrals to Q_{95} values. Q_{95} values are considered low-flow values of streams on Maui. Note that the hypsometric integrals are inversely proportional to the Q_{95} values. Purple markers are streams with at least 50% of its watershed impounded by dikes. Green markers are streams with less than 50% of its watershed impounded by dikes. Open markers (both purple and green) are intermittent streams.

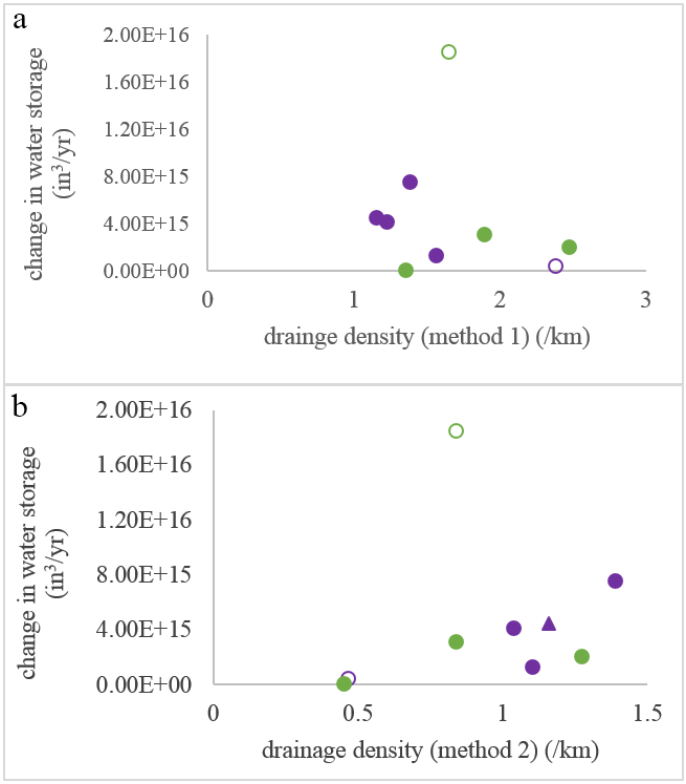

Figure 28. Plots comparing drainage density to change in water storage, ΔS. (a) Drainage densities calculated from Method 1 stream network. Note the slight inverse correlation. (b) Drainage densities calculated from Method 2 stream networks. Note the positive correlation. Purple markers are streams with at least 50% of its watershed impounded by dikes. Green markers are streams with less than 50% of its watershed impounded by dikes. Open markers (both purple and green) are intermittent streams.

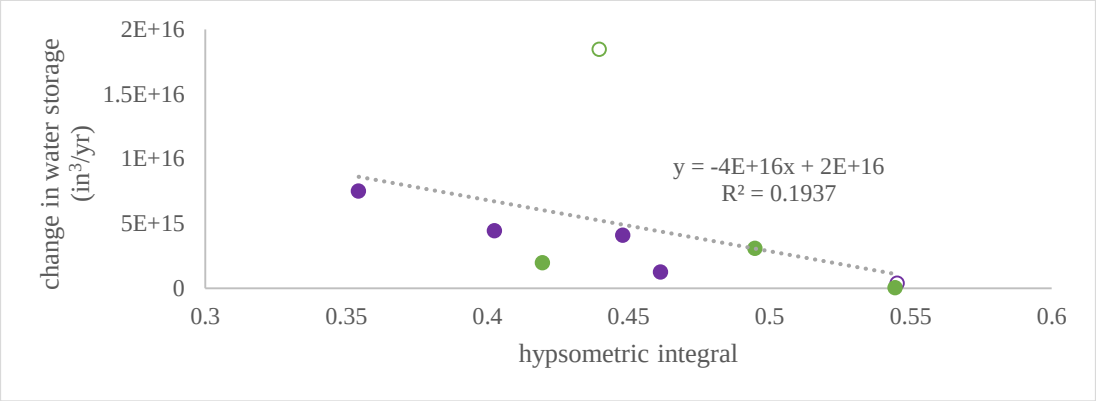

Figure 29. Plot comparing hypsometric integrals to change in water storage, ΔS. Note that the hypsometric integrals are inversely proportional to ΔS, except for ʻOheʻo Gulch (open green circle). Purple markers are streams with at least 50% of its watershed impounded by dikes. Green markers are streams with less than 50% of its watershed impounded by dikes. Open markers (both purple and green) are intermittent streams.

To predict the hydrologic values of currently ungaged streams on Maui, plots comparing drainage densities, concavity indices, and hypsometric integrals to recession constants, low-flow values, and change in storage values were fitted with 95% confidence intervals (Figure 30). The equations fit to the best-fit line and confidence intervals were used to recalculate the hydrologic variables for the currently gaged streams on Maui to evaluate the validity of the best-fit equations of each geomorphic variable. The predictions are listed in Tables 3-5.

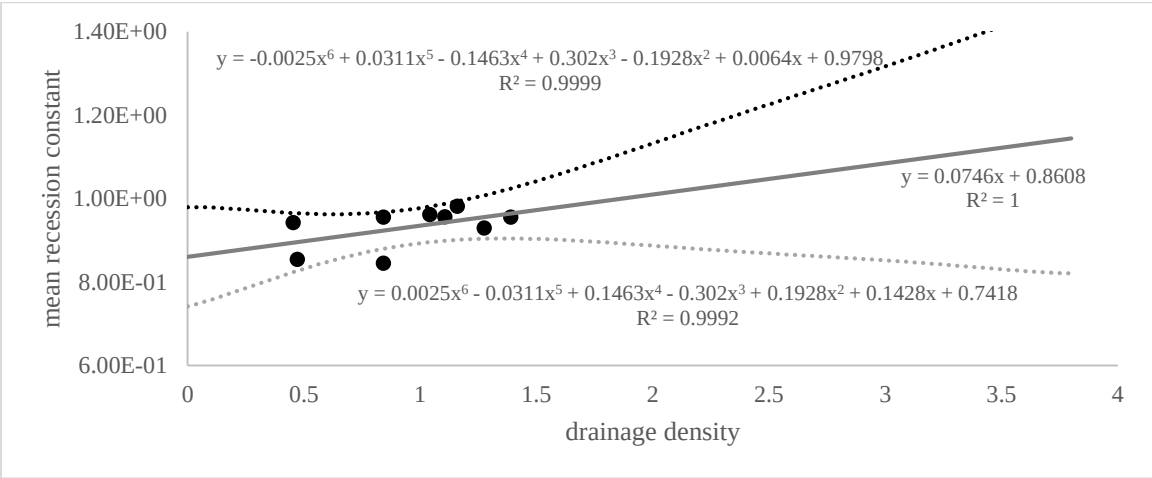

Figure 30. Plot comparing drainage density against mean recession constants and 95% confidence intervals. Black circles are the actual values from currently gaged streams on Maui. Solid grey line is the best-fit line for the actual data, dashed black line is the upper limit confidence interval calculated based on the actual data, and dashed grey line is the lower limit confidence interval calculated based on the actual data. A linear equation was fit to the best-fit line to calculate the predicted recession constants of the ungaged streams and 6-order polynomial equations were fit to the upper and lower confidence intervals to determine the error bars of the predictions. All of the confidence interval plots can be found in Appendix J.

Table 3. Predicted recession constants (along with upper and lower standard deviations) of nine currently gaged streams of Maui, four ungaged streams of southern Maui, and five ungaged streams of northern Maui. Predicted recession constants were computed from best-fit line equation based on three different geomorphological variables (drainage density, concavity index, and hypsometric integral). Upper and lower recession constants were computed from 95% confidence interval equations. Recession constants are dimensionless.

				Drainage Density method			Concavity Index method			Hypsometric Integral method		
	Stream	USGS ID	Actual k	Predicted k	Upper SD	Lower SD	Predicted k	Upper SD	Lower SD	Predicted k	Upper SD	Lower SD
Gaged Streams	Honokōhau	16620000	0.962	0.939	0.981	0.896	0.991	1.016	0.965	0.934	0.985	0.883
	Kahakuloa	16618000	0.957	0.943	0.988	0.988	0.942	0.961	0.924	0.931	0.982	0.880
	Waiheʻe	16614000	0.982	0.947	0.994	0.944	0.969	0.991	0.948	0.947	1.004	0.889
	ʻĪao	16604500	0.956	0.964	1.024	0.905	0.950	0.969	0.931	0.960	1.034	0.884
	Honopou	16587000	0.943	0.895	0.966	0.966	0.549	0.203	0.894	0.908	0.978	0.838
	Waikamoi	16552800	0.855	0.896	0.965	0.965	0.845	0.882	0.807	0.908	0.978	0.837
	West Wailuaiki	16518000	0.93	0.956	0.956	0.904	0.930	0.948	0.911	0.942	0.996	0.888
	Hanawi	16508000	0.956	0.924	0.968	0.880	0.936	0.954	0.917	0.922	0.976	0.867
	ʻOheʻo	16501200	0.846	0.924	0.968	0.880	0.881	0.907	0.856	0.937	0.988	0.885
Southern Ungaged Streams	Kahoma	16638500	-	0.949	0.996	0.902	1.022	1.056	0.987	0.933	0.984	0.882
	Malalowaiaole	16647500	-	1.002	1.111	0.892	0.874	0.902	0.846	0.929	0.980	0.878
	Kealia	-	-	0.988	1.077	0.899	1.223	1.336	1.111	0.997	1.160	0.835
	Unnamed	16664200	-	0.906	0.963	0.849	0.768	0.832	0.704	0.961	1.038	0.883
Northern Ungaged Streams	South Waiehu	205426156313601	-	0.949	0.996	0.902	1.104	1.169	1.039	0.954	1.020	0.888
	Honolua	16623000	-	0.978	1.053	0.902	0.826	0.871	0.781	0.939	0.991	0.886
	Makapipi	16507000	-	0.964	1.024	1.024	0.997	1.024	0.970	0.953	1.018	0.888
	Kawaipapa	16502900	-	0.920	0.965	0.965	0.869	0.898	0.839	0.924	0.977	0.872
	Koʻolau	16523000	-	0.905	0.963	0.963	0.844	0.882	0.805	0.922	0.977	0.868

Table 4. Predicted low-flow values, Q_{95}, (along with upper and lower standard deviations) of nine currently gaged streams of Maui, four ungaged streams of southern Maui, and five ungaged streams of northern Maui. Predicted Q_{95} values were computed from best-fit line equation based on three different geomorphological variables (drainage density, concavity index, and hypsometric integral). Upper and lower Q_{95} values were computed from 95% confidence interval equations. Q_{95} values are in cfs units.

				Drainage Density method			Concavity Index method			Hypsometric Integral method		
	Stream	USGS ID	Actual Q_{95}	Predicted Q_{95}	Upper SD	Lower SD	Predicted Q_{95}	Upper SD	Lower SD	Predicted Q_{95}	Upper SD	Lower SD
Gaged Streams	Honokōhau	16620000	11	9.376	18.922	-0.171	17.183	31.636	2.669	8.779	18.515	-0.960
	Kahakuloa	16618000	4	10.456	20.333	0.578	10.467	21.054	-0.150	7.402	17.132	-2.329
	Waiheʻe	16614000	33	11.367	21.667	1.067	14.233	26.267	2.154	13.472	24.499	2.443
	ʻĪao	16604500	16	15.250	28.632	1.867	11.534	22.328	0.705	18.436	32.796	4.074
	Honopou	16587000	0.47	-0.542	15.275	-16.36	-44.339	-241.324	152.681	-1.172	12.257	-14.604
	Waikamoi	16552800	1.65	-0.258	15.170	-15.69	-3.153	18.527	-24.836	-1.248	12.241	-14.740
	West Wailuaiki	16518000	2.2	13.309	24.910	1.707	8.710	19.318	-1.924	11.712	22.030	1.392
	Hanawi	16508000	2.2	5.999	15.792	-3.794	9.526	20.067	-1.043	3.945	14.409	-6.521
	ʻOheʻo	16501200	0.44	5.999	15.792	-3.794	1.994	16.815	-12.837	9.639	19.467	-0.190
Southern Ungaged Streams	Kahoma	16638500	-	11.756	22.273	1.238	21.514	41.115	1.826	8.210	17.923	-1.505
	Malalowaiaole	16647500	-	23.640	48.151	-0.872	0.927	16.964	-15.118	6.866	16.639	-2.909
	Kealia	-	-	20.483	40.380	0.585	49.570	113.279	-14.600	32.825	63.849	1.798
	Unnamed	16664200	-	1.965	14.686	-10.756	-13.829	22.647	-50.306	18.930	33.719	4.140
Northern Ungaged Streams	South Waiehu	205426156313601	-	11.737	22.243	1.230	33.000	69.818	-4.011	16.248	28.910	3.584
	Honolua	16623000	-	18.246	35.120	1.373	-5.726	19.996	-31.451	10.448	20.422	0.472
	Makapipi	16507000	-	15.233	28.598	1.868	18.062	33.424	2.634	15.832	28.211	3.451
	Kawaipapa	16502900	-	5.155	15.326	-5.016	0.236	17.126	-16.660	5.038	15.154	-5.081
	Koʻolau	16523000	-	1.744	14.703	-11.216	-3.278	18.594	-25.154	4.279	14.626	-6.069

Table 5. Predicted change in storage, ΔS, (along with upper and lower standard deviations) of nine currently gaged streams of Maui, four ungaged streams of southern Maui, and five ungaged streams of northern Maui. Predicted ΔS values were computed from best-fit line equation based on three different geomorphological variables. Upper and lower ΔS values were computed from 95% confidence interval equations. ΔS values are in in^3/yr.

				Drainage Density method			Concavity Index method			Hypsometric Integral method		
	Stream	USGS ID	Actual ΔS	Predicted ΔS	Upper SD	Lower SD	Predicted ΔS	Upper SD	Lower SD	Predicted ΔS	Upper SD	Lower SD
Gaged Streams	Honokōhau	16620000	4.10E+15	5.13E+15	7.38E+15	6.79E+15	1.43E+16	1.15E+17	-8.6E+16	6.56E+15	2.99E+16	1.14E+15
	Kahakuloa	16618000	1.25E+15	5.32E+15	6.93E+15	7.50E+15	1.33E+16	6.91E+16	-4.1E+16	6.16E+15	2.89E+16	1.83E+15
	Waiheʻe	16614000	4.44E+15	5.48E+15	6.57E+15	8.07E+15	1.39E+16	9.21E+16	-6.3E+16	7.93E+15	3.28E+16	-8.3E+14
	ʻĪao	16604500	7.51E+15	6.17E+15	5.05E+15	1.05E+16	1.34E+16	7.48E+16	-4.7E+16	9.37E+15	3.57E+16	-2.7E+15
	Honopou	16587000	4.27E+13	6.63E+15	1.41E+16	-2.24E+15	4.52E+15	-2.49E+17	2.61E+17	3.66E+15	2.01E+16	9E+15
	Waikamoi	16552800	3.77E+14	3.41E+15	1.38 E+16	-1.91E+15	1.11E+16	4.04E+16	-1.7E+16	3.64E+15	2.0E+16	9.1E+15
	West Wailuaiki	16518000	1.99E+15	5.83E+15	5.82E+15	9.28E+15	1.30E+16	6.08E+16	-3.4E+16	7.41E+15	3.17E+16	-1.3E+14
	Hanawi	16508000	3.08E+15	4.53E+15	9.09E+15	4.28E+15	1.31E+16	6.45E+16	-3.7E+16	5.15E+15	2.61E+16	3.98E+15
	ʻOheʻo	16501200	1.84E+16	4.53E+15	9.09E+15	4.28E+15	1.19E+16	4.27E+16	-1.7E+16	6.81E+15	3.05E+16	7.45E+14
Southern Ungaged Streams	Kahoma	16638500	-	5.55E+15	6.42E+15	8.32E+15	1.50E+16	1.59E+17	-1.3E+17	6.39E+15	2.95E+16	1.42E+15
	Malalowaiaole	16647500	-	7.66E+15	-8.02E+14	1.84E+16	1.17E+16	4.15E+16	-1.7E+16	6.00E+15	2.85E+16	2.12E+15
	Kealia	-	-	7.1E+15	2.13E+15	1.47E+16	1.95E+16	7.45E+17	-7.1E+17	1.36E+16	4.51E+16	-9.4E+15
	Unnamed	16664200	-	3.81E+15	1.19E+16	5.08E+14	9.38E+15	4.92E+16	-2.8E+16	9.51E+15	3.59E+16	-2.9E+15
Northern Ungaged Streams	South Waiehu	205426156313601	-	5.55E+15	6.42E+15	8.30E+15	1.68E+16	3.27E+17	-2.9E+17	8.73E+15	3.44E+16	-1.9E+15
	Honolua	16623000	-	6.70E+15	3.60E+15	1.27E+16	1.07E+16	4.18E+16	-1.9E+16	7.05E+15	3.10E+16	3.91E+14
	Makapipi	16507000	-	6.17E+15	5.06E+15	1.05E+16	1.45E+16	1.23E+17	-9.4E+16	8.61E+15	3.41E+16	-1.7E+15
	Kawaipapa	16502900	-	4.38E+15	9.61E+15	3.56E+15	1.16E+16	4.10E+16	-1.6E+16	5.47E+15	2.71E+16	3.22E+15
	Koʻolau	16523000	-	3.77E+15	1.21E+16	2.76E+14	1.11E+16	4.04E+16	-1.7E+16	5.25E+15	2.64E+16	3.74E+15

The actual hydrologic values of the nine currently gaged streams were plotted against the predicted hydrologic values to reveal which geomorphologic variable would produce the most accurate results (Figures 31-33). For clearer visualization, the differences between the actual and predicted values can be found in Appendix K.

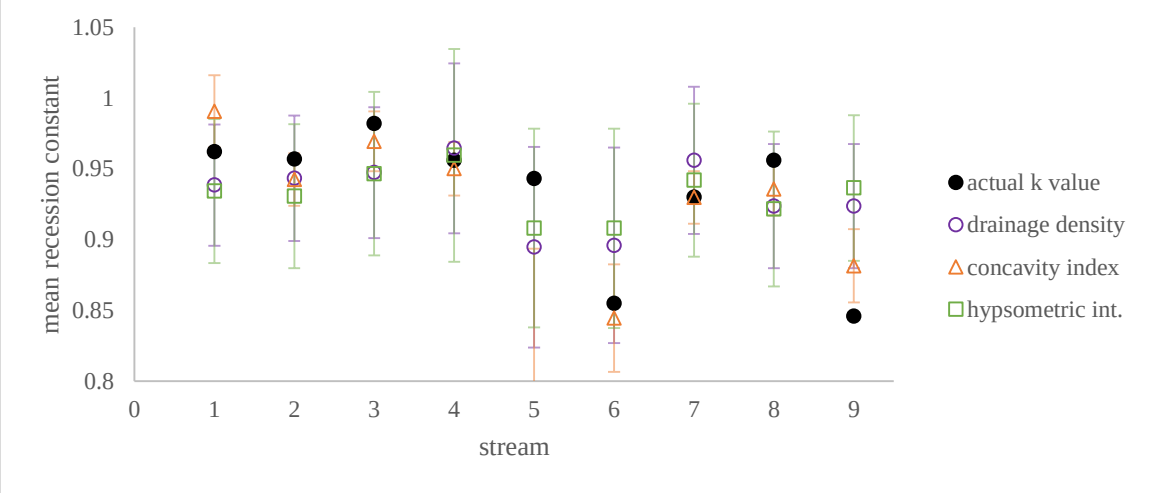

Figure 31. Plot comparing the predicted recession constants of the nine currently gaged streams on Maui. Recession constant symbology is coordinated according to the geomorphologic parameter used to compute the predicted recession constant. The predictions are compared to the actual recession constant (closed black circle) for each stream. Error bars were calculated from the 95% confidence interval equations and are color coordinated to the geomorphologic parameter. Stream data is organized in order of Table 3's gaged streams [1.Honokōhau; 2.Kahakuloa; 3.Waiheʻe; 4 ʻĪao; 5.Honopou; 6.Waikamoi; 7.West Wailuaiki; 8.Hanawi; 9. ʻOheʻo].

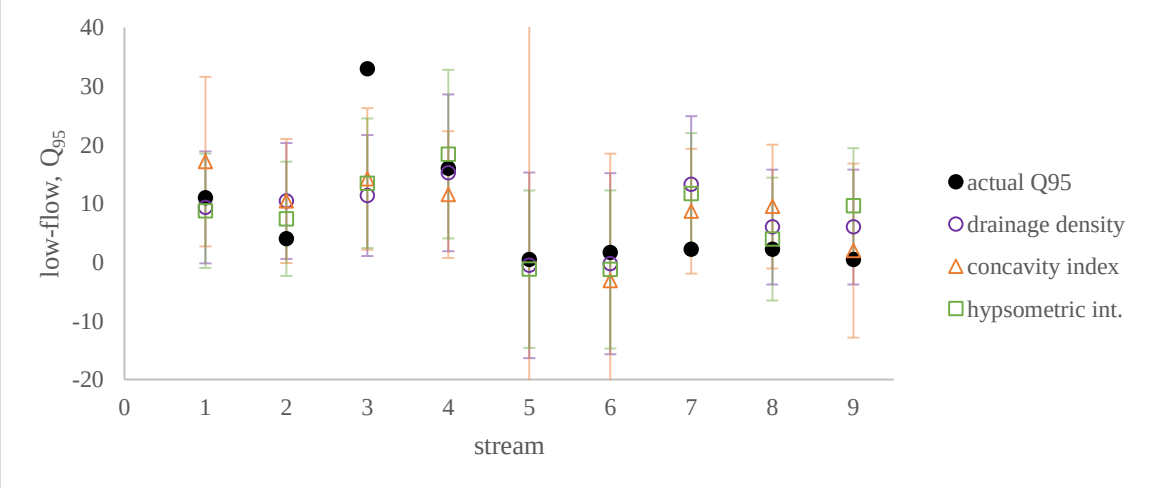

Figure 32. Plot comparing the predicted Q_{95} (low-flow) values of the nine currently gaged streams on Maui. Q_{95} symbology is coordinated according to the geomorphologic parameter used to compute the predicted Q_{95}. The predictions are compared to the actual Q_{95} (closed black circle) for each stream. Error bars were calculated from the 95% confidence interval equations and are color coordinated to the geomorphologic parameter. Stream data is organized in order of Table 4's gaged streams [1.Honokōhau; 2.Kahakuloa; 3.Waiheʻe; 4.ʻĪao; 5.Honopou; 6.Waikamoi; 7.West Wailuaiki; 8.Hanawi; 9. ʻOheʻo].

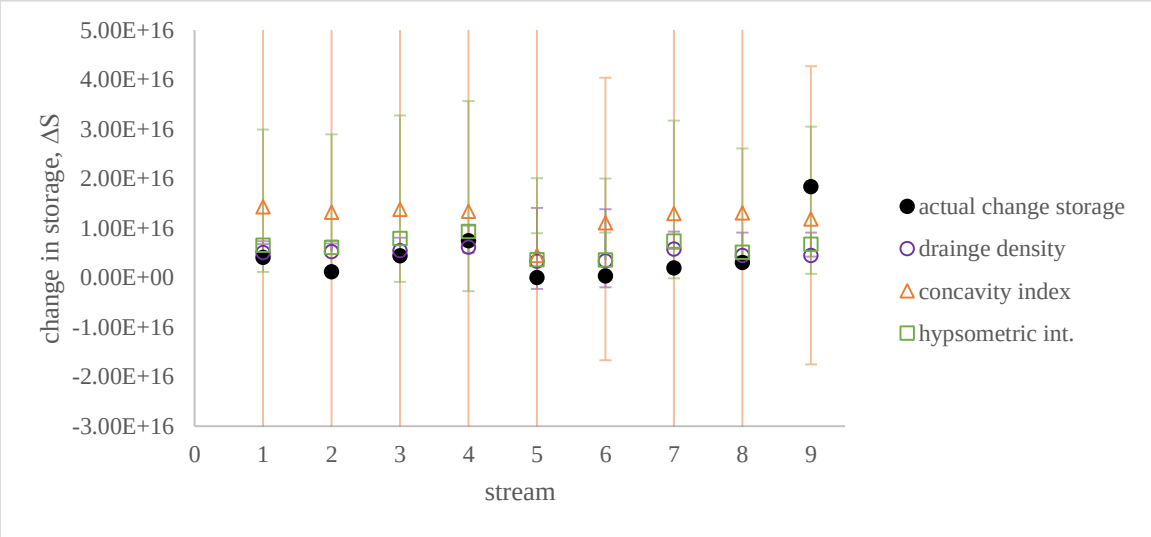

Figure 33. Plot comparing the predicted change in storage, ΔS, values of the nine currently gaged streams on Maui. ΔS symbology is coordinated according to the geomorphologic parameter used to compute the predicted ΔS. The predictions are compared to the actual ΔS (closed black circle) for each stream. Note that ΔS values predicted from drainage density and hypsometric integral variables were the closest to the actual ΔS. Error bars were calculated from the 95% confidence interval equations and are color coordinated to the geomorphologic parameter. Stream data is organized in order of Table 5's gaged streams [1.Honokōhau; 2.Kahakuloa; 3.Waiheʻe; 4.ʻĪao; 5.Honopou; 6.Waikamoi; 7.West Wailuaiki; 8.Hanawi; 9. ʻOheʻo].

I then compared the predicted recession constants, Q_{95} values, and ΔS values based on all three geomorphologic variables to determine which geomorphologic variable would produce the most accurate prediction (Figures 34-36). Figures 34-36 generally show that the predictions calculated based on drainage densities and hypsometric integrals produced similar results. In most situations, the values calculated based on concavity indices are outliers.

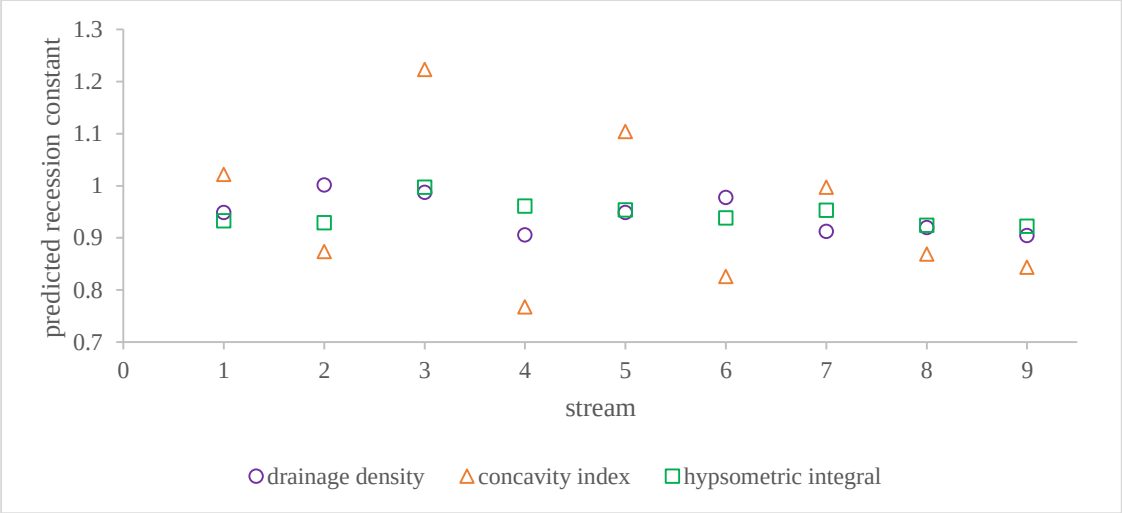

Figure 34. Plot comparing the predicted recession constants from Table 3 of the nine ungaged streams on Maui. Stream numbers along x-axis are coordinated to numeric value assigned in the table. Recession constant symbology is coordinated according to geomorphologic parameter used to compute the predicted recession constant. Note the very similar recession constant values between the drainage density and hypsometric integral predictions. Stream data is organized in order of Table 3's ungaged streams [1.Kahoma; 2.Malalowaiaole; 3.Kealia; 4.Unnamed; 5.South Waiehu; 6.Honolua; 7.Makapipi; 8.Kawaipapa; 9.Koʻolau], where streams 1-4 are on the southern side of the island and streams 5-9 are on the northern side of the island.

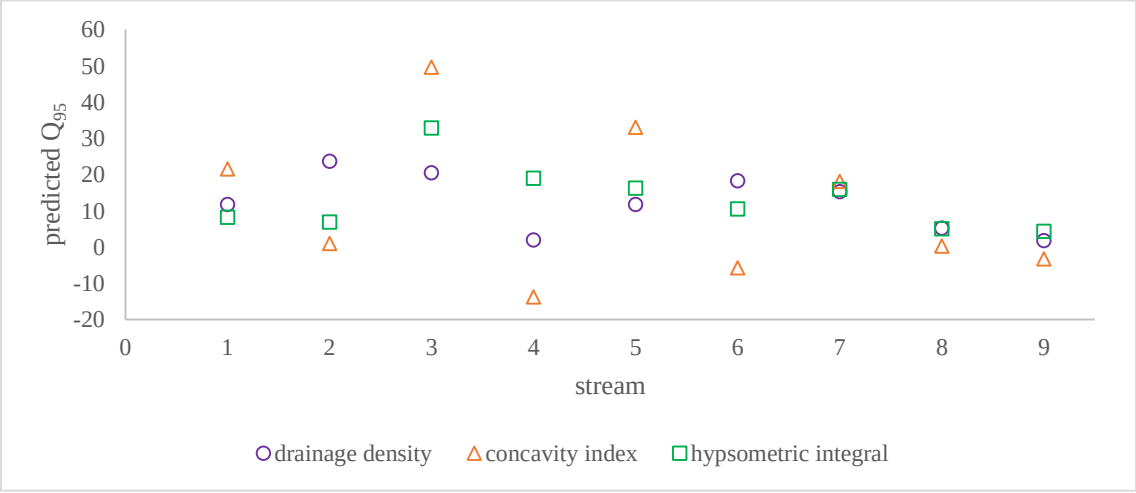

Figure 35. Plot comparing the predicted Q_{95} (low-flow) values from Table 4 of the nine ungaged streams on Maui. Stream numbers along x-axis are coordinated to numeric value assigned in the table. Q_{95} symbology is coordinated according to geomorphologic parameter used to compute the predicted recession constant. Note the general similarity in Q_{95} values between drainage density and hypsometric integral predictions. Stream data is organized in order of Table 4's ungaged streams [1.Kahoma; 2.Malalowaiaole; 3.Kealia; 4.Unnamed; 5.South Waiehu; 6.Honolua; 7.Makapipi; 8.Kawaipapa; 9.Koʻolau], where streams 1-4 are on the southern side of the island and streams 5-9 are on the northern side of the island.

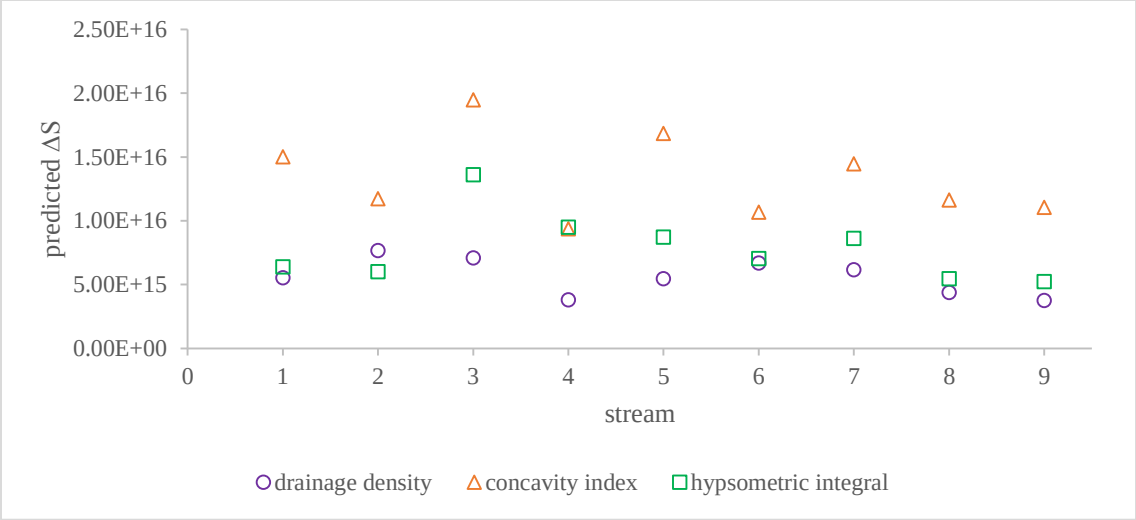

Figure 36. Plot comparing the predicted change in storage values, ΔS, from Table 5 of the nine ungaged streams on Maui. Stream numbers along x-axis are coordinated to numeric value assigned in the table. ΔS symbology is coordinated according to geomorphologic parameter used to compute the predicted recession constant. Note the general similarity in ΔS values between drainage density and hypsometric integral predictions. Stream data is organized in order of Table 5's ungaged streams [1.Kahoma; 2.Malalowaiaole; 3.Kealia; 4.Unnamed; 5.South Waiehu; 6.Honolua; 7.Makapipi; 8.Kawaipapa; 9.Koʻolau], where streams 1-4 are on the southern side of the island and streams 5-9 are on the northern side of the island.

I then carried out the same methods for three currently gaged streams on Oʻahu. The actual and predicted hydrologic values for the three streams are displayed in Table 6. The predictions calculated for each hydrologic variable based on all three geomorphologic variables are displayed in Figures 37-39. Drainage densities and hypsometric integrals from the streams on Oʻahu produced hydrologic predictions similar to those of the streams on Maui, and the concavity indices also produced predictions displayed as outliers.

Table 6. Predicted recession constants (k), low-flow values (Q_{95}), and change in storage (ΔS) values of three currently gaged streams of O'ahu. Predicted values were computed from best-fit line equation based on three different geomorphological variables (drainage density, concavity index, and hypsometric integral) of currently gaged streams on Maui. Upper and lower values were computed from 95% confidence interval equations. Recession constants are dimensionless, Q_{95} values are in cfs units, and ΔS are in in^3/yr.

			Drainage Density method			Concavity Index method			Hypsometric Integral method		
Stream	USGS ID	Actual k	Predicted k	Upper SD	Lower SD	Predicted k	Upper SD	Lower SD	Predicted k	Upper SD	Lower SD
Kalihi	16229000	0.938	1.008	1.118	0.897	1.411	2.462	0.360	0.967	1.055	0.878
Kamananui	16325000	0.830	0.973	1.040	0.907	0.890	0.914	0.866	0.936	0.988	0.885
Waikāne	16294900	0.979	1.009	1.122	0.897	1.696	23.712	-20.32	0.975	1.081	0.869
		Actual Q_{95}	Predicted Q_{95}	Upper SD	Lower SD	Predicted Q_{95}	Upper SD	Lower SD	Predicted Q_{95}	Upper SD	Lower SD
Kalihi	16229000	0.68	25.77	49.94	1.607	75.74	674.3	-524.1	21.12	38.00	4.249
Kamananui	16325000	0.01	17.68	32.22	3.133	3.186	16.81	-10.45	9.612	19.44	-0.214
Waikāne	16294900	3.80	26.14	50.74	1.541	115.4	12678	-12451	24.20	44.41	3.978
		Actual ΔS	Predicted ΔS	Upper SD	Lower SD	Predicted ΔS	Upper SD	Lower SD	Predicted ΔS	Upper SD	Lower SD
Kalihi	16229000	7.90E+14	8.40E+15	2.70E+16	-6.6E+15	2.37E+16	2.60E+18	-2.6E+18	1.02E+16	3.73E+16	-3.8E+15
Kamananui	16325000	1.12E+15	7.15E+15	2.00E+16	-8.5E+14	1.21E+16	4.45E+16	-1.9E+16	6.80E+15	3.04E+16	7.57E+14
Waikāne	16294900	7.28E+14	8.46E+15	2.73E+16	-6.8E+15	3.00E+16	2.07E+19	-2.1E+19	1.10E+16	3.92E+16	-5.2E+15

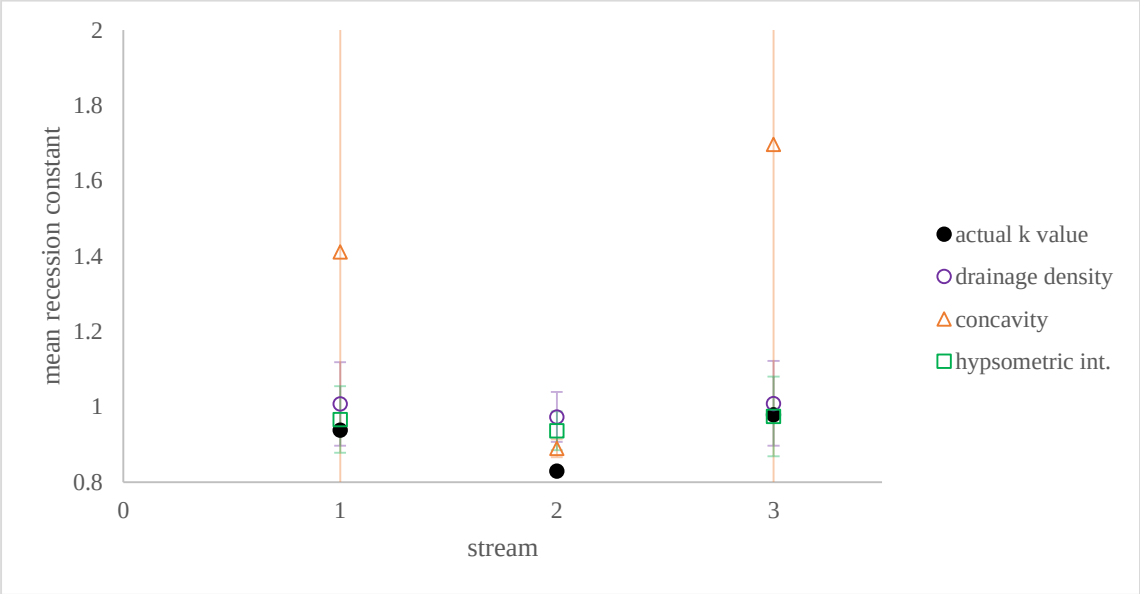

Figure 37. Plot comparing the predicted recession constants of three currently gaged streams on O‘ahu. Recession constant symbology is coordinated according to the geomorphologic parameter used to compute the predicted recession constant. The predictions are compared to the actual recession constant (closed black circle) for each stream. Error bars were calculated from the 95% confidence interval equations and are color coordinated to the geomorphologic parameter.

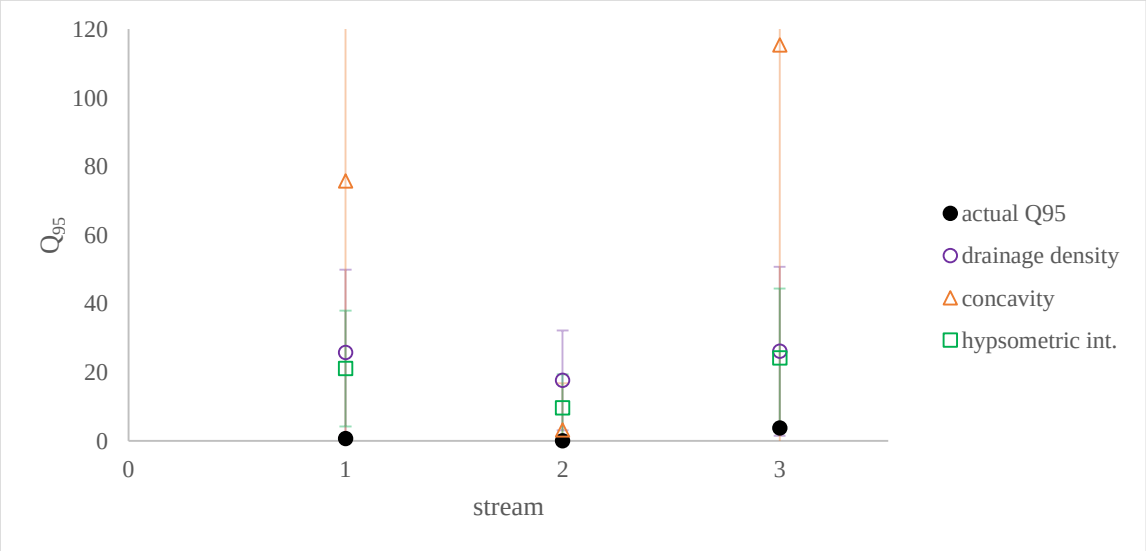

Figure 38. Plot comparing the predicted Q_{95} (low-flow) values of three currently gaged streams on O‘ahu. Q_{95} symbology is coordinated according to the geomorphologic parameter used to compute the predicted Q_{95}. The predictions are compared to the actual Q_{95} (closed black circle) for each stream. Error bars were calculated from the 95% confidence interval equations and are color coordinated to the geomorphologic parameter.

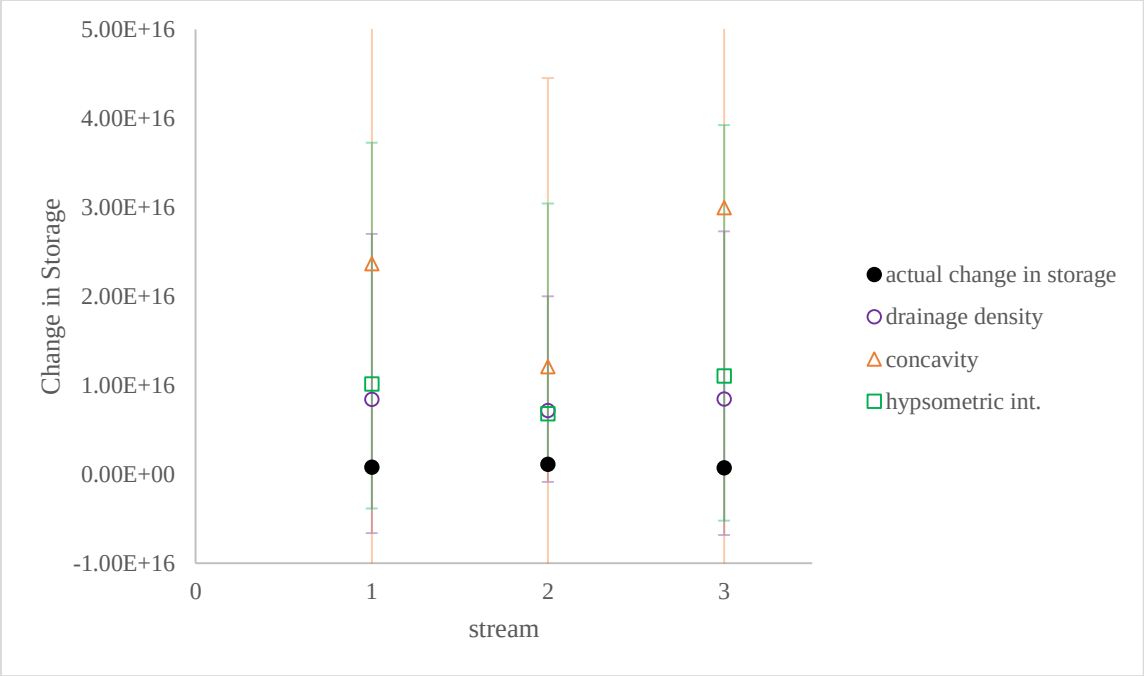

Figure 39. Plot comparing the predicted change in storage, ΔS, values of three currently gaged streams on Oʻahu. ΔS symbology is coordinated according to the geomorphologic parameter used to compute the predicted ΔS. The predictions are compared to the actual ΔS (closed black circle) for each stream. Error bars were calculated from the 95% confidence interval equations and are color coordinated to the geomorphologic parameter.

To assess my second question of whether hydrologic and/or geomorphic variables can recognize groundwater sharing between Waiheʻe and ʻĪao streams, I used the variables calculated for the first question and focused specifically on whether Waiheʻe and ʻĪao's values were particularly prominent.

Table 7. Recharge and baseflow values for the nine currently gaged streams on Maui. Note that Waiheʻe and Honopou are the only streams that have a higher baseflow value than recharge value.

Stream	Recharge (cfs)	Baseflow (cfs)	Baseflow/recharge (%)
Honokōhau	38.80	17.46	45.0
Kahakuloa	15.42	6.722	43.6
Waiheʻe	28.47	45.41	159.1
ʻĪao	35.86	27.59	76.9
Honopou	1.539	1.957	127.2
Waikamoi	7.607	0.074	0.97
West Wailuaiki	21.46	6.918	32.24
Hanawi	48.92	5.437	11.1
ʻOheʻo	94.23	2.782	2.95

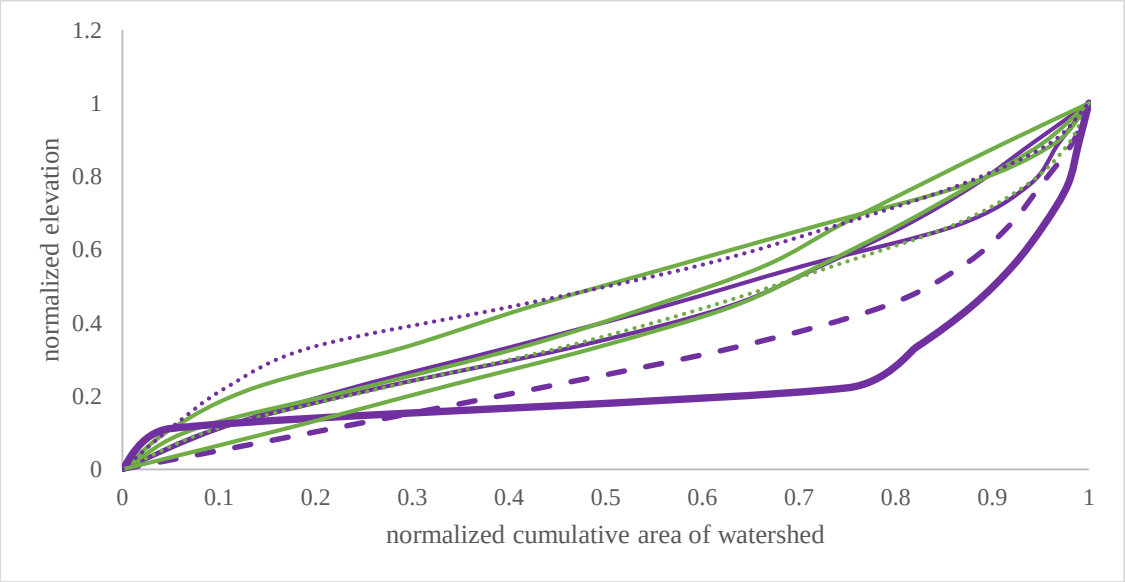

Figure 40. Hypsometric curve plot comparing normalized cumulative area of watershed against normalized elevation. Purple lines are streams that belong to watersheds with at least 50% of its area impounded by dikes. Green lines are streams that belong to watersheds with less than 50% of its area impounded by dikes. Note that Waiheʻe's hypsometric curve (bolded purple) strays away from the other curves, which are all generally clustered together. Also note that although not as drastic as Waiheʻe, ʻĪao's hypsometric curve (bolded dashed purple) lies between Waiheʻe's curve and the other curves.

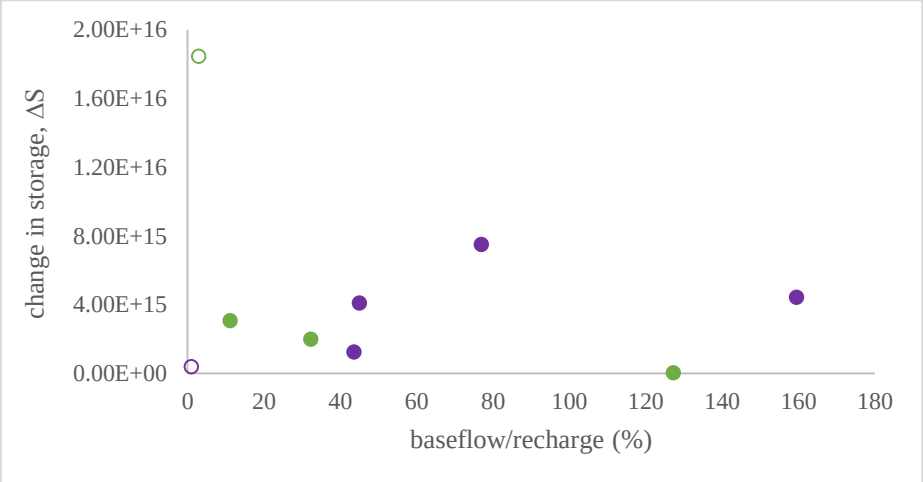

Figure 41. Plot comparing baseflow/recharge with change in storage. Note the lack of correlation between the two variables.

4. Discussion

The goal of this thesis is to use Maui as a case study to determine which streams produce the most ideal groundwater resources by analyzing relationships between hydrologic and geomorphologic variables of a watershed. This thesis then used O‘ahu as a test case to determine if this analysis can produce valid results for other islands in Hawai‘i. The geomorphologic variables used were drainage density, hypsometric integral, and concavity index. The hydrologic variables used were recession constants, low-flow values, and change in storage values.

4.1 Comparisons between hydrologic and geomorphologic variables

The three hydrologic variables were compared to the three geomorphologic variables to determine if it is possible to predict streamflow conditions based on the geomorphologic characteristics of a drainage basin. Two different methods were used to determine stream networks, and after calculating the drainage densities with both stream network methods, I realized how important the cell-accumulation threshold is while calculating the drainage density. When I used Method 1 to determine one general stream network for the entire island, some of the watersheds' drainage densities were not as realistic as they should have been. The drainage densities on the eastern side of the island were too high because the stream network included artificial streams. This is obvious when the streams were matched against the hillshade of the island (Figure 14), because streams from the stream network were laid over relatively flat land. Since the drainage densities of half the watersheds were too high, this caused a positive correlation between drainage densities and hypsometric integrals (Figure 22a). When I used Method 2 to create a stream network for individual watersheds to match the USGS's stream network, the drainage densities inversely correlated with the hypsometric integrals (Figure 22b). This inverse correlation is more logical than the relationship found with the Method 1 calculations because lower hypsometric integrals reflect relatively evolved basins while lower drainage densities reflect relatively young basins. Based on the relationships found between drainage densities and hypsometric integrals, I propose that the drainage densities created with Method 2 stream networks are the most realistic. The relationship makes sense considering the general definitions of what drainage densities and hypsometric integrals reflect (Bierman and Montgomery, 2014). This relationship also matches the relationship found between drainage densities and hypsometric integrals in a study conducted by Bloomfield et al. (2011).

The drainage densities computed with Method 1 and Method 2 stream networks were then compared to the recession constants of the streams. The drainage densities calculated with the

Method 1 stream network were inversely correlated to the recession constants of the watersheds (Figure 24a, 24b). This contradicts the relationship found by Brandes et al. (2005). However, this is because Brandes et al. (2005) defines their recession constant as α, whereas I defined my recession constant as $k = e^{-\alpha}$ (Equation 2). When my recession constants, k, were converted to α (Table 1), the recession constants and α values became inversely related, and the drainage density and α values were positively correlated, just as Brandes et al. (2005) found. The drainage densities calculated with the Method 2 stream networks were found to be positively correlated to the recession constants of the watersheds (Figure 24c, 24d), which now disagrees with Brandes et al. (2005). Despite the fact that our results are not correlated in the same way, the Brandes et al. (2005) study is set in a different location with different geologic and climatic conditions, so it is difficult to properly compare their results to mine, especially since recession constants are not influenced solely by drainage density. If the positive correlation between recession constants and drainage densities is true, then I propose the relationship could be explained as follows: higher recession constants reflect basins that are typically of lower permeability (i.e. dikes). If a basin has a lower permeability, then the water is more likely to accumulate above the material of lower permeability since it is not easily able to seep down into the ground. If more water accumulates at or near the surface, a larger volume of water exerts concentrated pressure on the surface, eroding deep incisions into the mountain slopes, and eventually creating steep valleys. The steep valleys narrow the area of the drainage basins because the volume of water is concentrated in the valleys rather than widely flowing over the basin. These narrow drainage basins are clearly identifiable in Figure 15. Since drainage density is the total stream length divided by the total drainage area, the narrowed drainage basin areas result in a higher drainage density. This indicates a positive correlation between recession constants and drainage densities, which I propose could explain the relationship seen in Figure 24c and 24d.

Concavity index values reflect the surface processes hypothesized to have formed the stream channels and drainage basins (Bierman and Montgomery, 2014). A stream's recession constant was found to be inversely related to the concavity index of the stream (Figure 25). The more negative the concavity index, the more concave the stream profile will be, whereas streams with a positive concavity index have a convex stream profile. This correlation can also be supported by the proposed interpretation explaining the relationship between recession constants and drainage densities. If a stream has a high recession constant, its basin is of lower permeability. If the basin is of lower permeability, then water is more likely to accumulate at the surface of the basin and cut deep incisions into the landscape. If this process is true, then the deep incisions would result

in stream profiles of greater concavity. Therefore, I propose that these profiles will result in lower concavity indices. This then results in an inverse correlation between recession constants and concavity indices.

Hypsometric integrals provide information of the erosional extent of a drainage basin as well as the processes and factors controlling the formation of the basin (Sarp et al., 2011). The hypsometric integral describes the development stages of the watershed and its susceptibility to erosional processes (Singh, 2008). The values also indicate the amount of land mass found at different elevations, where high hypsometric integrals are typical of younger basins and low hypsometric integrals are typical of older basins (Bierman and Montgomery, 2014). A stream's mean recession constant, *k*, and low-flow value, Q_{95}, were observed to be inversely related to the hypsometric integral of the watershed (Figure 26 and 27). The erosion of a watershed is greatly affected by surface runoff and sediment loss, which hypsometric integrals indicate (Singh, 2008). If a watershed has a high Q_{95} value, that means the watershed has a large discharge with lots of runoff. If there is more runoff, then more erosion can occur, generating a lower hypsometric integral, which is in agreement with the relationship between Q_{95} values and hypsometric integrals in Figure 27.

A stream's change in storage, ΔS, is the amount of water lost to factors other than discharge and evapotranspiration, such as reservoirs, lakes, soil, etc. (Fetter, 2000). When drainage densities were calculated with Method 1 stream networks, the drainage density was inversely correlated to a stream's change in storage, ΔS (Figure 28a). When drainage densities were calculated with Method 2 stream networks, the drainage density was positively correlated to ΔS (Figure 28b). If a watershed has a large drainage density, water is flowing over longer distances through longer streams. If water is flowing over longer distances, there are more opportunities for the water to leave the stream network and increase the ΔS value. It then makes sense, that the ΔS values are positively correlated to the drainage density of a watershed using Method 2 stream networks. If the positive correlation is true, I propose it is possible that drainage densities indicate the relative amount of ΔS of watersheds. This explanation also reinforces my belief that the drainage densities calculated with the Method 2 stream networks are most reliable.

I also found the change in storage value, ΔS, to be inversely correlated to the hypsometric integral of the watershed (Figure 29), which should be as expected since hypsometric integrals and drainage densities are inversely correlated (Figure 22b) and drainage densities and change in storage values are positively correlated (Figure 28b). As mentioned earlier, high hypsometric

integrals reflect younger basins and low hypsometric integrals reflect older, heavily eroded basins (Bierman and Montgomery, 2014). If a basin is heavily eroded, then there are potentially more reservoirs for water to escape to, therefore increasing the ΔS value. If a basin is young, it will typically have a lower stream order (Table 2). If a basin has a lower stream order, then water flows through less tributaries, therefore providing less opportunities for the water to be lost along the way. If there are fewer ways for water to be lost within the drainage basin, then I suspect the change in storage value should be lower. A watershed with a large ΔS may not be desirable for water resources because a lot of the precipitation it receives is lost before it can be collected for use. The ΔS value, of course, must be analyzed in relation to the overall amount of precipitation a watershed receives. A watershed with a high ΔS value but also a very high precipitation level could still discharge more water than a watershed with a low ΔS value and a low precipitation. Even though stream orders were calculated for these streams, they are not the most distinguishing characteristic to analyze because there was little difference between stream orders since most of the streams in the drainage basins are relatively young (Table 2).

4.2 Predicting hydrologic variables

The relationships found between the hydrologic and geomorphologic variables of the gaged streams are used to predict the unknown hydrologic variables of the ungaged streams on Maui. Each geomorphologic variable of the nine currently gaged Maui streams was plotted against each hydrologic variable of the nine currently gaged Maui streams in order to determine a best-fit equation and 95% confidence interval equations (Figure 30 and Appendix J), which could then be used to calculate predicted hydrologic values of the ungaged streams (Tables 3-5).

4.2.a Comparing actual vs predicted hydrologic variables of currently gaged streams on Maui

The actual hydrologic values were compared to the predicted hydrologic values of the nine currently gaged streams on Maui (Figures 31-33). Out of the three geomorphologic variables analyzed, drainage densities and hypsometric integrals produced the most accurate hydrologic predictions for ungaged streams.

The recession constants of Honokōhau and Honopou were accurately predicted with the watershed's drainage density, ʻĪao was most accurately predicted with the hypsometric integral, and Kahakuloa, Waiheʻe, Waikamoi, Hanawi, and ʻOheʻo were most accurately predicted with the concavity index (Figure 31). Despite the observation that most recession constants were most accurately predicted from the concavity index, the concavity index values also produced some of

the largest standard deviations relative to the standard deviations produced by drainage densities and hypsometric integrals. The large standard deviations could be because of the concavity index's lack of basin area sensitivity. Since channels with different gradients could have the same concavity index, the relationships including concavity indices could be weak, resulting in larger standard deviations. The groups of streams predicted by each geomorphologic variable do not have the same external characteristics in common (i.e. location, basin area, average precipitation), which suggests that there is no particular reason why certain geomorphologic variables were able to better predict the recession constants of certain streams. The lack of consistency of which geomorphologic variables produce the best recession constant predictions may be due to the fact that recession constants cannot be analyzed based on individual geomorphologic variables. As mentioned in the introduction, recession constants are complex and can be affected by various factors. The recession constants are dependent not only on the geomorphology of the drainage basin, but on the general hydrology of the basin and time as well. All of these factors could affect the predictions made and therefore result in a lack of consistency amongst the geomorphologic variables.

While comparing the actual low-flow values, Q_{95}, with the predicted Q_{95}, there was no clear geomorphic variable that produced the most accurate predictions, but the hypsometric integral produced the most predictions closest to the actual Q_{95} (Figure 32). The standard deviations calculated for the Q_{95} values were all relatively similar, except for Honopou, which had a very large concavity index standard deviation. While comparing actual ΔS values with the predicted ΔS values, it was found that the drainage densities and hypsometric integrals produced the most accurate values compared to the concavity indices (Figure 33). In this case, the drainage densities had some of the smallest standard deviations and the concavity indices had some of the largest standard deviations, therefore making the concavity indices less reliable than the drainage density and hypsometric integral predictions.

Based on the comparisons made between the actual data and the predicted data for the nine currently gaged streams on Maui, the drainage densities and hypsometric integrals of the watersheds should provide the best insight into predicting recession constants, low-flow values, and change in storage values for the ungaged streams. Since drainage densities and hypsometric integrals have a strong inverse correlation (Figure 22b), it is understandable why both variables prove to be ideal indicators of hydrologic variables rather than one over the other. The drainage density and hypsometric integral ultimately quantify the same characteristic of a watershed – landscape dissection – but measure it in different ways. They should ideally be treated as the

same variable rather than two separate attributes, explaining the similar predictions calculated by both variables. The predictions calculated based on drainage densities and hypsometric integrals were closest in accuracy to the actual hydrologic values and typically had the smallest standard deviations, making them more precise relative to the predictions calculated based on concavity indices.

4.2.b Predicting hydrologic variables of ungaged Maui streams

Based on the comparisons of actual and predicted hydrologic values of the nine currently gaged streams on Maui, the drainage density and hypsometric integral of the watersheds should produce relatively accurate predictions of the hydrologic variables of Maui's ungaged streams. The hypothesis that drainage densities and hypsometric integrals of a watershed would produce relatively accurate hydrologic variable predictions was true in all three cases of predicting recession constants, low-flow values, and change in storage values for the nine ungaged streams on Maui. When predicting the hydrologic variables for the ungaged basins, I found that the drainage densities and hypsometric integrals produced similar results relative to the concavity indices (Figures 34-36). With the ungaged streams, actual recession constants, low-flow values, and change in storage values were not calculated because the streams' discharges are no longer monitored. Therefore, the actual values were not used to verify the validity of the predictions, as was done with the currently gaged streams in section 4.2.a. Since the hydrologic predictions computed from the drainage density equation were similar to the predictions computed from the hypsometric integral equation (Figures 34-36), I propose that those predicted hydrologic variables are most accurate to what the actual hydrologic variables would be. The concavity index may not be the best geomorphologic parameter to use while predicting hydrologic variables of ungaged streams because unlike the hypsometric integrals, the concavity indices are not sensitive to basin size. Both a large and small watershed could have the same concavity index, but for different reasons. The large watershed could have a low concavity index because the stream is heavily eroded to the point where its profile is very concave. A small watershed could have a low concavity index because its short length causes the slope to increase. Even though both streams have similar concavity indices, their basin areas are different, which I suspect could impact the amount of water that is discharged from the stream. Concavity index interpretations are debatable since the values are affected by various factors such as, rate of uplift, base level, and climate (Zaprowski et al., 2005). In contrast, the drainage density and hypsometric integral take basin size into account, and thus produce more representative values. The drainage densities and

hypsometric integrals are affected by surficial and underground water processes that are reflected in the results (Singh, 2008).

The five ungaged streams on the northern side of the island (Figure 15) were predicted to have less variability between the three geomorphologic variables compared to the ungaged streams on the southern side of the island (Figure 15). This is likely because the ungaged streams on the northern side of the island are most similar to the currently gaged streams. Since the streams are located on the northern side, they receive the same general amount of annual precipitation (Figure 2) and experience the same general climatic changes. It is interesting that the hydrologic predictions were most consistent with watersheds that are impounded by dikes. In Figures 31-33, streams 1, 5, and 6 have at least 50% of their watersheds impounded by dikes, and streams 8 and 9 have at least 44% of their watersheds impounded by dikes. The predictions computed based on drainage densities and hypsometric integrals are very close to each other for those streams, suggesting that along with those two geomorphologic variables, watersheds with dike-impounded groundwater, or that have a lower permeability, can potentially provide more accurate hydrologic predictions.

Based on these variables, it is challenging to determine which streams would have the most ideal streamflow conditions because Q_{95} and ΔS are both positively correlated to the recession constant, *k* (Figures 18 and 20). In section 4.1.a, higher recession constants typically indicate perennial streams (rather than intermittent), so it is now necessary to determine whether high or low Q_{95} and ΔS values are preferable. Since Q_{95} values indicate the value at which the flow is expected to exceed 95% of the time, then higher Q_{95} values are desirable since they should correlate with larger discharges. Low ΔS values are desirable because if a stream has a large ΔS, then the stream is losing a lot of water to unknown reservoirs before reaching the gaging station. However, if you look for a high Q_{95} value to give you a high *k* value, you could also have a high ΔS value, since both are positively correlated to *k*. It is then perhaps best to look for *k* values that are somewhere in the middle (perhaps ranging between 0.925-0.96), and balance between a large low-flow value and a small change in storage value.

For the island of Maui, it seems that the streams on the northern side of the island have the most ideal streamflow conditions since they receive the most precipitation and have recession constants predicted to be within the range of 0.925-0.96. The northern streams on the western side of the island are predicted to have higher low-flow values, suggesting higher water discharge values. However, the northern streams on the eastern side of the island had lower change in storage values, which are preferable since they suggest that high volumes of water are not shared. The

northwestern streams have higher ΔS values, but if groundwater sharing is indeed occurring between Waiheʻe and ʻĪao stream (which are located on the northwest side of the island), it is possible that groundwater sharing could be happening between other streams located near Waiheʻe and ʻĪao. Therefore, even though the groundwater is being lost from a stream with a high ΔS value, that groundwater could be escaping to an adjacent watershed, from which water can still be collected as water resources.

4.2.c Predicting hydrologic variables of streams on Oʻahu

Hydrologic predictions were computed for three currently gaged streams on Oʻahu (Table 6) to determine if the same conclusions could be made for other islands in Hawaiʻi or if the above conclusions are restricted only to Maui. The predictions and standard deviations computed for Oʻahu are very high compared to the actual values. In general, it seems that the hypsometric integral and drainage density produced the closest predictions, especially compared to the predictions computed from the concavity indices, but those predictions are still much higher than the actual values (Figures 37-39). I propose that it is indeed possible to predict streamflow conditions of Oʻahu's ungaged streams under the same methods used to predict streamflow conditions of Maui's ungaged streams in this thesis. However, it does not seem appropriate to use the same equations to predict the hydrologic variables between islands. Even though the islands all experience the same general climate systems and have the same general lithology, slight differences in environmental and anthropogenic conditions can greatly impact the calculations and predictions. For example, Oʻahu is much more heavily populated than Maui, has a lower maximum elevation, and is older in age, which should be reflected by mountains more eroded than Maui (Engott et al., 2015). All of these factors could impact the way the groundwater flows throughout the watersheds. Therefore, in order to best predict the streamflow conditions of Oʻahu's ungaged streams, it would be ideal to calculate best-fit equations for Oʻahu based on discharge values of Oʻahu's streams rather than Maui's streams.

Based on the results from this thesis, the geomorphologic variables can indeed be used to estimate the hydrologic characteristics of a drainage basin. Studies such as Bloomfield et al. (2011) found that if relationships can be determined and quantified between the lithology, hydrology, and geomorphology of an area, then those physical characteristics can be used to estimate the hydrologic features of ungaged basins. Results from this thesis could be used for other areas within Hawaiʻi and around the world, but with caution. Even though the hydrology of an area is related to its geomorphology, every area is unique. There are many factors that influence a

watershed's hydrology, so it is possible for relationships to vary. Overall, the general relationships found between the geomorphologic and hydrologic variables should be relatively similar in other locations, but as seen with the Brandes et al. (2005) study, relationships can vary, especially when it comes to the recession constants. Since recession constants are time-dependent, not as easily determined as other hydrologic characteristics (such as low-flow values), and have a relatively small range, there is a higher chance that the recession constants will have different relationships with other features of the drainage basins. Therefore, extra precaution should be taken while calculating recession constants; not only because of their sensitivity, but because of their usefulness while estimating streamflow conditions. Bevans (1986) found that under certain conditions, recession constants can be used to estimate aquifer properties. By analyzing baseflow recession curves, you are able to determine stream-aquifer interactions without necessarily having to use digital groundwater flow models, which can be very expensive and difficult to operate (Bevans, 1986). If recession constants can be calculated for streams, the recession constants can potentially identify perennial and intermittent streams, therefore suggesting the stream's usefulness as a water resource.

4.3 Groundwater Sharing

The main components likely to identify groundwater sharing were the recharge and baseflow values calculated for each watershed. Table 7 shows that Honopou had a higher baseflow than recharge value, but I suspect that is because Honopou is an anomaly rather than a stream with groundwater sharing. Honopou has a very small basin area relative to the other watersheds, is isolated from the other gaged streams, and does not necessarily receive as much rainfall as the other watersheds (Figure 2). So, I suspect that Honopou's characteristics are too dissimilar from the other watersheds to confidently say that it is experiencing groundwater sharing. Table 7 also shows that Waiheʻe Stream has a larger baseflow than recharge value, indicating that Waiheʻe is receiving water from another source. It is expected that Waiheʻe is receiving groundwater from ʻĪao, which is adjacent to Waiheʻe, although most hydrologic and geomorphic variables did not show strong evidence of this.

The only other parameter that showed slight evidence of groundwater sharing is the hypsometric curve. Figure 40 shows that Waiheʻe stream's curve is more concave and strays away from the rest of the curves, which could indicate evidence of groundwater sharing. A concave hypsometric curve reflects a watershed with a greater amount of its rock volume located lower in the basin, whereas a convex hypsometric curve reflects a watershed with a greater amount of its rock

volume located higher in the basin (Bierman and Montgomery, 2014). If the curve is concave, then more material has been eroded and transported downstream. If a stream receives more groundwater from groundwater sharing, then I suspect that the larger volume of water can erode more material, resulting in a concave hypsometric curve. This could explain why Waiheʻe's hypsometric curve is the most concave relative to the eight other hypsometric curves in Figure 40. The issue now, is understanding why ʻĪao's hypsometric curve is so concave when it is supposedly losing groundwater to Waiheʻe. I would assume that if a stream is losing a lot of its water, it will not be able to erode as much material, resulting in a convex hypsometric curve. However, ʻĪao receives more precipitation than Waiheʻe (Table 1), so perhaps ʻĪao can afford to lose some of its groundwater to Waiheʻe while still eroding and transporting material downstream to result in a concave hypsometric curve. This explains how a stream receiving extra water and a stream losing water could both have concave hypsometric curves, and suggest that hypsometric curves could indeed detect possible groundwater sharing between watersheds. However, since Waiheʻe and ʻĪao are the only streams with potential groundwater sharing, it is difficult to conclude whether the hypsometric curves are indicative of this process, or if it is just a coincidence that Waiheʻe's curve strays.

I also looked at how the baseflow/recharge values compared to the change in storage values, ΔS, (Figure 41) because the change in storage could possibly relate to groundwater sharing. As mentioned earlier, if streams have higher ΔS values, the streams are losing a lot of water to unknown reservoirs. That reservoir could be another watershed. If ΔS reflects groundwater sharing, then streams with high baseflow/recharge values should correlate to low ΔS values, therefore indicating that the streams are on the receiving-end of the sharing. However, when plotted, Figure 41 lacked sufficient evidence that ΔS could be an indicator of groundwater sharing. The data did not have a strong correlation between the two variables and it is difficult to determine if they actually share an inverse relationship. Since a correlation is not seen between baseflow/recharge and change in storage values, the groundwater sharing may be occurring on a smaller local scale. I suggest that it would be best to analyze smaller portions of the island to search for localized groundwater sharing.

5. Summary and Conclusions

The main objective of this thesis was to determine if Maui's streamflow conditions could be predicted based on quantifiable hydrologic and geomorphologic variables. Hydrologic variables such as baseflow recession constants (k), low-flow values (Q_{95}), and change in storage (ΔS) were computed for currently gaged streams on Maui and analyzed against computed geomorphologic variables such as drainage density, hypsometric integral, and concavity index. The relationships found between the hydrologic and geomorphologic variables were used to predict the hydrologic values of ungaged basins on Maui in order to determine the potential streamflow conditions of those ungaged streams. The analysis was then carried over to O'ahu to determine if the same relationships between hydrologic and geomorphologic variables could be used for O'ahu's watersheds.

When recession constants were computed for the island of Maui, I found that streams with recession constants greater than 0.95 were generally located in areas of the island with dike-impounded groundwater and streams with recession constants less than 0.95 were generally located in areas with groundwater that is not dike-impounded. Streams with recession constants less than 0.90 are expected to be intermittent or nearly perennial streams because the stream discharge is very low and sometimes drops to zero. Recession constants could be useful for water resource management because the recession constants can predict the streamflow conditions (whether a stream is perennial or intermittent) which could indicate whether a stream is ideal for water resources.

When the actual hydrologic values were compared to the predicted hydrologic values of the currently gaged streams on Maui, I found that the drainage densities and hypsometric integrals produced the most accurate predictions. The same was found for the ungaged Maui streams, where the drainage densities and hypsometric integrals generally produced the most similar hydrologic predictions. The similarity between drainage density and hypsometric integral predictions is due to the fact that the two variables ultimately measure the same watershed characteristic (landscape dissection), but in different ways. The northern ungaged streams had the least amount of variability relative to the southern ungaged streams, most likely because the currently gaged streams are also located on the northern side of the island, therefore are placed under similar environmental and climatic conditions as the currently gaged streams.

I propose that the same analysis conducted on Maui can also be done for the island of O'ahu. The drainage densities and hypsometric integrals produced hydrologic predictions most similar to the

actual hydrologic values, relative to the concavity indices. However, since the differences between the actual and predicted hydrologic values were much greater than those of Maui, the slight environmental and anthropogenic differences between Maui and Oʻahu may affect the results of the analysis. Therefore, it would be most ideal to use relationships found on Oʻahu in order to predict the streamflow conditions.

The second objective of this thesis was to determine if the hydrologic and geomorphologic variables can predict/explain potential groundwater sharing between adjacent watersheds. However, since there was a lack of known watersheds that share groundwater, conclusive evidence was not found. Recharge and baseflow values seemed to be the best indicators since basins with larger baseflow values than recharge values indicates that the stream is receiving water from other sources besides precipitation recharge. Hypsometric curves show potential for determining if groundwater sharing is occurring, due to the intense concavity of streams that receive extra groundwater. Change in storage values could also reflect groundwater sharing, but due to the lack of correlation between ΔS and baseflow/recharge, this hypothesis should be further explored on a smaller, localized scale.

This thesis concludes that relationships between a watershed's hydrologic and geomorphologic characteristics can be used to predict streamflow conditions, and that drainage densities and hypsometric integrals have the potential to estimate hydrologic variables. This thesis calculates the baseflow recession constants of Maui streams, which has never been done for the state of Hawaiʻi, and uses those values, along with whole-scale basin parameters to assess the relationship between the island's hydrology and geomorphology. These assessments can be used to predict potential streamflow conditions, which are critical for the island's water resource management.

Acknowledgements

I would like to thank my readers and professors for helping me throughout this process and the last four years of my undergraduate career. Special thanks to Delwyn Oki, Adam Johnson, Maoya Bassiouni, and everybody at the USGS Pacific Islands Water Science Center welcoming me over the summer, answering my many emails throughout the year, and for sharing all of your knowledge with me. Thank you to my family for always supporting me, and finally, thank you to my amazing friends for keeping me sane and providing me with caffeine.

Works Cited

Bevans, H.E., 1986, Estimating Stream-Aquifer Interactions in Coal Areas of Eastern Kansas by Using Streamflow Records: U.S. Geological Survey Water-Supply Paper 2290, p. 51-64.

Bierman, P.R. and Montgomery, D.R., 2014, Key Concepts in Geomorphology: New York, W.H. Freeman and Company Publishers, 494 p.

Bloomfield, J.P., Bricker, S.H., and Newell, A.J., 2011, Some relationships between lithology, basin form and hydrology: a case study from the Thames basin, UK: Hydrological Processes, v. 25, p. 2518-2530, doi: 10.1002/hyp.8024.

Brandes, D., Hoffmann, J.G., & Mangarillo, J.T., 2005, Base flow recession rates, low flows, and hydrologic features of small watersheds in Pennsylvania, USA: Journal of the American Water Resources Association, v. 41, issue 5, p. 1177-1186.

Carlston, C.W., 1963, Drainage Density and Streamflow: U.S. Geological Survey Professional Paper 422-C, C1-C8.

Cox, D.C., 1954, Notes: Research in ground-water hydrology in Hawaii: Pacific Science, v.8, p. 230-233.

El-Kadi, A.I., Moncur, J.E.T., 2006. The history of groundwater management and research in Hawaii. In: Proceedings, 2006 Jeju-Hawaii Water Forum, July 21-22, 2006. Jeju, Korea, pp. 222-241.

Engott, J.A., 2015, Mean annual water-budget components for the Island of Oahu, Hawaii, for average climate conditions, 1978-2007 rainfall and 2010 land cover. Vector Digital Data Set (Polygon), available at http://pubs.usgs.gov/sir/2015/5010/.

Engott, J.A., Johnson, A.G., Bassiouni, M., and Izuka, S.K., 2015, Spatially distributed groundwater recharge for 2010 land cover estimated using a water-budget model for the island of Oʻahu, Hawaiʻi: U.S. Geological Survey Scientific Investigations Report 2015-5010, 49 p., http://dx.doi.org/10.3133/sir20155010.

Fetter, C.W., 2001, Applied Hydrogeology Fourth Edition: New Jersey, Prentice-Hall, 533 p.

Harlin, J.M., 1984, Watershed morphometry and time to hydrograph peak: Journal of Hydrology, v. 67, p. 141-154.

Giambelluca, T.W., Q. Chen, A.G. Frazier, J.P. Price, Y.-L. Chen, P.-S. Chu, J.K. Eischeid, and D.M. Delparte, 2013: Online Rainfall Atlas of Hawai'i. *Bull. Amer. Meteor. Soc.* 94, 313-316, doi: 10.1175/BAMS-D-11-00228.1

Gingerich, S.B., 2008, Ground-water availability in the Wailuku area, Maui, Hawaiʻi: U.S. Geological Survey Scientific Investigations Report 2008-5236, 95 p., *http://pubs.usgs.gov/sir/2008/5236/*.

Gingerich, S.B., & Oki, D.S., 2000, Ground Water in Hawaii: U.S. Geological Survey FS 126-00, hi.water.usgs.gov/publications/pubs/fs/fs126-00.pdf.

Hirashima, G.T., 1963, Influence of water-development tunnels on streamflow-groundwater relations in Haiku-Kahaluu area, Oahu, Hawaii: Hawaii Div. Water and Land Devel. Circ. C21, 11 p.

Johnson, A.G., 2014, Mean annual water-budget components for the Island of Maui, Hawaii, 1978-2007, Vector Digital Data Set (Polygon), available at http://pubs.usgs.gov/sir/2014/5168/.

Johnson, A.G., Engott, J.A., and Bassiouni, M., 2014, Spatially distributed groundwater recharge estimated using a water-budget model for the Island of Maui, Hawai‘i, 1978-2007: U.S. Geological Survey Scientific Investigations Report 2014-5168, 53 p., *http://dx.doi.org/10.3133/sire20145168*.

Knisel Jr., W. G. *(*1963*),* Baseflow recession analysis for comparison of drainage basins and geology, J. Geophys. Res., 68*(*12*),* 3649–3653, *doi:*10.1029/JZ068i012p03649.

Kowall, S.J. (1976), The Hypsometric Integral and Low Streamflow in Two Pennsylvania Provinces: Water Resources Research, vol. 12, p. 497-502.

Langbein, W.B. et al., 1947, Topographic Characteristics of Drainage Basins: U.S. Geological Survey Water-Supply Paper 968-C, p. 125-157.

Maupin, M.A., Kenny, J.F., Hutson, S.S., Lovelace, J.K., Barber, N.L., and Linsey, K.S., 2014, Estimated use of water in the United States in 2010: U.S. Geological Survey Circular 1405, 56 p., http://dx.doi.org/10/3133/cir1405.

Oki, D.S., 2004, Trends in Streamflow Characteristics at Long-Term Gaging Stations, Hawaii: U.S. Geological Survey Scientific Investigations Report 2004-5080, 120 p.

Oki, D.S., Rosa, S.N., and Yeung, C.W., 2010, Flood-frequency estimates for streams on Kaua‘i, O‘ahu, Moloka‘i, Maui, and Hawai‘i, State of Hawai‘i: U.S. Geological Survey Scientific Investigations Report 2010-5035, 121.

Pyrce, R., 2004, Hydrological Low Flow Indices and their Uses: Watershed Science Centre WSC Report No. 04-2004, Peterborough, Ontario, 33p.

Rea, Alan, and Skinner, K.D., 2012, Geospatial datasets for watershed delineation and characterization used in the Hawaii StreamStats web application: U.S. Geological Survey Data Series 680, 12 p.

Rodriguez-Iturbe, I. and Valdes, J.B., 1979, The Geomorphologic Structure of Hydrologic Response: Water Resources Research, vol. 15, no. 6, p. 1409-1420.

Sarp, G., Toprak, V. & Duzgun, S. (2011) Hypsometric properties of the hydrolic basins located on western part of Nafz. 34th International Symposium on Remote Sensing of Environment, Sidney, 2011. www.isprs.org/proceedings/2011/isrse-34/211104015Final00591.pdf.

Singh, O., Sarangi, A., Sharma, M.C., 2008, Hypsometric Integral Estimation Methods and its Relevance on Erosion Status of North-Western Lesser Himalayan Watersheds: Water Resources Management, v. 22, pg. 1545-1560.

Stearns, H.T., and Macdonald, G.A., 1942, Geology and ground-water resources of the island of Maui: territory of Hawaii, Hawaii Division of Hydrography Bulletin 7, 344 p.

Tallaksen, LM, (1995). A review of baseflow recession analysis. Journal of Hydrology, 165: 349-370.

Thomas, B.F., Vogel, R.M., Kroll, C.N., Famiglietti, J.S., 2013, Estimation of base flow recession constant under human interference: Water Resources Research, vol. 49, p. 7366-7379.

Vogel, R.M., and Kroll, C.N., 1992, Regional Geohydrologic-Geomorphic Relationships for the Estimation of Low-Flow Statistics: Water Resources Research, vol. 28, no. 9, p. 2451-2458.

Vogel, R.M., and Kroll, C.N., 1996, Estimation of Baseflow Recession Constants: Water Resources Management, vol. 10, p. 303-320.

Zaprowski, B.J., Pazzaglia, F.J., and Evenson, E.B., 2005, Climatic influences on profile concavity and river incision: Journal of Geophysical Research, vol. 110, F03004, doi: 10.1029/2004JF00138.

Zecharias, Y.B., and Brutsaert, W., 1988, Recession Characteristics of Groundwater Outflow and Base Flow From Mountainous Watersheds: Water Resources Research, vol. 24, no. 10 p. 1651-1658.

Appendix A: Median Discharge, Q_{95} Exceedance Percentile, and Flow-Duration Curves

1. Input all of the discharge values of one stream into a single column in an Excel sheet. The discharge data should be the same continuous data used for the same years as the recession constants.
2. Sort the discharge values from largest to smallest.
3. In a new column, assign a rank to each value (where the largest value is 1)
4. For each value, calculate the Weibull plotting position m/(n+1), where m is the rank and n is the total number of values.
5. If trying to determine the median discharge, search for the Weibull number that is closest to 0.5.
6. If trying to determine the Q_{95} exceedance percentile, search for the Weibull number that is closest to 0.95.
7. This method can be used to plot flow duration curves.

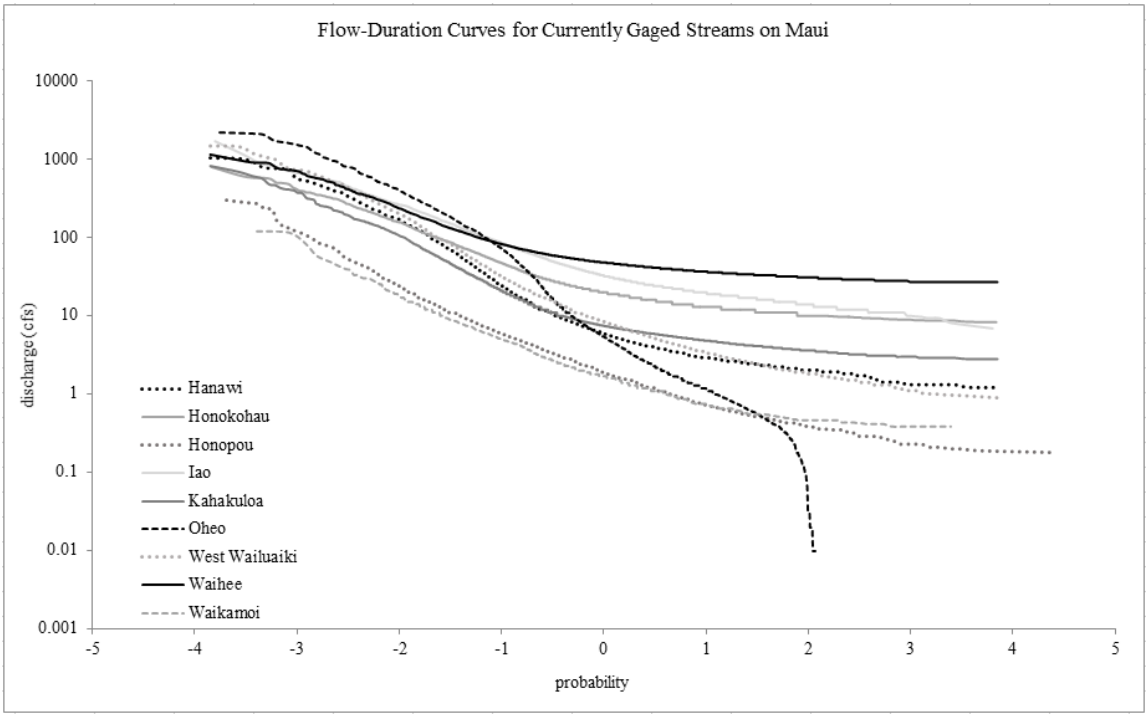

Appendix B: Converting Recharge from in/yr to cfs

1. In ArcMap, clip mean annual water-budget components file provided by the USGS Pacific Islands Water Science Center (http://water.usgs.gov/GIS/metadata/usgswrd/XML/sir2014-5168_Maui_water-budget_components.xml) according to the desired watersheds.
2. Calculate the area (in square meters) of each polygon within the watershed by adding a new variable in the attribute table and calculating geometry.
3. Copy the data from the attribute table and paste in an Excel file.
4. Calculate the new recharge in cfs of each polygon with the equation recharge/12/86400/365*area*10.7639, where the recharge in the equation is in in/yr and the area is in m^2.
5. You can then add all of the new recharge values within the entire watershed to get the total recharge of the watershed in cubic feet per second.

Appendix C: Computing Baseflow with Wahl and Wahl program (1995)

(files provided by the USGS Pacific Islands Water Science Center c/o Adam Johnson)

1. Instructions to run the Wahl and Wahl (1995) program, provided by the USGS
    a. Run bfi415.exe
        i. Input is the .crd file that contains streamflow data from NWIS (i.e. st16614000.crd [for Waiheʻe Stream]. Bfi415.exe and .crd file must be in the same folder.
        ii. Choose ‘h’ to name output hydrograph file. Choose ‘f’ (use 0.9). Choose ‘N’ (use 1). Program output files will be st16614000.q, st16614000.bfi, st16614000.n.
    b. Run bfigetn.exe to get rid of text in output file st16614000.q
        i. Input: st16614000.q
        ii. Output: st16614000notext.q
    c. Run bfigetn.exe program to select only streamflow and baseflow values for the N that you specify (i.e. 1)
        i. Input .crd file: (i.e. st1614000.crd)
        ii. Input no text file: (i.e. st16614000notext.q)
        iii. Input N value: (i.e. 3; this varies by station, so please see table 4 of Johnson et al. (2014) report (SIR-2014-5168

[http://pubs.usgs.gov/sir/2014/5168/pdf/sir2014-5168.pdf]) to determine N value for each stream).

iv. Output file: (i.e. st16614000n3.q)

2. Calculate annual average baseflow
    a. Import data from .q file (i.e. st16614000n3.q) into an Excel file
    b. Calculate the average baseflow of each water year (October 1 – September 30) and average all of the averages to get the annual average baseflow. Baseflow values are in cfs.

Appendix D: Using the Mosaic tool in ArcGIS

The Mosaic tool in ArcGIS is used to stitch multiple rasters into a single raster.

1. Stitch the rasters together:
    a. ArcToolbox > Raster > Raster Dataset > Mosaic to New Raster
    b. Input rasters: select all of the rasters you wish to stitch together
    c. Output location: choose a location for your file
    d. Raster Dataset Name with Extension: whatever you choose to name your fully stitched raster and follow the extension instructions on the right
    e. Number of Bands: 1

Appendix E: Creating a Stream Network in ArcGIS

1. Fill your DEM to eliminate empty cells:
    a. ArcToolbox > Spatial Analyst > Hydrology > Fill
    b. Input: [your initial DEM (i.e. Maui_dtm)]
    c. Output: [whatever you choose to name your filled layer (i.e. Maui_dtm_fill)]
2. Inform GIS which direction the water in the stream is flowing:
    a. ArcToolbox > Spatial Analyst > Hydrology > Flow Direction
    b. Input: [your filled layer (i.e. Maui_dtm_fill)]
    c. Output: [whatever you choose to name your flow direction layer (i.e. Maui_FlowDir)]
3. Determine how many cells should be counted upstream from drainage area:
    a. ArcToolbox > Spatial Analyst > Hydrology > Flow Accumulation

b. Input: [your flow direction file (i.e. Maui_FlowDir)]
c. Output: [whatever you choose to name your flow accumulation file (i.e. Maui_FlowAcc)]
d. Output data type: INTEGER (saves space)

4. Calculate the log of the flow accumulation:
    a. ArcToolbox > Spatial Analyst > Map Algebra > Raster Calculator
    b. Double-click "Log10" from menu on right of Raster Calculator screen
    c. Double-click your flow accumulation file under *Layers and variables* menu on left
    d. Output: [whatever you choose to name your new flow accumulation file (i.e. log10_FlowAcc)]
5. Determine cell-threshold:
    a. ArcToolbox > Spatial Analyst > Map Algebra > Raster Calculator
    b. Double-click your new flow accumulation file (i.e. log10_FlowAcc) from the left menu
    c. Double-click ">=" symbol
    d. Type in 3.5
    e. Output: [whatever you choose to name your stream network file (i.e. Maui_strm_3p5)]
6. Link intersections of streams:
    a. ArcToolbox > Spatial Analyst > Hydrology > StreamLink
    b. Input stream raster: [your stream network file (i.e. Maui_strm_3p5)]
    c. Input flow direction raster: [your flow direction file (i.e. Maui_FlowDir)]
    d. Output: [whatever you choose to name your stream link file (i.e. Maui_strmL_3p5)]
7. Convert the streams into a feature:
    a. ArcToolbox > Spatial Analyst > Hydrology > Stream to Feature
    b. Input: [your stream link file (i.e. Maui_strmL_3p5)]
    c. Output: [whatever you choose to name your stream feature (i.e. Maui_strmF_3p5)]

Appendix F: Drainage Density

1. Creating Watershed Boundary
    a. If not already displayed, open the Drawing menu (Customize > Toolbars > Draw)
    b. Select Marker option from the Drawing toolbar
    c. Place a marker on the cell of interest on your stream (my marker was placed as close to the gaging station as possible since that was the lowest point at which incoming water could have been measured)
    d. Create the pour point by converting the marker to feature from the Drawing pulldown menu (Drawing > Convert Graphics to Features) and save it as a layer to the map (i.e. Waihee_pp). Once the marker is a layer on the map, you can delete the original marker, which should be displayed above the feature.
    e. Create watershed
        i. ArcToolbox > Hydrology > Watershed
        ii. Input flow direction raster: [your flow direction file (i.e. Maui_FlowDir)]
        iii. Input raster or feature pour point data: [your marker feature (i.e. Waihee_pp)]
        iv. Output raster: [whatever you choose to name your watershed raster (i.e. Waihee_ws)]
    f. Convert watershed to shapefile
        i. ArcToolbox > Conversion Tools > From Raster > Raster to Polygon
        ii. Input raster: [your watershed raster (i.e. Waihee_wtrshd)
        iii. Output polygon features: [whatever you choose to name your watershed (i.e. Waihee_watershed)]
2. Calculate Drainage Basin Area
    a. Right-click your watershed layer (i.e. Waihee_watershed) > Open Attribute Table
    b. Click Table Option pulldown menu > Add Field
        i. Name: Area
        ii. Type: Double (gives a more precise value)
    c. If not already displayed, open Editor toolbar (Customize > Toolbars > Editor)
    d. Click Editor > Start Editing
    e. In the Start Editing window, find and select the layer you want to edit (i.e. Waihee_waterhsed) (Be sure the same layer is selected from the Create Features sidetab)

f. Right-click Area title cell in Attribute Table > Calculate Geometry
    i. Property: Area
    ii. Units: Square Kilometers [sq km]
g. The area of the drainage basin will be displayed in the Attribute Table in square kilometers

3. Extract Streams within Watersheds
    a. ArcToolbox > Spatial Analyst Tools > Extract by Mask
    b. Input raster: [your stream network file (i.e. Maui_strmF_3p5)]
    c. Input raster or feature mask data: [your watershed shapefile (i.e. Waihee_watershed)]
    d. Output raster: [whatever you choose to name your extracted stream (i.e. Waihee_extract)]
4. Calculate Stream Length
    a. Right-click your extracted stream layer (i.e. Waihee_extract) > Open Attribute Table
    b. Click Table Option pulldown menu > Add Field
        i. Name: Length
        ii. Type: Double (gives a more precise value)
    c. Click Editor > Start Editing > select layer you want to edit (i.e. Waihee_extract)
    d. Right-click Length title cell in Attribute Table > Calculate Geometery
        i. Property: Length
        ii. Units: Kilometers [km]
    e. The length of the extracted streams will be displayed in the Attribute Table in kilometers
5. Calculate Drainage Density
    a. Divide stream length by drainage basin area (I chose to do this in Excel)

Appendix G: Hypsometric Integral

(Reproduced from instructions found at http://gis4geomorphology.com/hypsometric-index-integral/).

1. Convert DEM mosaic from floating point to integer
    a. Spatial Analyst > Math > Int
    b. Input raster or constant value: the DEM mosaic
    c. Output raster: whatever you choose to name it

2. Extract by mask: extract the new integer DEM for each watershed
3. Reclassify the new watersheds
    a. Spatial Analyst > Reclassify
    b. Input raster: the new watershed shapefile
    c. Classify > Method: Equal Interval > Classes: 20
    d. Output raster: name_hyprec
4. Open the properties of the reclassified watershed and take note of the mean, max, and min elevation.
5. HI = (mean elevation – min elevation)/(max elevation – min elevation)

Appendix H: Channel Concavity Index

(Reproduced from instructions found at http://gis4geomorphology.com/concavity-soon/).

1. Create a point marker at the headwaters of the stream trunk and covert graphic to feature (i.e. Waihee_cpp)
2. Mark out the stream trunk
    a. Spatial Analyst > Cost Path
    b. Input raster or feature destination data: your new point (i.e. Waihee_cpp)
    c. Input cost distance raster: your flow accumulation (i.e. flowacc)
    d. Input cost backlink raster: your flow direction (i.e. flowdir)
    e. Output raster: save it [Waihee_trunk]
3. Clip out only the trunk within your drainage basin
    a. Spatial Analyst > Extract by Mask
    b. Input raster: Waihee_trunk
    c. Input raster or feature mask data: your watershed shapefile (i.e. Waihee_watershed.shp)
    d. Output raster: Waihee_trcl
4. Extract DEM from trunk
    a. Spatial Analyst > Extract by Mask
    b. Input raster: your filled DEM (i.e. full_mosaic)
    c. Input raster or feature mask data: Waihee_trcl
    d. Output Raster: Waihee_t.dem
5. Determine slope of the trunk
    a. Spatial Analyst > Slope

    b. Input raster: Waihee_t.dem
    c. Output raster: Waihee_t.slope
    d. Output measurement: PERCENT_RISE
6. Extract flow of the trunk
    a. Spatial Analyst > Extract by Mask
    b. Input raster: flowacc
    c. Input raster or feature mask data: Waihee_trcl
    d. Output raster: Waihee_t.flow
7. Get points from trunk
    a. Conversion > From Raster > Raster to Point
    b. Input raster: Waihee_trcl
    c. Output point features: Waihee_t.points
8. Extract slope to points
    a. Spatial Analyst > Sample
    b. Input rasters: Waihee_t.slope
    c. Input location raster or point features: Waihee_t.points
    d. Output table: Waihee_slope_data
    e. Open the table that is created; copy the data from the table and paste into Excel
9. Extract flow to points
    a. Spatial Analyst > Sample
    b. Input rasters: Waihee_t.flow
    c. Input location raster or point features: Waihee_t.points
    d. Output table: Waihee_flow_data
    e. Open the table that is created; copy the data from the table and paste into Excel
        i. Cut the flow data column and paste it next to the slope data column from earlier (you can delete the other data from the flow section since it's the same as the slope section).
10. Making a channel concavity plot
    a. Delete all rows where the slope is zero
    b. Create a new column titled "drainage area" and fill it with the equation =(flow*(pixel size*pixel size))/1000000
    c. Plot drainage area on x-axis and slope on y-axis (with both axes on log scale)
    d. Fit a power trend line and display the line's equation
    e. The concavity index is the exponent of the equation

Appendix I: Calculating 95% Confidence Intervals

(95% confidence intervals were calculated based on instructions found at http://www.tushar-mehta.com/publish_train/data_analysis/16.htm).

1. Let's say we want to compare drainage density (x-axis) with recession constants (y-axis). Add your drainage density and recession constant data as two columns in Excel and graph it with a best-fit line; display the equation of the best-fit line. Make note of the slope (**m**) and y-intercept (**b**) of the best fit line in the Excel sheet.

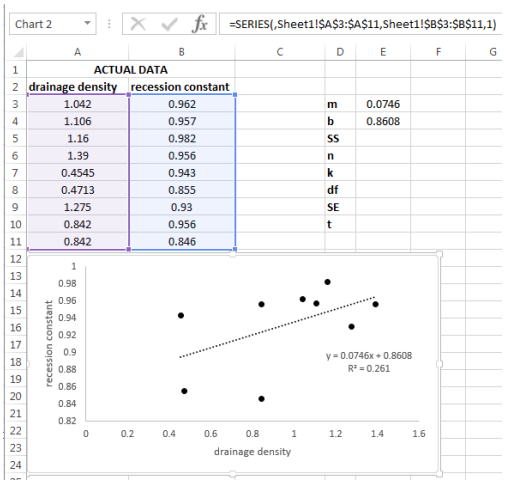

2. Calculate **ŷ**, the value predicted for each x value, with the equation ŷ=mx+b, where m is the slope of the best-fit line, x is the drainage density value, and b is the y-intercept of the best-fit line. Calculate the residual (error), **y-ŷ**, where y is the recession constant. Then, square the residual to get **(y-ŷ)²**. Calculate **SS**, which is the sum of all the $(y-\hat{y})^2$ values (the sum of the values that remain unexplained) with the equation $=SUM((y-\hat{y})^2)$.

	A	B	C	D	E
1	ACTUAL DATA				
2	drainage density	recession constant			
3	1.042	0.962		m	0.0746
4	1.106	0.957		b	0.8608
5	1.16	0.982		SS	0.013766
6	1.39	0.956		n	
7	0.4545	0.943		k	
8	0.4713	0.855		df	
9	1.275	0.93		SE	
10	0.842	0.956		t	
11	0.842	0.846			
12					
13					
14	ŷ	y-ŷ	(y-ŷ)^2		
15	0.9385332	0.0234668	0.000550691		
16	0.9433076	0.0136924	0.000187482		
17	0.947336	0.034664	0.001201593		
18	0.964494	-0.008494	7.2148E-05		
19	0.8947057	0.0482943	0.002332339		
20	0.89595898	-0.04095898	0.001677638		
21	0.955915	-0.025915	0.000671587		
22	0.9236132	0.0323868	0.001048905		
23	0.9236132	-0.0776132	0.006023809		

3. Plug in the appropriate value for **n**, which is the number of rows of actual data, and **k**, which is the number of columns of actual data. Calculated the degrees-of-freedom, **df**, which is the difference between n and k. Calculate the standard error of the regression, **SE**, with the equation SE = $\sqrt{\frac{SS}{(n-k)}}$. Calculate the critical t-value, **t**, with the formula =TINV(0.05,df), where 0.05 is the probability that corresponds to the 95% confidence.

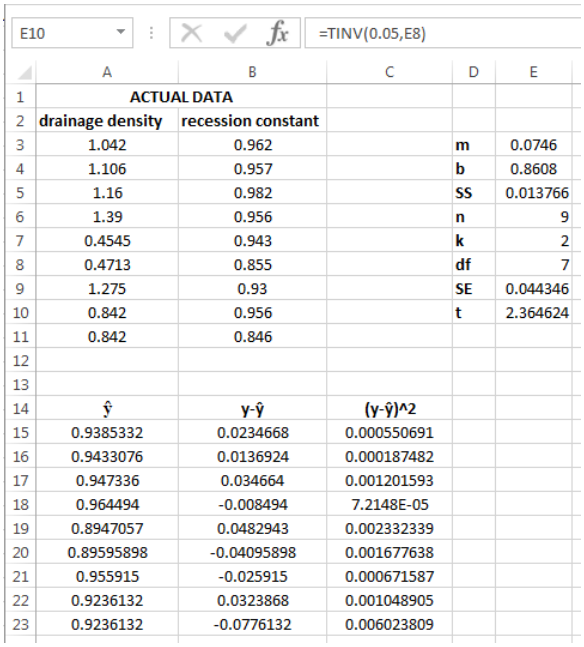

E10 =TINV(0.05,E8)

	A	B	C	D	E
1	ACTUAL DATA				
2	drainage density	recession constant			
3	1.042	0.962		m	0.0746
4	1.106	0.957		b	0.8608
5	1.16	0.982		SS	0.013766
6	1.39	0.956		n	9
7	0.4545	0.943		k	2
8	0.4713	0.855		df	7
9	1.275	0.93		SE	0.044346
10	0.842	0.956		t	2.364624
11	0.842	0.846			
12					
13					
14	ŷ	y-ŷ	(y-ŷ)^2		
15	0.9385332	0.0234668	0.000550691		
16	0.9433076	0.0136924	0.000187482		
17	0.947336	0.034664	0.001201593		
18	0.964494	-0.008494	7.2148E-05		
19	0.8947057	0.0482943	0.002332339		
20	0.89595898	-0.04095898	0.001677638		
21	0.955915	-0.025915	0.000671587		
22	0.9236132	0.0323868	0.001048905		
23	0.9236132	-0.0776132	0.006023809		

4. Make a new column in Excel with a list of "predictable" drainage densities from which you wish to predict recession constants. In the next column, calculate the predicted recession constants with the best-fit line equation mx_1+b, where x_1 is the "predictable" drainage density you just typed in.

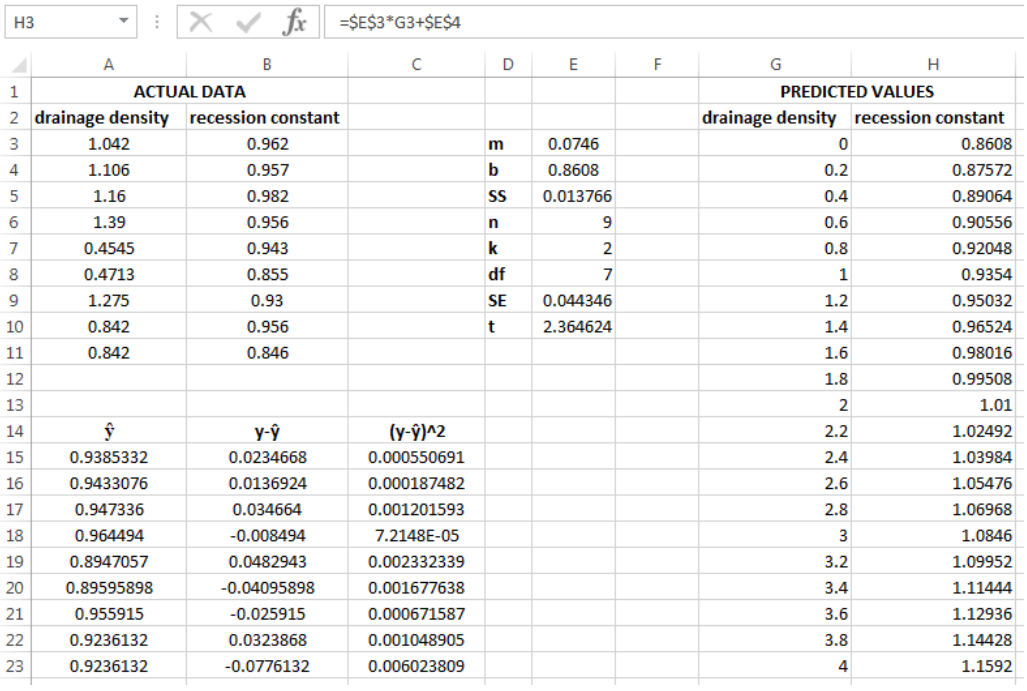

H3 =$E$3*G3+$E$4

	A	B	C	D	E	F	G	H
1	ACTUAL DATA						PREDICTED VALUES	
2	drainage density	recession constant					drainage density	recession constant
3	1.042	0.962		m	0.0746		0	0.8608
4	1.106	0.957		b	0.8608		0.2	0.87572
5	1.16	0.982		SS	0.013766		0.4	0.89064
6	1.39	0.956		n	9		0.6	0.90556
7	0.4545	0.943		k	2		0.8	0.92048
8	0.4713	0.855		df	7		1	0.9354
9	1.275	0.93		SE	0.044346		1.2	0.95032
10	0.842	0.956		t	2.364624		1.4	0.96524
11	0.842	0.846					1.6	0.98016
12							1.8	0.99508
13							2	1.01
14	ŷ	y-ŷ	(y-ŷ)^2				2.2	1.02492
15	0.9385332	0.0234668	0.000550691				2.4	1.03984
16	0.9433076	0.0136924	0.000187482				2.6	1.05476
17	0.947336	0.034664	0.001201593				2.8	1.06968
18	0.964494	-0.008494	7.2148E-05				3	1.0846
19	0.8947057	0.0482943	0.002332339				3.2	1.09952
20	0.89595898	-0.04095898	0.001677638				3.4	1.11444
21	0.955915	-0.025915	0.000671587				3.6	1.12936
22	0.9236132	0.0323868	0.001048905				3.8	1.14428
23	0.9236132	-0.0776132	0.006023809				4	1.1592

5. Calculate the distance of the confidence interval with the equation, **CI**, with the equation $\mathrm{CI} = (\mathrm{t})(\mathrm{SE})\sqrt{\frac{1}{\frac{[\mathrm{COUNT(x:x)}+(\mathrm{x_1}-\mathrm{AVERAGE(x:x)})]^2}{\mathrm{DEVSQ(x:x)}}}}$, where COUNT, AVERAGE, and DEVSQ are functions in Excel, x_1 is each "predicted" drainage density value, and x:x is the range of actual drainage density values. Calculate the **lower CI** by subtracting the CI from the "predicted" recession constant (i.e. J3=H3-I3 in the Excel sheet). Calculate the **upper CI** by adding the CI with the "predicted" recession constant (i.e. K3=H3-I3 in Excel).

I3 =$E$10*$E$9*SQRT(1/COUNT($A$3:$A$11)+(G3-AVERAGE($A$3:$A$11))^2/DEVSQ($A$3:$A$11))

	A	B	C	D	E	F	G	H	I	J	K
1	ACTUAL DATA						PREDICTED VALUES				
2	drainage density	recession constant					drainage density	recession constant	CI	lower CI	upper CI
3	1.042	0.962		m	0.0746		0	0.8608	0.112533046	0.748267	0.973333
4	1.106	0.957		b	0.8608		0.2	0.87572	0.091475185	0.784245	0.967195
5	1.16	0.982		SS	0.013766		0.4	0.89064	0.071261736	0.819378	0.961902
6	1.39	0.956		n	9		0.6	0.90556	0.05287025	0.85269	0.95843
7	0.4545	0.943		k	2		0.8	0.92048	0.038971711	0.881508	0.959452
8	0.4713	0.855		df	7		1	0.9354	0.035338759	0.900061	0.970739
9	1.275	0.93		SE	0.044346		1.2	0.95032	0.044557426	0.905763	0.994877
10	0.842	0.956		t	2.364624		1.4	0.96524	0.061060651	0.904179	1.026301
11	0.842	0.846					1.6	0.98016	0.08048568	0.899674	1.060646
12							1.8	0.99508	0.10116318	0.893917	1.096243
13							2	1.01	0.122460345	0.88754	1.13246
14	ŷ	y-ŷ	(y-ŷ)^2				2.2	1.02492	0.144102691	0.880817	1.169023
15	0.9385332	0.0234668	0.000550691				2.4	1.03984	0.165955229	0.873885	1.205795
16	0.9433076	0.0136924	0.000187482				2.6	1.05476	0.187944654	0.866815	1.242705
17	0.947336	0.034664	0.001201593				2.8	1.06968	0.210027975	0.859652	1.279708
18	0.964494	-0.008494	7.2148E-05				3	1.0846	0.232178403	0.852422	1.316778
19	0.8947057	0.0482943	0.002332339				3.2	1.09952	0.254378406	0.845142	1.353898
20	0.89595898	-0.04095898	0.001677638				3.4	1.11444	0.27661605	0.837824	1.391056
21	0.955915	-0.025915	0.000671587				3.6	1.12936	0.298882933	0.830477	1.428243
22	0.9236132	0.0323868	0.001048905				3.8	1.14428	0.321172973	0.823107	1.465453
23	0.9236132	-0.0776132	0.006023809				4	1.1592	0.343481662	0.815718	1.502682

6. Against the predicted drainage densities, graph the predicted recession constants, lower CI values, and upper CI values. You can add a trendline and display the equations. For the lower and upper CI trendlines, I found that a 6-order polynomial line matched best. You should have a graph with three lines that looks similar to the graphs displayed in Appendix J.

Appendix J: 95% Confidence Interval Graphs

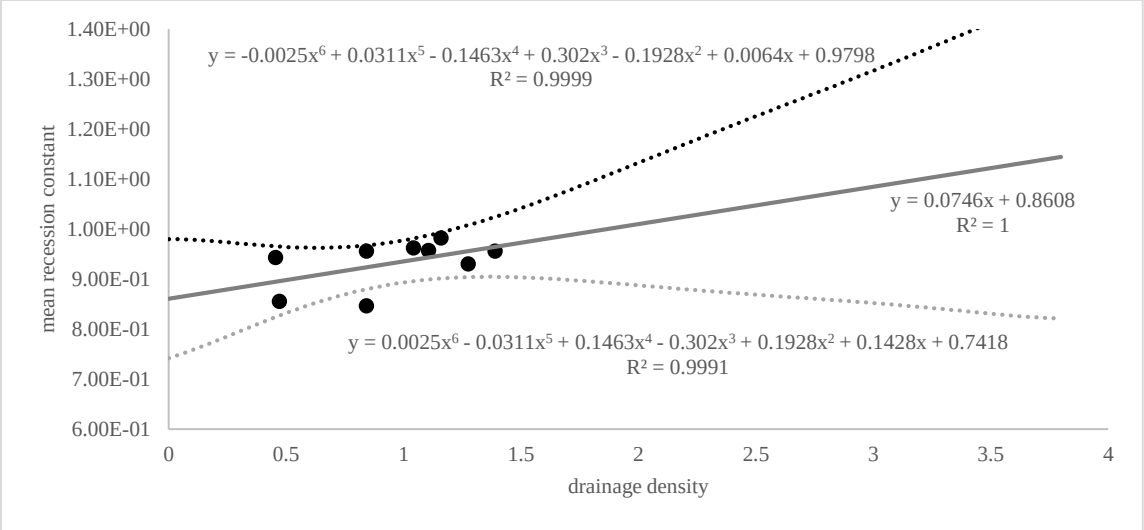

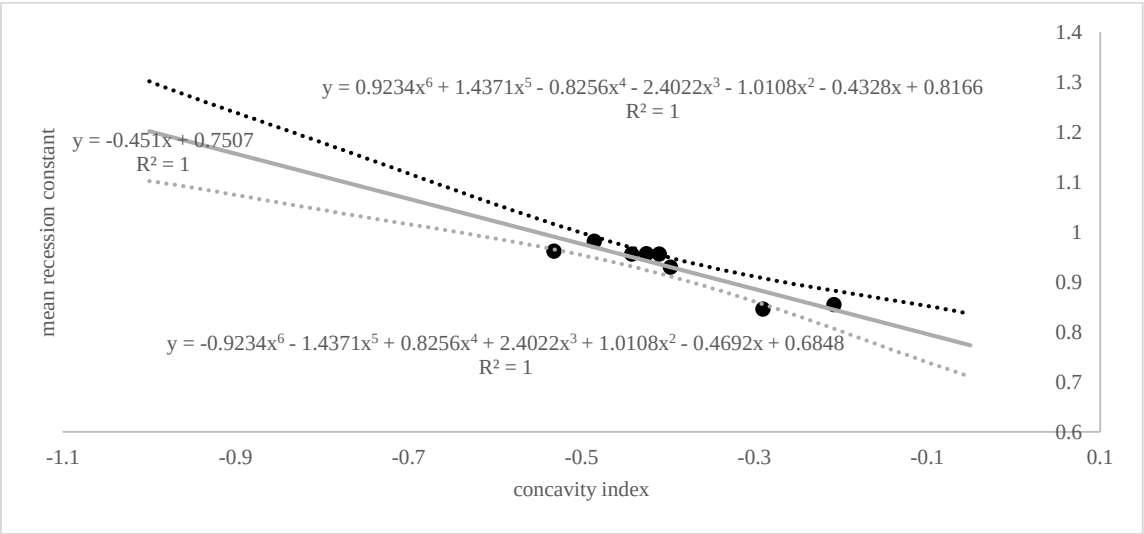

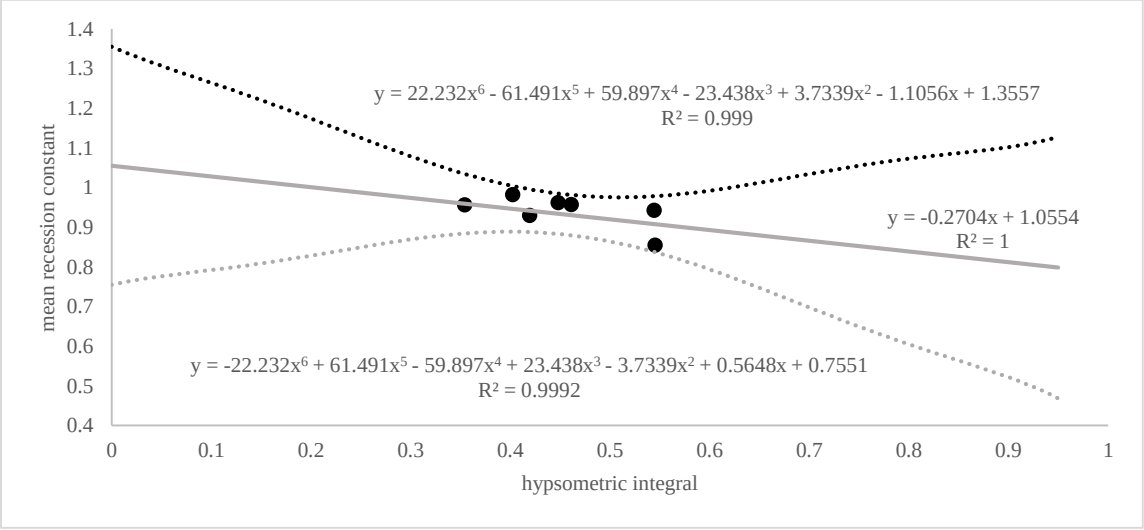

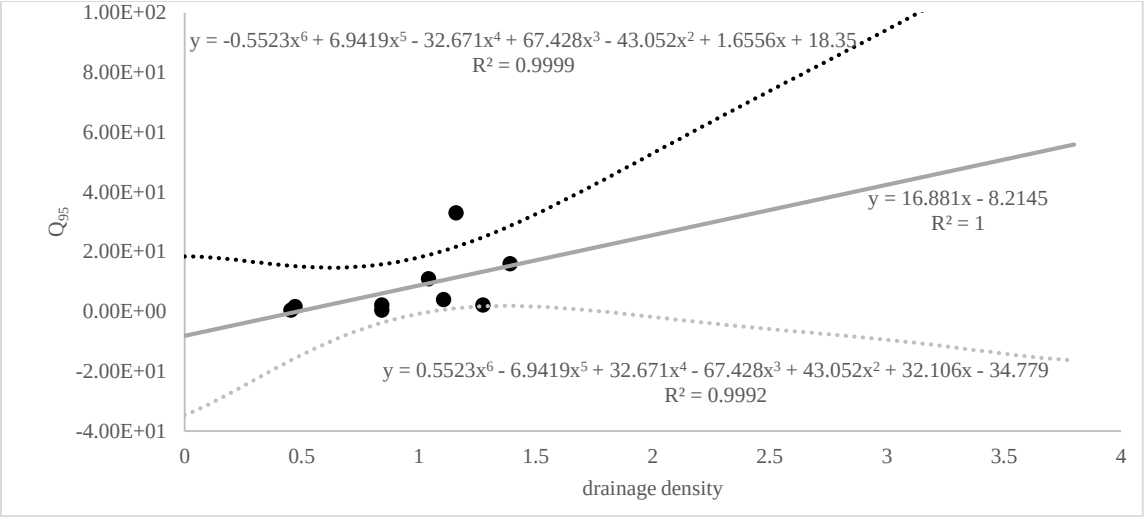
y = -0.5523x⁶ + 6.9419x⁵ - 32.671x⁴ + 67.428x³ - 43.052x² + 1.6556x + 18.35
R² = 0.9999
y = 16.881x - 8.2145
R² = 1
y = 0.5523x⁶ - 6.9419x⁵ + 32.671x⁴ - 67.428x³ + 43.052x² + 32.106x - 34.779
R² = 0.9992
Q95
drainage density

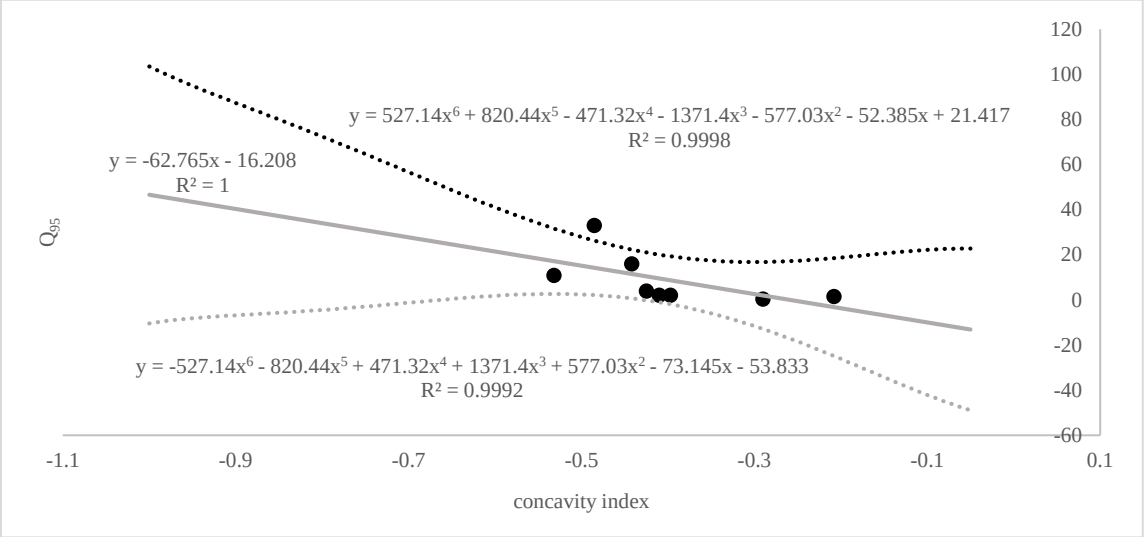
y = 527.14x⁶ + 820.44x⁵ - 471.32x⁴ - 1371.4x³ - 577.03x² - 52.385x + 21.417
R² = 0.9998
y = -62.765x - 16.208
R² = 1
y = -527.14x⁶ - 820.44x⁵ + 471.32x⁴ + 1371.4x³ + 577.03x² - 73.145x - 53.833
R² = 0.9992
Q95
concavity index

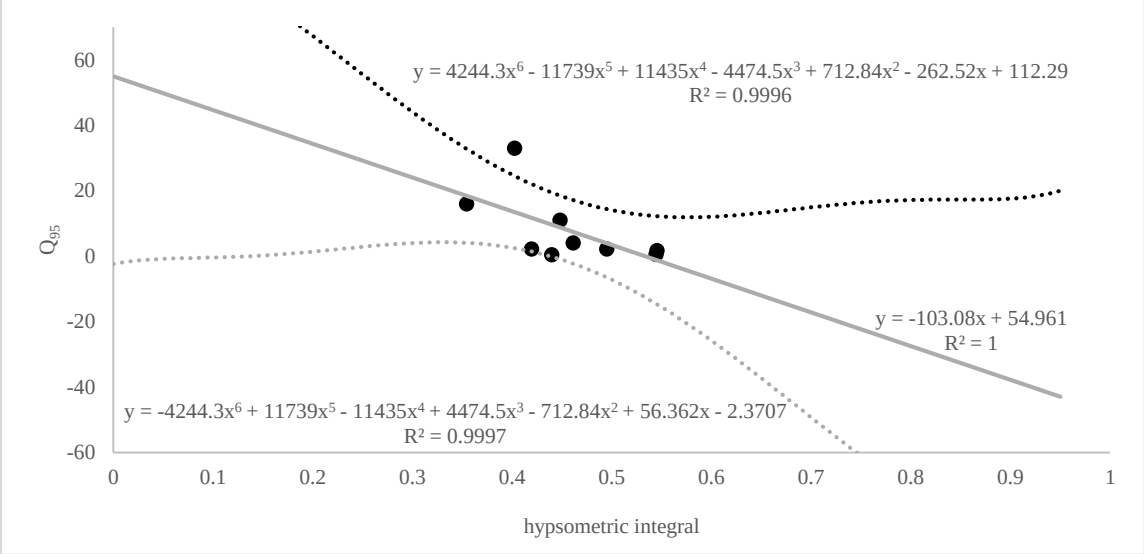
y = 4244.3x⁶ - 11739x⁵ + 11435x⁴ - 4474.5x³ + 712.84x² - 262.52x + 112.29
R² = 0.9996
y = -103.08x + 54.961
R² = 1
y = -4244.3x⁶ + 11739x⁵ - 11435x⁴ + 4474.5x³ - 712.84x² + 56.362x - 2.3707
R² = 0.9997
Q95
hypsometric integral

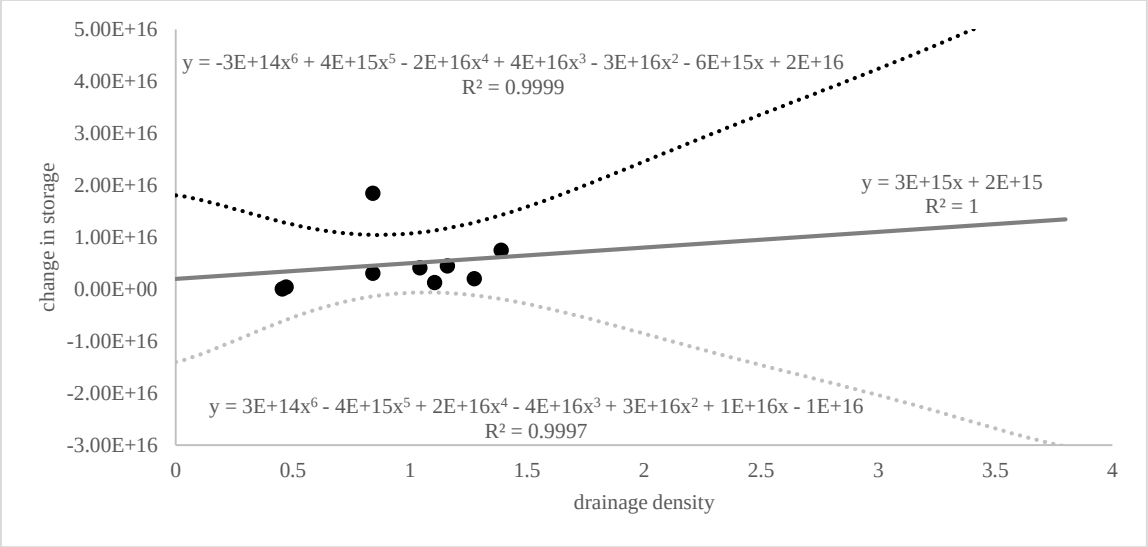
y = -3E+14x⁶ + 4E+15x⁵ - 2E+16x⁴ + 4E+16x³ - 3E+16x² - 6E+15x + 2E+16
R² = 0.9999
y = 3E+15x + 2E+15
R² = 1
y = 3E+14x⁶ - 4E+15x⁵ + 2E+16x⁴ - 4E+16x³ + 3E+16x² + 1E+16x - 1E+16
R² = 0.9997
change in storage
drainage density

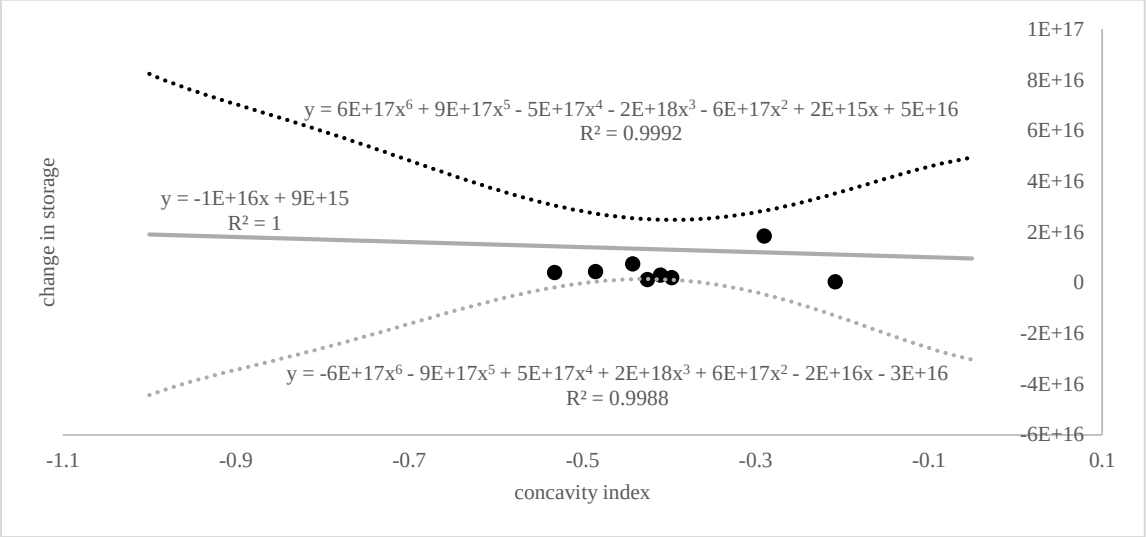
y = 6E+17x⁶ + 9E+17x⁵ - 5E+17x⁴ - 2E+18x³ - 6E+17x² + 2E+15x + 5E+16
R² = 0.9992
y = -1E+16x + 9E+15
R² = 1
y = -6E+17x⁶ - 9E+17x⁵ + 5E+17x⁴ + 2E+18x³ + 6E+17x² - 2E+16x - 3E+16
R² = 0.9988
change in storage
concavity index

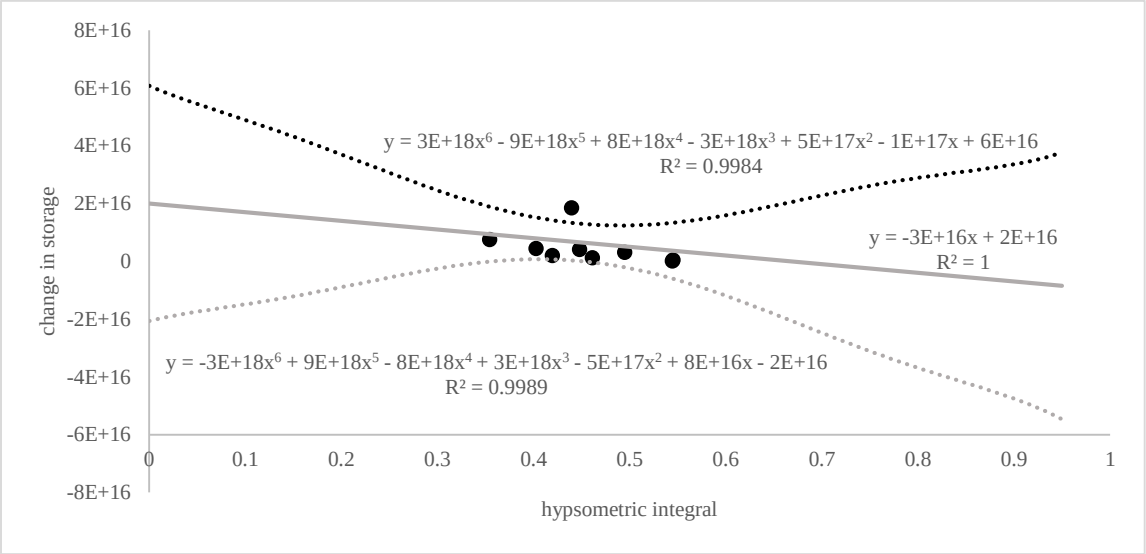
y = 3E+18x⁶ - 9E+18x⁵ + 8E+18x⁴ - 3E+18x³ + 5E+17x² - 1E+17x + 6E+16
R² = 0.9984
y = -3E+16x + 2E+16
R² = 1
y = -3E+18x⁶ + 9E+18x⁵ - 8E+18x⁴ + 3E+18x³ - 5E+17x² + 8E+16x - 2E+16
R² = 0.9989
change in storage
hypsometric integral

Appendix K: Differences between actual and predicted hydrologic values for currently gaged streams on Maui